MECHANISTIC UNDERSTANDING OF BIOGEOCHEMICAL TRANSFORMATIONS OF TRACE ELEMENTS IN CONTAMINATED MINEWASTE MATERIALS UNDER REDUCED CONDITIONS

by

RANJU RANI KARNA

M.S., Southern Illinois University Edwardsville, 2009

AN ABSTRACT OF A DISSERTATION

submitted in partial fulfillment of the requirements for the degree

DOCTOR OF PHILOSOPHY

Department of Agronomy
College of Agriculture

KANSAS STATE UNIVERSITY
Manhattan, Kansas

2014

Abstract

The milling and mining operations of metal ores are one of the major sources of heavy metal contamination at earth's surface. Due to historic mining activities conducted in the Tri-State mining district, large area of land covered with mine waste, and soils enriched with lead (Pb), zinc (Zn) and cadmium (Cd) remain void of vegetation influencing ecosystem and human health. It has been hypothesized that if these minewaste materials are disposed of in the flooded subsidence pits; metals can be transformed into their sulfide forms under reduced conditions limiting their mobility, and toxicity. These mine waste materials are high in pH, low in organic carbon (OC) and sulfur (S). The objective of this study was to examine the effect of OC and S addition on the biogeochemical transformations of Pb, Zn and Cd in submerged mine waste containing microcosms. Advanced molecular spectroscopic and microbiological techniques were used to obtain a detail, mechanistic, and molecular scale understanding of the effect of natural and stimulated redox conditions on biogeochemical transformation and dynamics of Pb, Zn and Cd essential for designing effective remediation and mitigation strategies.

The results obtained from these column studies indicated that Pb, Zn and Cd were effectively immobilized upon medium (119-day) and long-term (252-day) submergence regardless of treatment. The OC plus S treatment enhanced sulfide formation as supported by scanning electron microscopy- energy dispersive X-ray technique, and synchrotron based bulk-, and micro-X-ray fluorescence and absorption spectroscopy analyses. Microbial community structure changed with OC and S addition with the enhancement sulfur reducing bacteria genes (dsrA/B), and decreased metal resistance genes over time. The long-term submergence of existing mine tailings with OC plus S addition reduced trace metals mobility most likely through dissimilatory sulfate reduction under stimulated reduced conditions. Colloidal assisted metal

transportation (<1% of both Pb and Cd) occurred during initial submergence. Retention filters are suggested to avoid colloidal metal transport in order to meet the maximum concentration limit for Pb and Cd in surface and groundwater.

This research enhances our understanding of the redox processes associated with the sequestration of non-redox sensitive metals through dissimilatory reduction of sulfates in mine waste materials and/or waste water and provides regulators with useful scientific evidence for optimizing remediation goals.

MECHANISTIC UNDERSTANDING OF BIOGEOCHEMICAL TRANSFORMATIONS OF TRACE ELEMENTS IN CONTAMINATED MINEWASTE MATERIALS UNDER REDUCED CONDITIONS

by

RANJU RANI KARNA

M.S., Southern Illinois University Edwardsville, 2009

A DISSERTATION

submitted in partial fulfillment of the requirements for the degree

DOCTOR OF PHILOSOPHY

Department of Agronomy
College of Agriculture

KANSAS STATE UNIVERSITY
Manhattan, Kansas

2014

Approved by:

Major Professor
Ganga M. Hettiarachchi

Copyright

Abstract

The milling and mining operations of metal ores are one of the major sources of heavy metal contamination at earth's surface. Due to historic mining activities conducted in the Tri-State mining district, large area of land covered with mine waste, and soils enriched with lead (Pb), zinc (Zn) and cadmium (Cd) remain void of vegetation influencing ecosystem and human health. It has been hypothesized that if these minewaste materials are disposed of in the flooded subsidence pits; metals can be transformed into their sulfide forms under reduced conditions limiting their mobility, and toxicity. These mine waste materials are high in pH, low in organic carbon (OC) and sulfur (S). The objective of this study was to examine the effect of OC and S addition on the biogeochemical transformations of Pb, Zn and Cd in submerged mine waste containing microcosms. Advanced molecular spectroscopic and microbiological techniques were used to obtain a detail, mechanistic, and molecular scale understanding of the effect of natural and stimulated redox conditions on biogeochemical transformation and dynamics of Pb, Zn and Cd essential for designing effective remediation and mitigation strategies.

The results obtained from these column studies indicated that Pb, Zn and Cd were effectively immobilized upon medium (119-day) and long-term (252-day) submergence regardless of treatment. The OC plus S treatment enhanced sulfide formation as supported by scanning electron microscopy- energy dispersive X-ray technique, and synchrotron based bulk-, and micro-X-ray fluorescence and absorption spectroscopy analyses. Microbial community structure changed with OC and S addition with the enhancement sulfur reducing bacteria genes (dsrA/B), and decreased metal resistance genes over time. The long-term submergence of existing mine tailings with OC plus S addition reduced trace metals mobility most likely through dissimilatory sulfate reduction under stimulated reduced conditions. Colloidal assisted metal

transportation (<1% of both Pb and Cd) occurred during initial submergence. Retention filters are suggested to avoid colloidal metal transport in order to meet the maximum concentration limit for Pb and Cd in surface and groundwater.

This research enhances our understanding of the redox processes associated with the sequestration of non-redox sensitive metals through dissimilatory reduction of sulfates in mine waste materials and/or waste water and provides regulators with useful scientific evidence for optimizing remediation goals.

Table of Contents

List of Figures

List of Tables

Acknowledgements

I am extremely grateful to my major supervisor Dr. Ganga M. Hettiarachchi for her continuous encouragement, tremendous support and guidance during my study. I would like to extend my gratitude to my Ph.D. committee members Dr. Gary Pierzynski, Dr. Charles W. Rice, Dr. Gerard J. Kluitenberg and Dr. Saugata Datta. I also highly acknowledge the Graduate School Chairman Dr. Paul E. Smith. My thanks goes to all the agronomy faculties and staffs who were very nice and helpful throughout my Ph. D. I would like to thank Jared Henry from Advanced Manufacturing Institute at K-State for making the columns for my study. I am very thankful to Dr. Yared A. Mullisa for his help with statistical analysis. This project would not be able to be completed without support from my laboratory colleagues and student workers. My gratitude goes to Dorothy Menefee, Phillip Defoe, Pavithra Pitumpe, Chammi Attanayake, Buddhika Galkaduwa, Joseph Weeks, Joy Pierzynski, Kasun Dissanayake, Rojee Pradhan, and Prabha Bajracharya. I would also like to thank Ms. Betsy Edwards at IT-help desk. I am very thankful to my family for their continuous support, encouragement and sacrifices especially my husband, Rajesh Kumar Labh.

Dedication

To my Parents

Krishna Kumar Karna

Ram Lali Karna

My husband

Rajesh Kumar Labh

My daughter

Sanvi Labh

Chapter 1 - Introduction

The milling, mining, and smelting operations are one of the main sources of heavy metal contamination of surface waters, groundwater, soils, and sediments in the world, especially generation of sulfide rich tailings, have a heavy impact on the neighboring water bodies (Edwards et al., 2000; Baker et al., 2003; Bhattacharya et al., 2006). The acid mine drainage resulting from the exposure of sulfide rich minerals to oxygen rich water leads to the leaching of several contaminants affecting groundwater quality (Johnson et al., 2005; Vega et al., 2006). Thus, metal contamination and acid mine drainage are highly prioritized environmental concern in any part of the world (Nordstrom et al., 1999; Concas et al., 2006).

The Tri-State mining district situated in parts of southeast Kansas, southwest Missouri, and northeast of Oklahoma has a history of 120 years of Pb, and Zn-ore mining activities. After the first commercial ore discovery of Pb was made in southwestern Missouri in 1838, it was mined only for Pb to be used in making bullets for initial 20 years (KGS, 2001). Zinc production started after the civil war in 1870 as mining became easier with access to heavy mining equipment via railroad transportation. The production from the Tri-State mining peaked between 1918 and 1941 (Pope, 2005). The extensive mining left a very large quantity of minewaste on the surface as chat and tailings which contain trace levels of various sulfide minerals such as pyrite (FeS_2), galena (PbS), sphalerite (ZnS), and others (Newfields, 2003). Metals have been dispersed heterogeneously throughout the district via aerial and fluvial transport (Beyer et al., 2004). The movement of soluble metals and metal-laden sediments from the landscape into surface waters via surface runoff are the primary ecological concerns for both aquatic and terrestrial organisms (Pierzynski and Vaillant, 2006).

Research has been done on the application of different amendments to stabilize and reduce the bioavailability of trace elements in minewaste materials in the Tri-State mining district (Pierzynski et al., 1993; 2005; Hettiarachchi et al., 2001; Baker et al., 2014). Application of high rates of compost, P amendment, and the mixture of biosolids, lime and compost in the minewaste materials have been somewhat successful in reducing the bioavailability and toxicity of Pb and Zn, however frequent application of amendments are required (Gudichuttu et al., 2013; Baker et al., 2014; Brown et al., 2014). Disposal of minewaste materials in flooded subsidence pits (i.e., wetland treatment) was the most preferred remediation strategy proposed by the USEPA. It has been hypothesized that if these minewaste materials are disposed of in the flooded subsidence mine pits, these metals can be transformed back into their sulfide forms, limiting their mobility and toxicity. Subsurface submergence of minewaste may result in seepage of leachate containing some Pb and Zn into groundwater regardless of liners/barriers. Requiring large volumes of clean soil for capping, and long term continuous monitoring could make this remedial action expensive (USEPA, 2010). The pre-assessment and screening was conducted in Waco, MO in order to evaluate the ability of this treatment to reduce metal loading to surface water. A flooded subsidence pit was backfilled with $4.4x10^4$ m^3 tailings, and then capped with 45 cm of topsoil/ biosolids mixture. Water samples collected from four nearby ponds for one year, two shallow aquifer wells, and a central well indicated no changes in parameters except for a short-term spike in Zn concentration observed at one site (Newfields, 2003).

The minewaste materials are low in dissolved OC and that could have a significant impact on redox processes (Zhang et al., 2005; Hayes et al., 2006; Stein et al., 2007) as OC is the driver of biogeochemical cycling of major and trace elements (Evans et al., 2006; Borch et al., 2010). As a consequence of leaving minewaste materials on the surface, more S would leach out

as compared to immobile trace elements like Pb, Zn and Cd. Therefore, insufficient S content in minewaste materials could limit sulfide formations and promote carbonate precipitation depending on pH and carbonate concentration (Falkowski et al., 2000; Toevs et al., 2006). Remediation approach that involves microbial sulfate reduction for metal remediation comprises reduction of metals via biogenic sulfide formation (Labrenz et al., 2000; Finneran et al., 2002; Moreau and Banfield, 2004), which is going to be affected by a multitude of complex and interactive biogeochemical processes such as sorption/desorption, precipitation/dissolution and redox transformations (Wang et al., 2006; Violante et al., 2010). The toxicity exerted by heavy metals may suppress the microbial community and may lead to a shift in community structure affecting the related microbial processes. For example, enzymes controlling C-cycling are least affected due to presence of heavy metals compared to the enzymes involved in N, P and S cycling (Fliegbach et al. 1994). Therefore, the mobilities of metals depend on the metal speciation that is highly controlled by a dynamic interplay of physical, chemical, and biological processes in wetlands (Adriano et al., 2001; Gadd et al., 2004; Toevs et al., 2006). A multiple approach is required to fully understand these complex systems. The effectiveness of OC and S addition on reducing the bioavailability of trace elements were assessed by measuring solution chemistry dynamics. Scanning electron microscopy-energy dispersive X-ray (SEM-EDXA) was used to obtain an indirect evidence of metal sulfide formations via measuring colocalization of metals with S. Any possible colloidal assisted trace metals transport were measured to continuously meet the maximum concentration limits for Pb, Zn and Cd in groundwater. A synchrotron based X-ray technique; X-ray fluorescence (XRF) was used to assess the elemental distribution, and their relationship. Direct Pb and Zn speciation were done via synchrotron based X-ray absorption near edge structure (XANES), and X-ray absorption fine structure (XAFS) to

understand underlying mechanisms responsible for effluent water chemistry indicating metal transformations and sequestrations. The impact of OC and S on the dynamic of microbial community structure, and the role of SRB gene in metal sulfide formations were assessed via advanced microbial analysis; functional gene array (GeoChip 4.2). This dissertation consists of three studies, and their specific objectives are given below:

1. The objectives of the first study; Biogeochemical transformations of trace elements in a contaminated minewaste material under reduced conditions (Chapter 3), were to understand the role(s) and mechanisms of biogeochemical redox transformations of Pb, Zn and Cd, and their dynamics under submerged conditions over time.
2. The objectives of the second study; Understanding subsurface transformation and dynamics of Pb and Zn in contaminated minewaste materials using synchrotron based X-ray analysis (Chapter 4), were to determine biogeochemical transformations of Pb and Zn by identification and semi quantification of the dominant forms of Pb and Zn minerals in submerged columns containing treated and non-treated materials with OC and S.
3. The objectives of the third study; Microbial population dynamics and role of SRB genes in stabilizing Pb and Zn under subsurface environment (Chapter 5), were to characterize the microbial communities playing a role in the biogeochemical transformation of Pb and Zn under reduced conditions, to measure the impact of OC and S on the dynamic of microbial community structure, and the role of SRB gene in the metal sulfide formation over time.

References

Adriano, D. C. 2001. Trace elements in terrestrial environments: Biogeochemistry, bioavailability, and risks of metals. Springer- Verlag, New York.

Bhattacharya, J., Ji, S. W., Lee, H. S., Cheong, Y. W., Yim, G. J., and Min, J. S. 2008. Treatment of acidic coal mine drainage: Design and operational challenges of successive alkalinity producing systems. Mine Water and the Environment. 27:12-19.

Beyer, W., Dalgarn, J., Dudding, S., French, J., Mateo, R., and Miesner, J. 2004. Zinc and lead poisoning in wild birds in the Tri-State mining district (Oklahoma, Kansas, and Missouri). Archives of Environmental Contamination and Toxicology. 48:108-117.

Borch, T., Kretzschmar, R., Kappler, A., Cappellen, P. V., Ginder-Vogel, M., and Voegelin, A. 2010. Biogeochemical redox processes and their impact on contaminant dynamics. Environmental Science and Technology. 44:15-23.

Brown, S., Mahoney, M., and Sprenger, M. 2014. A comparison of the efficacy and ecosystem impact of residual-based and topsoil-based amendments for restoring historic mine tailings in the Tri-State mining district. Science of the Total Environment. 48:624-632.

Concas, A., Ardau, C., Cristini, A., Zuddas, P., and Cao, G. 2006. Mobility of heavy metals from tailings to stream waters in a mining activity contaminated site. Chemosphere. 63: 244-253.

Edwards, K. J., Bond, P. L., Druschel, G. K., McGuire, M. M., Hamers, R. J., and Banfield, J. F. 2000. Geochemical and biological aspects of sulfide mineral dissolution: Lessons from iron mountain, California. Chemical Geology. 169:383-397.

Evans, M., Warburton, J., and Yang, J. 2006. Eroding blanket peat catchments: Global and local implications of upland organic sediment budgets. Geomorphology. 79:45-57.

Falkowski, P., Scholes, R. J., Boyle, E., Canadell, J., Canfield, D., and Elser, J. 2000. The global carbon cycle: A test of our knowledge of earth as a system. Science (New York, N.Y.). 290:291-296.

Finneran, K. T., Anderson, R. T., Nevin, K. P., and Lovley, D. R. 2002. Potential for bioremediation of uranium-contaminated aquifers with microbial U (VI) reduction. Soil and Sediment Contamination: An International Journal. 11:339-357.

Gadd, G. M. 2004. Microbial influence on metal mobility and application for bioremediation. Geoderma. 122:109-119.

Gudichuttu, V. 2013. Phytostabilization of multi-metal contaminated mine waste materials: Long-term monitoring of influence of soil amendments on soil properties, plants, and biota and the avoidance response of earthworms.

Hayes, J. M., and Waldbauer, J. R. 2006. The carbon cycle and associated redox processes through time. Philosophical Transactions of the Royal Society of London. Series B, Biological Sciences. 361:931-950.

Hettiarachchi, G., Pierzynski, G., and Ransom, M. 2001. In situ stabilization of soil lead using phosphorus. Journal of Environmental Quality. 30:1214-1221.

Baker, L. R., Pierzynski, G. M., Hettiarachchi, G. M., Scheckel, K. G., and Newville, M. 2014. Micro-X-ray fluorescence, micro-X-ray absorption spectroscopy, and micro-X-ray diffraction investigation of lead speciation after the addition of different phosphorus amendments to a smelter-contaminated soil. Journal of Environmental quality. 43:488-497.

Johnson, D. B., and Hallberg, K. B. 2005. Acid mine drainage remediation options: A review. Science of the Total Environment. 338:3-14.

http://www.kgs.ku.edu/Publications/pic17/pic17_2.html

Labrenz, M., and Banfield, J. 2004. Sulfate-reducing bacteria-dominated biofilms that precipitate ZnS in a subsurface circumneutral-pH mine drainage system. Microbial Ecology. 47:205-217.

Moreau, J. W., Webb, R. I., and Banfield, J. F. 2004. Ultrastructure, aggregation-state, and crystal growth of biogenic nanocrystalline sphalerite and wurtzite. American Mineralogist. 89:950-960.

Nordstrom, D. K., and Alpers, C. N. 1999. Negative pH, efflorescent mineralogy, and consequences for environmental restoration at the iron mountain superfund site, california. Proceedings of the National Academy of Sciences of the United States of America. 96:3455-3462.

Pierzynski, G. M., and Schwab, A. P. 1993. Bioavailability of zinc, cadmium, and lead in a metal-contaminated alluvial soil. Journal of Environmental Quality. 22:247-254.

Pierzynski, G. M., McDowell, R. W., Sims, J., and Sharpley, A. 2005. Chemistry, cycling, and potential movement of inorganic phosphorus in soils. Phosphorus: Agriculture and the Environment. 53-86.

Pierzynski, G. M., and Vaillant, G. C. 2006. Remediation to reduce ecological risk from trace element contamination: A decision case study. Journal of Natural Resources and Life Sciences Education. 35:85-94.

Pope, L. M. 2005. Assessment of contaminated stream bed sediment in the Kansas part of the historic Tri-State lead and zinc mining district, Cherokee County, 2004. USGS Scientific Investigations Report. 5251.

Stein, O. R., Borden-Stewart, D. J., Hook, P. B., and Jones, W. L. 2007. Seasonal influence on sulfate reduction and zinc sequestration in subsurface treatment wetlands. Water Research, 41:3440-3448.

Toevs, G. R., Morra, M. J., Polizzotto, M. L., Strawn, D. G., Bostick, B. C., and Fendorf, S. 2006. Metal (loid) diagenesis in mine-impacted sediments of Lake Coeur d'Alene, Idaho. Environmental Science and Technology. 40:2537-2543.

Vega, F. A., Covelo, E. F., and Andrade, M. 2006. Competitive sorption and desorption of heavy metals in mine soils: Influence of mine soil characteristics. Journal of Colloid and Interface Science. 298:582-592.

Violante, A., and Pigna, M. 2002. Competitive sorption of arsenate and phosphate on different clay Minerals and Soils. Soil Science Society of America Journal. 66:1788-1796.

Wang, Y., Morin, G., Ona-Nguema, G., Menguy, N., Juillot, F., and Aubry, E. 2008. Arsenite sorption at the magnetite–water interface during aqueous precipitation of magnetite: EXAFS evidence for a new arsenite surface complex. Geochimica Et Cosmochimica Acta. 72:2573-2586.

Zhang, S., Xue, X., Liu, R., and Jin, Z. 2005. Current situation and prospect of the comprehensive utilization of mining tailings. Mining and Metallurgical Engineering. 3:44-48.

Chapter 2 - Literature Review

History of the Tri-State Mining District

The Tri-State Mining District located in southeast Kansas, southwest of Missouri, and northeast of Oklahoma covers an area of 6475 square km and has a history of 120 years of Pb and Zn ore mining activities. The district has been mined for the sulfide forms of Pb (galena) and Zn (sphalerite) and to a lesser extent for Zn carbonate (smithsonite), Pb carbonate (cerrusite), Pb phosphate (pyromorphite), and other less abundant ores (Beyer et al., 2004). Since the first commercial ore discovery of Pb was made in southwestern Missouri in 1838, it was mined only for Pb that was used for making bullets for initial 20 years (KGS, 2001). Zinc production started after the civil war in 1870 as mining became easier with an access to heavy mining equipment via railroad transportation (Pope, 2005). More smelters were constructed in the early 1900's after the discovery of a shallow gas field in southeastern Kansas. That is how the production from the Tri-State mining peaked between 1918 and 1941 (KGS, 2001). The shallow mining that was done by using hand tools and a simple hoisting devices (man-made or animal-powered) were replaced by deeper mining with the improved blasting equipment, drills, hoists, and pumps. During this period the value of the Tri-State mining region production exceeded one billion dollars, and until 1945 it was the world's leading producer of Pb, and Zn concentrate. The process of mining galena, and sphalerite generated some smelter slag, and plenty of chat, and mine tailings were skimmed off and discarded that were typically stored on the site. The groundwater flooding control was lost when pumpage declined in 1950's, and 1960's, and became a threat to the quality of neighboring ground and surface water (Bark, 1977). In the lack of efficient milling and mining, residual Pb and Zn remained in chat and tailings. An average

concentration of Pb and Zn in chat ranges 360-1500 mg kg^{-1}, and 6000-13000 mg kg^{-1} respectively (USEPA, 1997). In addition Hettiarachchi et al. (2001) reported that Pb and Zn concentration in slag ranges 9111- 25313 mg kg^{-1}, and 42592- 67654 mg kg^{-1} respectively. With such elevated trace elements concentration, the movement of soluble metals and metal-laden sediments from the landscape into surface waters via surface runoff can be of great concern.

Effect of Pb, Zn, and Cd on Human Health

Any trace metals at an elevated concentration can be toxic to plant productivity, ecosystem, and human health (Rasmussen, and Gardener, 2009). The potential health risk assessment calculated using USEPA model based on life time exposure (ingestion and inhalation) determined Zn, Cd, Pb, Co, Ni, Cu, Cr and Mn as the cumulative carcinogenic and non-carcinogenic risk for children and adults (ASTDR, 2008). Lead is a soft metal and can exist in the form of very small particles in air. Therefore Pb is ubiquitous in air through volcanic eruptions, and increased anthropogenic activities like smelting, milling and mining operations, soil erosion, waste incinerations, battery recycling, and renovations of old unsafe houses with Pb-based paint (Brown et al., 2004). An inhalation of dust with high concentration of Pb is the main exposure pathway in adult, whereas ingestion pathway is mainly associated with hand and mouth activities among children (Pierzynski and Gehl, 2004). There is no known physiological benefits of Pb in the body; however, it has numerous harmful effects as it interferes with a variety of human body system (Hsiang et al., 2011). Exposure to Pb is more dangerous for unborn, and young children. The fetus can get exposed through mother resulting premature births, reduced growth, and decreased mental ability in infant and unborn children. A child who ingests large amounts of Pb may develop blood anemia, severe stomachache, muscle weakness, brain damage, and also death is probable if blood Pb level is 150 µg dL^{-1}. Even with smaller

ingestion, Pb can affect a young childrens' mental and physical growth (ATSDR, 2007). Therefore, the effect of Pb in soil is always associated with elevated Pb blood levels in children (ASTDR, 2007). With elevated Pb, Zn and Cd (result of smelting locally mined ores), children in Joplin, MO area were detected with higher levels of Pb in blood (Ryan et al., 2001). The children blood Pb level of concern recommended by the United States Center for Disease Control and Prevention (CDC) is 10 μg dL-1 (ATSDR, 2007).

Zinc is a bluish-white shiny metal, naturally occurring in the earth's crust. It is also produced from smelting, milling, and mining operations, and is ubiquitous in air, soil and water. Zinc compounds are widely used in industry to make paint, rubber, dyes, wood preservatives, and ointments. In addition, Zn is considered to be relatively non-toxic to humans (Fosmire, 1990), and is considered as an essential trace element not only for humans, but for all organisms. It plays very significant role for human health as it is a constituent of more than 300 enzymes, and even higher number of proteins. Therefore sufficient amount of Zn is required in the body for proper functioning of protein metabolism, and cell growth (Vallee et al., 1993). Despite all such importance, Zn could also be an ecological risk, because it is known to adversely affect aquatic receptors and can be phytotoxic at high concentrations (US EPA, 2003). In addition, an excess of Zn can cause brain lethargy, focal neuronal deficits, nausea, vomiting, and epigastric pain (ATSDR, 2005). Three major exposure pathways; inhalation, absorption through skin, and ingestion have been suggested for their entry into the human body (Plum, 2010).

Cadmium is a natural element in the earth's crust, and is found as a mineral in combination with other elements such as CdO, $CdCl_2$, $CdSO_4$, and CdS. Mostly all soils, rocks including coals, and fertilizers contain some amount of Cd. Cadmium is usually extracted along with other metals like Pb, Zn and Cu (Adriano, 2001). Cadmium has commercial use in

producing batteries, pigments, metal coatings, and plastics. In typical inactive metal mine districts, huge piles of sulfide containing minewaste also contain Cd. Mostly inhalation of the dust containing Cd is the main exposure pathway. After few days of acute Cd inhalation, severe pulmonary edema, and chemical pneumonitis develop leading to death due to respiratory failure. Chronic exposure to Cd causes itai itai disease in elderly women that results in decrease of bone mineral density, increased risk for fractures, and osteoporosis. The Department of Health and Human Services has identified Cd as a human carcinogen (Seidal et al., 1993).

Impact of mining on surface and groundwater quality

Water is required to support all flora, and fauna (Vanloon and Duffy, 2005), and it is gained from two principal natural sources; surface water (fresh water, lakes, rivers, and streams), and groundwater (borehole water and well water) (Mendie, 2005). Due to its unique properties, such as polarity, and hydrogen bonds, it can dissolve, absorb, adsorb or suspend various compounds (WHO, 2007). Therefore, water is more susceptible to a wide varieties of contaminants that persists in all dissolved, particulate, and colloidal phases (Adepoju-Bello et al., 2009).

The milling and mining operations of metal ores are one of the major sources of heavy metal contamination on the earth's surface, in particular, the generation of sulfide rich tailings has a heavy impact on neighboring water bodies (Baker et al., 2003). Acid mine drainage resulting from the exposure of sulfide rich minerals to oxygen rich water leads to leaching of several contaminants that may impact on surface and groundwater quality (Vega et al., 2006). Thus, metal contamination and acid mine drainage are high priority environmental concerns, particularly where minewaste materials rich in metal-sulfides are abandoned without any

mitigation provisions in place (Concas et al., 2006).The groundwater quality is affected by the characteristics of media through which water passes on its way to the groundwater zone of saturation indicating a significant relationship between surface and ground water contamination (Adeyemi et al., 2007).

In addition, the heavy metals discharged by industries, traffic, municipal wastes, and hazardous waste sites as well as from fertilizers for agricultural purposes and accidental oil spillages from tankers can result in a steady rise in contamination of groundwater (Igwilo et al., 2006). Therefore, it is essential to supply high-quality water for the overall health of the high Plains agricultural economy, the viability of its cities and rural communities, and the environmental well-being of the landscape by running consistent with maximum contamination limit for all possible (eg., USEPA MCL for Pb in groundwater is 15 µg L^{-1}, and Cd is 5 µg L^{-1}) (McMahon et al., 2007).

Remediation

As mentioned earlier, a primary source of Pb, Zn and Cd contamination in soils is the mining and smelting of ores containing these trace elements. In addition, mining related highly contaminated wastes such as rocks, chat, and tailings represent potential sources of metals that can be redistributed to the surrounding environment by aerial and fluvial transport (Schaider et al, 2007). When Pb, Zn and Cd are present in soils at high concentrations that can affect human health and environment, this is specifically true for Pb (Davies and Wixson, 1988). Given the widespread contamination of soil with Pb, Zn and Cd due to anthropogenic activities, and the associated potential human and ecological risks require remediation of contaminated soils. There are several commonly used remedial processes that includes excavation, and landfilling of smelter/mine contaminated soil/minewaste materials. However, presently less invasive, and

inexpensive *in situ* remediation techniques focus on reducing metal bioavailability have been favored (Adriano, 1997).

Excavation of metal-contaminated soils

Excavation of metal contaminated soils is not always practical due to an excessive cost involved with magnitude (area, depth and volume) of the contaminated soil/minewaste materials that needs to be excavated along with the degree of disruption incurred at the site. Containment alternatives such as soil caps, are often inconsistent with the desired end use for the site and may be viewed negatively by the regulatory community and the public (Mulligan et al., 2001).

Phytoremediation

Phytoremediation refers to a diverse collection of plant-based technologies that use either naturally occurring or genetically engineered plants, and associated microbiota to extract, contain, or immobilize contaminants (Flathman and Lanza, 1998; Helmisari et al., 2007). This technology is an innovative, cost-effective alternative to the more established treatment methods used at hazardous waste sites (Zhang et al., 2010). Plants should be tolerant of site conditions (e.g., low pH, high metal concentration, and salinity), rapidly growing with higher biomass, relatively dense roots to provide an additional surface area for metal precipitation or adsorption to occur (Berti et al., 1998). Red fescue (*Festuca rubra L.)* is frequently used to establish vegetative cover in mine impacted soils previously treated with stabilization amendments (Vangronsveld and Cunningham, 1998; Li et al., 2000).

Phytoremediation technologies have different applications; phytoextraction (Jadia and Fulekar, 2009), phytostabilization, phytodegradation and phytovolatilization (Long et al., 2002). Phytoextraction technology refers to the process in which plants absorb metals from soil and

translocate, or further accumulate in the shoots that are subsequently harvested to remove the contaminants from soils (Salt et al., 1995).

In phytostabilization, contaminant mobility and bioavailability in the soil is limited by use of plant in combination with *in situ* inactivation or chemical stabilization via addition of soil amendments. This technique has been effective for remediating Cd, Cu, As, Zn and Cr, and it is very effective when rapid immobilization is needed to preserve ground and surface waters (USEPA, 2000). Phytodegradation is also known as phytotransformation. This approach remediates organic compounds, including herbicides, insecticides, chlorinated solvents, and inorganic contaminants (Pivetz, 2001) via breaking down by plant produce enzymes such as dehalogenase and oxygenase that help catalyze degradation. In this approach, plants and the associated microbial communities play a significant role in attenuating contaminants. In phytovolatilization, the plants uptake contaminants from the soil, and transform them into volatile forms to further release into the atmosphere (USEPA, 2000). Phytovolatilization of Se has been reported by Banuelos (2000), where Se is transformed into dimethylselenide and dimethyldiselenide in high Se media, and released into the atmosphere.

Phytoremediation techniques are not as well developed but could be useful for areas of low contamination, where longer treatment times may be necessary to remediate contaminants. There are several issues associated with this technique such as enhancing the accumulation of metals by plants, developing methods to extract meals from plants and determining correlations between soil components and bioavailability. However, for mining/smelter impacted areas less invasive, and inexpensive *in situ* remediation methods such as in place inactivation through soil amendments and phytostabilization, have been favored to reduce ecosystem health risk (Adriano, 1997).

In situ Remediation

There are seven commonly identified *in situ* remediation technologies such as solidification/stabilization, vitrification, electrokinetic remediation, soil flushing, phytoextraction, phytostabilization, and chemical stabilization. Altogether, in situ remediation approach is based on three remedial strategies; isolation, removal, and stabilization. The isolation technologies refer to those that are implemented to reduce contaminant availability by reducing the exposed surface area, reducing the soil permeability, and/or reducing the contaminant solubility. Removal technologies refer to those that are employed *in situ* to remove metals from a contaminated soil matrix through the use of physical and/or chemical processes (Ruby et al., 2004; Zhang et al., 2010). For the purpose of this thesis we will be focusing on chemical stabilization.

Chemical stabilization

Chemical stabilization technologies include those that involve the use of chemical amendment(s) and/or plants to reduce the leachability and/or bioavailability of metals in contaminated soils. *In situ* stabilization like other approaches such as natural attenuation, *in situ* capping and *in situ* confinement, has several advantages as it is less expensive, and less disruptive to ecosystem compared to *ex situ* methods (Smith et al., 1995).

Types of amendments

Numerous studies have been conducted using different chemical amendments that include organic material, alkaline material, phosphate fertilizer, and metal oxides adsorbents for remediation of Cd, Pb and Zn (Sauve et al., 2003; Bhattacharya et al., 2006; Baker et al., 2008). The general mechanisms underlying the immobilization of metals are adsorption, surface complexation, precipitation/co-precipitation, and cation exchange.

Organic amendment

With the proven significant role of soil organic matter (OM) in the restoration, and sustainability of ecosystem processes, organic amendments have also been used in the remediation of heavy metal contaminated soils (Clemente et al., 2005). Mine tailings are often characterized by poor soil properties including very low organic C, P, N, and low to neutral pH. Organic matter often has high CEC and may adsorb metals on pH-dependent exchange sites. It also forms strong complexes with Pb, Cu or Zn present in contaminated soils or mine spoils. Some organic amendments that contain high levels of P or Fe or have a high pH may have additional capacity to inactivate soil metals. Many organic materials e.g., composts, sludges, manures have been in use to improve the soil properties such as water holding capacity, enhanced water infiltration, increased nutrient supply, improved aggregation, proper aeration, and higher microbial activity. As OC is consumed by microbial communities, the large amount of organic amendment is required to be done over time to establish a new equilibrium at which the contaminants can be retained and ecosystem functions can be restored (Sauve et al., 2003; Bhattacharya et al., 2006; Baker et al., 2008).

It has been reported that the adsorption ability of heavy metals on OM is 30 times higher than clay minerals (Sauve et al., 2003). The stability complex may influence the bioavailability and extraction of heavy metals by plants, and affect the acidity, and redox properties of soils (Walker et al., 2003). Therefore, in recent years, composted materials or biosolids application have been done in attempt to remediate heavy metal contaminated soils. Application of OM in forms of cattle manure, pig manure, chicken manure, peat and crop straw are inexpensive, highly available and feasible in the restoration of heavy metal contaminated soils, however the

outcomes may be site specific, and therefore it is difficult to make any generalization (Walker et al., 2003).

Phosphorus amendments

The majority of bench-scale laboratory investigations have been conducted in particular to evaluate the effects of phosphate amendments on Pb solubility, reporting phosphate as an effective amendment at stabilizing Pb. The phosphate minerals have the potential to sorb and/or co-precipitate trace metals (Cunningham, 1997; Chaney et al., 1997; Hettiarachchi and Pierzynski, 2002) forming highly insoluble Pb phosphate minerals with low bioavailability and mobility that are stable under different environmental conditions (Ruby et al., 1994). Phosphates may be added to contaminated soil or mine spoil as phosphoric acid, di- and tri-basic potassium phosphate, calcium phosphates, sodium phosphate, mono- and di-ammonium phosphate, and rock phosphate or apatite (Berti et al., 1997).

Alkaline Materials Amendment

Several studies have used alkaline materials for *in situ* chemical stabilization of heavy metals. The alkaline materials commonly used in agricultural practice, and mine spoil re-vegetation are $CaCO_3$, $CaCO_3$+$MgCO_3$), $Ca(OH)_2$, CaO and they have been used to raise soil pH desirable for plant growth (Gray et al., 2006). In addition, liming materials may also be used to immobilize metals in waste products (sludges, composts, slags, flyashes), or in contaminated sludge-amended soils and sediments (Berti et al., 1998). Generally, an increase in soil pH ionizes pH-dependent exchange sites, raising cation exchange capacity (CEC), which subsequently increases metal sorption to soil particles (Lindsay, 1979). Additionally, increased soil pH, and carbonate buffering can lead to the formation of metal carbonate precipitates, complexes, and the formation of secondary minerals that decrease metal solubility, and mobilities. However, the

effect of added alkaline materials may no longer take effect after pH-buffering capacity of the amendment is depleted. Therefore frequent application of alkaline materials is required especially in mine impacted area with lower pH (Berti et al., 1998). The researches show that alkaline materials may not always be successful as an individual treatment. However when combined with other inorganic and organic amendments, it will provide more binding sites to effectively immobilize the cationic contaminants. The increased pH by alkaline materials will further enhance effectiveness by making surface adsorption sites more reactive due to reduced competition with proton. The lime and composted manure applied simultaneously reduced the extractable concentration of both Pb and Zn (Lothenbach et al., 1998). Additionally, it should be noted that the addition of alkaline materials may increase DOC concentration resulting in high contaminant mobility through dispersion of organically bound metals (Korthals et al., 1996). Majority of the studies are focused on Pb because of its known negative impacts on human health (Nriagu, 1984). There is a significant concern regarding As mobility with phosphate amendments, however that can be potentially mitigated by inclusion of Fe as hydrous ferric oxide along with phosphate amendment (Jones, 1997). Another concern is the continuous uptake of P due to plant growth that could reduce the effectiveness of P amendments on Pb bioavailability, unless sufficient excess was applied or P amendment added in combination with other sorbents such as Mn oxides (Hettiarachchi and Pierzynski, 2002). In fact many contaminated sites contain several trace elements simultaneously, which commonly possess different chemical properties controlling their mobility and toxicity. As such, no single additive is expected to immobilize all inorganic contaminants. Therefore, a combination of soil amendments is needed for immobilizing co-existing multi-element contaminants in soil and sediments through synergistic, and superposition effects (Schreier et al., 1994). Still, it is

unrealistic to assume that once metal is complexed or precipitated in a solid phase, it is removed from the system forever, therefore, stability of immobilized contaminants over time should be examined (Scheckel, and Ryan, 2002). In addition, more research need to be conducted in multiple soil chemical environments with different amendments.

Wetland Treatment Systems

The high cost of conventional remedial approach has emphasized to explore creative, cost effective, and environmentally sound technology from contaminants removal (Woulds and Ngwenya, 2004). Wetland construction is an alternative low cost means to remove heavy metals from soil, and water (Matagi et al., 1998; Woulds and Ngwenya, 2004). Wetlands are defined as the land where water surface is near the ground surface long enough to maintain saturated conditions, along with the related vegetation. Wetlands are both naturally, and artificially constructed. The naturally constructed wetlands are marshes, bogs and swamps that have been used as a sink where a very large amounts of environmental contaminants are assimilated (Gray et al., 2000). Constructed wetland systems are simulated natural wetland systems which can be controlled, and manipulated, therefore usually the contaminants load rate, and their removal efficiency rate is higher in constructed wetland compared to natural ones (Mays and Edwards, 2001). There are two types of artificially constructed wetlands; free water surface and subsurface flow. The free water surface type wetlands are mainly basins or channels with a barrier to prevent any seepage; however they are provided with suitable depth of porous media. Subsurface wetland has water above the media; it provides enough surface for treatment, and the risk of odor, exposure, and vectors are inhibited. Therefore subsurface type wetland is advantageous over free water surface wetland, especially for the metals that needs to stay reduced for stabilization. Multiple processes undergoing in the wetlands are responsible for such as uptake of

nutrient by plants, bacterially mediated degradation, oxidation of contaminants, sedimentation, and adsorption of particles, and dissolved substances in the waste on the substrate, and deposition of suspended solids due to low flow rates. (Mays and Edwards, 2001; Marchand et al., 2010). However, the efficiency of systems depend strongly on inlet contaminant concentrations and hydraulic loading (Kadlec and Knight, 1996). In addition to adsorption, precipitation and co-precipitation, the redox reactions play a significant role in contaminant removal under subsurface environment. Metals can also form insoluble compounds through reductive or oxidative sorption; for example, under chemically reducing conditions (Eh < 50 mV) sulfates can be reduced to sulfides that can further combine with various elements, and form CuS<PbS<CdS<ZnS<NiS<FeS<MnS that are relatively insoluble precipitates (Murray-Gulde et al., 2005; Stein et al., 2007).

Biogeochemistry of Pb, Zn, and Fe in subsurface environment

When soil is submerged, the pore space is mostly filled with water, and O_2 in soil becomes insignificant a few hours after submergence. It creates a barrier between the water and atmosphere via limited movement of O_2 into soil. Reduction of submerged soil proceeds roughly in the sequence. Descending from aerobic to anaerobic conditions, the major electron acceptors available for microbial respiration are: O_2, NO_3^-/N_2+, NO_2^-/N_2, Mn^{2+}, Fe^{2+}, SO_4^{2-} and CO_2. The sequence of these electron acceptors more or less follows the order of decreasing free energy change, and explains the utilization order for microbial respiration. Functional microbial community changes as aerobic organisms are replaced by facultative or obligate anaerobes. During anaerobic respiration, OM is oxidized and redox sensitive soil components are reduced (Ponnamperuma, 1972; Kirk, 2004). In addition, submerging soil brings about a variety of results in several electrochemical changes such as decrease in redox potential, an increase in pH of acid

soils and a decrease in pH of alkaline soils, changes in specific conductance and ionic strength, drastic shifts in mineral equilibria, cation and anion exchange reactions, and sorption and desorption of ions. Similarly, in subsurface wetlands, after soil reduction occurs, mainly four mechanisms affect metal removal processes (Lesage et al., 2007a): (1) adsorption to fine textured sediments and organic matter (Gambrell, 1994), (2) precipitation as insoluble salts (mostly sulfides and oxyhydroxides), (3) absorption and induced changes in biogeochemical cycles by plants and bacteria (Kadlec and Knight, 1996), and (4) deposition of suspended solids due to low flow rates. All these reactions lead to accumulation of metals in the substrate of wetlands. The efficiency of systems depends strongly on (i) inlet metal concentrations and (ii) hydraulic loading (Kadlec and Knight, 1996).

Sorption is the mechanism in which transfer of ions from a soluble phase to a solid phase occurs. It is an important mechanism for removal of metals in wetlands as it helps in short-term retention or long-term stabilization of metals. Sorption refers to a group of processes including i) adsorption, ii) absorption and iii) precipitation.

Adsorption is a surface process resulting in the accumulation of a dissolved substance (an adsorbate) at the interface of a solid (adsorbent) and the solution phase. This interfacial region incorporates the volume of soil solution under the direct influence of surface, and is commonly referred as solid-solution interphase (Essington, 2004). Adsorption processes could occur via physical processes with weak bindings (physisorption), or chemical processes with strong bindings (chemisorption). Metals are adsorbed to particles by either ion exchange depending upon factors such as the type of element and the presence of other elements competing for adsorption sites (Seo et al., 2008) or chemisorption. Retention of Pb, Cu and Cr by adsorption is greater than Zn, Ni and Cd (Sheoran and Sheoran, 2006).

Absorption can retain inorganic, and organic substances via diffusion into three-dimensional framework of a solid structure. It also refers to a biochemical processes when a compound from the external media is entering into a living organism).

Precipitation reactions of an element can take place due to its high concentration in soil solutions. This reaction takes place when the solution becomes supersaturated with respect to that element. The precipitation refers to a mechanism via which the crystal structure of mineral increases in volume as a result of the three-dimensional growth of the structure. Metal carbonates are formed through precipitation at higher carbonate concentration under alkaline pH, and are effective for Pb and Ni. Despite metal carbonates are less stable than sulfides, they can contribute to initial sequestration of metals.

The degradation of OM rapidly lowers the redox potential (Gaillard et al., 1994). The reduction process in waterlogged soil enriched with OM influences the behavior of siderophilic (iron loving) trace elements. As redox progress due to Fe and Mn oxy(hydroxide) reductive dissolution, trace elements will be released in to soil solution, or get deposited via co-precipitation of Fe hydroxides or carbonates. Most metals in the pore water precipitate as metal oxides or adsorb on OM at redox potentials higher than 100 mV (Clark et al., 1998; Machemer et al., 1992; and Du Liang et al., 2009). Under chemically reducing conditions (Eh < 50 mV), in sulfate rich environment, sulfates can be reduced to sulfide minerals (Sheoran and Sheoran, 2006). Trace metals with the variable valence (Cr, Se, As and Mo) respond immediately to the decreasing redox potential in the soil (Fendorf et al., 2000). Trace elements with the constant valence (Co, Ni, Cu, Pb and Zn) respond indirectly by the reduction of iron (hydr)oxides as the carriers of heavy metals (Plekhanova et al., 2003). Upon a moderate decrease in redox potential, the mobility of heavy metals rises (Plekhanova et al., 1999). However, very strong reduction and

abundance of S in the soil lead to the opposite result, i.e., the formation of insoluble sulfides of heavy metals (Peltier et al., 2003).

Lead Minerals and Their Stability

The equilibrium reactions of different Pb minerals and complexes are summarized in Table 2-1. It is very unlikely that metallic Pb (Pb^0) may persist in natural environment that can be well explained by the following half-cell reaction:

$$Pb^{2+}\ 2e^- \longleftrightarrow Pb\ (c) \qquad \log K^0 = -4.33$$

Since Pb^{2+} in soil is expected to approach $10^{-8.5}$ M, an electron activity (pe) of < -6.41 is required for elemental Pb to form in soils. Thus it is unlikely for elemental Pb to form in soils as pe ranges from -6.0- 13.0 in soils (Sposito, 1989).

Table 2-1: Equilibrium reactions for some Pb minerals and their equilibrium constants at 25° C used for creating stability diagram 2-1.

No.	Equilibrium reaction	Log K°
1	$PbS\ (Galena) \Longleftrightarrow Pb^{2+} + S^{2-}$	-27.51
2	$PbO\ (yellow) + 2H^{+} \Longleftrightarrow Pb^{2+} + H_2O$	12.89
3	$PbO\ (red) + 2H^{+} \Longleftrightarrow Pb^{2+} + H_2O$	12.72
4	$Pb(OH)_2)\ (c) + 2H^{+} \Longleftrightarrow Pb^{2+} + 2H_2O$	8.16
5	$PbCO_3\ (cerussite) + 2H^{+} \Longleftrightarrow Pb^{2+} + CO_2(g) + H_2O$	4.65
6	$PbCO_3.Cl_2\ (Phosgenite) + 2H^{+} \Longleftrightarrow Pb^{2+} + CO_2(g) + H_2O + 2Cl^{-}$	-1.80
7	$Pb(CO_3)_2.(OH)_2\ (c) + 6H^{+} \Longleftrightarrow 3Pb^{2+} + 2CO_2(g) + 4H_2O$	17.39
8	$PbSO_4\ (anglesite) + 2H^{+} \Longleftrightarrow Pb^{2+} + SO_4^{2-}$	-7.79
9	$PbSO_4.PbO\ (c) + 2H^{+} \Longleftrightarrow 2Pb^{2+} + SO_4^{2-} + H_2O$	-0.19
10	$Pb_5(PO_4)_3OH\ (c)\ (hydroxypyromorphite) + 7H^{+} \Longleftrightarrow 5Pb^{2+} + 3H_2PO_4^{-}$	-4.14
11	$Soil\text{-}Pb \Longleftrightarrow Pb^{2+}$	-8.50

Adapted from Lindsay (1979).

Galena (PbS) is the most common mineral under reduced condition, it transforms into other common Pb minerals such as anglesite ($PbSO_4$), cerrusite ($PbCO_3$), and other phosphate minerals upon exposure to oxygen rich environment. In the oxidized system with higher pH values, Pb carbonates (cerrusite, $PbCO_3$), basic Pb carbonates ($Pb_3(CO_3)OH$), and Pb hydroxides ($Pb(OH)_2$) are the most stable minerals. Under low pH environment, Pb also forms many mixed minerals containing carbonate, sulfate, oxide, and chloride. These mixed minerals have an intermediate solubilities, and some even have very low solubility to be important in soils. For example, under lower pH, anglesite ($PbSO_4$) is predicted to have lower solubility compared to Pb carbonates, oxides, and hydroxides depending on the sulfate activity in that particular environment (Lindsay, 1979). Lead pyromorphite is one of the stable minerals among the Pb phosphates minerals under a wide range of environmental conditions. Figure 2-1 was constructed assuming sulfate activity to be 10^{-3} M that shows the relative solubility of several Pb minerals with respect to anglesite ($PbSO_4$). Of the minerals included in Figure 2-1, anglesite ($PbSO_4$) is most stable below pH 6, whereas cerrusite ($PbCO_3$) is most stable at higher pH. The oxides; PbO(red), and PbO(yellow) are the most soluble minerals of those depicted in the diagram. The $Pb(OH)_2$ (c) is considerably more stable at pH 8. Both $PbCO_3$, and $PbCO_3(OH)_2$ (c) have similar solubilities at 0.0003 atm of CO_2 (diagram is constructed based on 0.003 atm. With increase in CO_2, $PbCO_3$ is more stable (Figure 2-1). Among mixed Pb minerals, $PbSO_4$.PbO, and $Pb_3(CO_3)_2(OH)_2$ minerals are more stable compared to others that is explained in the diagram (Lindsay, 1979).

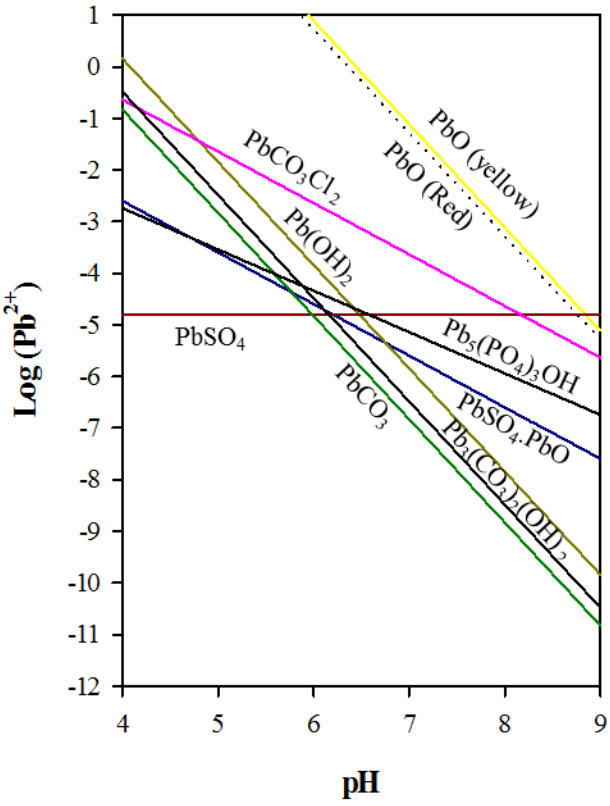

Figure 2-1: The solubility of selected various lead oxides, carbonates, and sulfates when SO_4^{2-} and Cl^- are 10-3 M and CO_2 is 0.003 atm.

Zinc Minerals and Their Stability

The oxidation state of Zn in natural environment like soils is Zn^{2+} exclusively. Metallic Zn(c) formation is possible only in highly reduced environments; it is unlikely to occur in soil environments as demonstrated by the reaction given below:

$$Zn^{2+} + 2e^- \longleftrightarrow Zn\ (c) \qquad \log K^0 = -25.80$$

Considering Zn^{2+} to be 1 M, an electron activity (pe) of -12.90 is required to form Zn(c). As discussed earlier, the pe in soils ranges from -6 to -13 (Sposito, 1989). Therefore, it is unlikely that Zn concentration will reach 1 M in solution, and metallic Zn will form in soils.

Table 2-2: Equilibrium reactions of some Zn minerals at 25 °C in soils used for creating stability in Figure 2-2.

No.	Equilibrium reaction	Log K°
1	Soil-Zn + $2H^+ \Longleftrightarrow Zn^{2+}$	5.80
2	ZnO (zincite) + $2H^+ \Longleftrightarrow Zn^{2+} + H_2O$	11.16
3	$Zn(OH)_2$) (amorphous) + $2H^+ \Longleftrightarrow Zn^{2+} + 2H_2O$	12.48
5	Zn_2SiO_4 (willemite) + $4H^+ \Longleftrightarrow 2Zn^{2+} + H_4SiO_4^0$	13.15
6	$ZnCO_3$ (smithsonite) + $2H^+ \Longleftrightarrow Zn^{2+} + CO_2(g) + H_2O$	7.91
7	$ZnFe_2O_4$(franklinite) + $8H^+ \Longleftrightarrow Zn^{2+} + 2Fe^{3+} + 4H_2O$	5.80

Adapted from Lindsay (1979).

Since the specific minerals controlling the activity of Zn^{2+} in soils are not known, reference solubility is used that permits Zn^{2+} solubility relationships to be compared to those of known Zn minerals (Novell and Lindsay, 1969; 1972). Most of the Zn production is done from Zn sulfide minerals; sphalerite, and wurtzite as they have higher percentage of Zn by weight compared to other minerals. Zinc sulfide minerals are common under reduced conditions, however on exposure to oxygen rich environment, ZnS are readily transformed into Zn silicate, oxide, carbonate, sulfate, and phosphate minerals.

The solubilities of different Zn minerals are plotted in figure 2-2. It shows that all of the $Zn(OH)_2$ minerals, ZnO (zincite), and $ZnCO_3$ (smithsonite) are too soluble to persist in soils. Willemite (Zn_2SiO_4) has intermediate solubility, and is highly dependent on H_4SiO_4 in soils that is further controlled by quartz (SiO_2) (Lindsay, 1979). Franklinite can be the most insoluble of these minerals, depending upon the Fe(III) oxides controlling Fe^{3+} activity. Zn minerals solubilities are highly influenced by pH, and with each unit of pH increase, solubility of all Zn minerals is increased by 100-fold (Fig 2-2). In addition, the existence of Zn phosphate mineral (hopeite) is highly dependent upon the concentration of phosphate in soils (Lindsay, 1979).

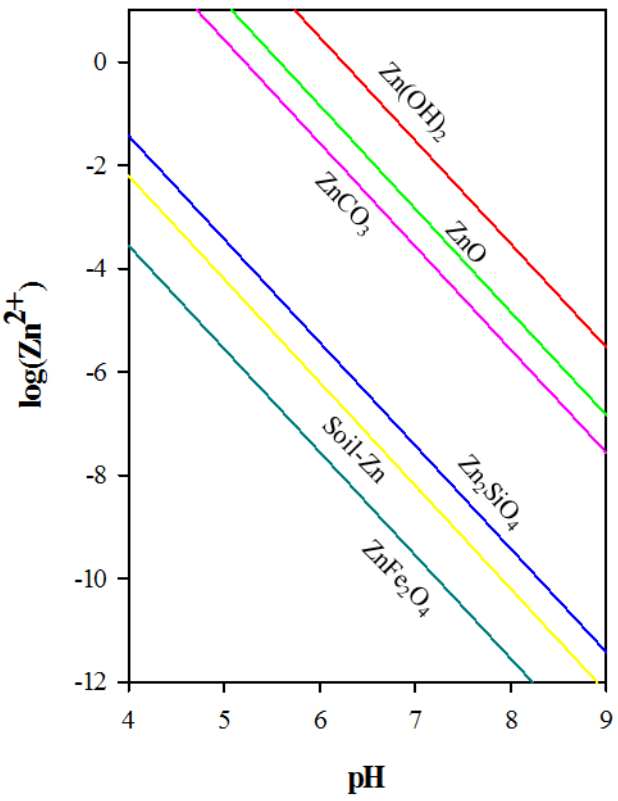

Figure 2-2: The solubility of several Zn minerals compared to soil-Zn.

Metal Sulfides and Their Solubility

The solubility relationships of the various S species and the sequence of metal sulfide precipitations are significant in soil particularly under submerged conditions, or exposed to fluctuating redox conditions (Lindsay, 1979). Sulfate is recognized as stable species in all but highly reduced soils. In highly reduced soils, hydrogen sulfide (H_2S) becomes an important solution species and is predominantly present below pH 7.02. Under this conditions relatively higher partial pressure of H_2S (g) is maintained that is sufficient enough to get released. Between pH 7.02 and 12.90 HS^- is a major solution species while S^{2-} is dominant above pH 12.90. Figure 2-3 was constructed using the thermodynamic equations provided in Lindsay (1979), and assuming SO_4^{2-} at 10^{-3} M. Figure 2-3 depicts the first formed sulfide as Hg_2S (c). The S (rhombic) formation is unlikely in soils due several reasons; required pe+pH of 2.5- 4.0, total S > $10^{-1.55}$ M, required confined system to avoid H_2S escape, and reaching all those conditions are not practical. Thus, the likely loss of H_2S (g) makes it unlikely to form CaS, and MgS in soils (Lindsay, 1979). βeta-Ag_2S (c) has similar solubility as α-Ag_2S. Pyrite (FeS_2) is the most stable mineral among all the iron sulfide minerals, however at lower redox some of the stability relationships may shift.

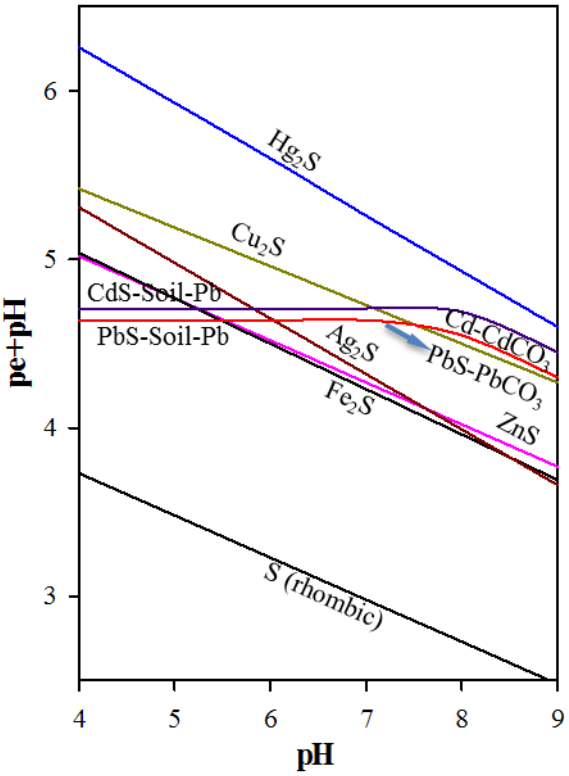

Figure 2-3: The redox at which various metal sulfides precipitate in soils when SO_4^{2-} is 10^{-3} M.

Activity of Zn^{2+} cannot be significantly depressed by ZnS (sphalerite) as redox is poised by the transformation of iron oxides into FeS_2 (Pyrite). Since soil has more Fe than Zn, this transformation will require sufficient enough S. Only after labile iron oxides transforms into pyrite, pe+pH will drop, and ZnS will precipitate to control Zn^{2+} solubility (Lindsay, 1979).

Biogeochemical cycling of Sulfur, Carbon, and Iron

Biogeochemical cycles describe the pathways by which chemical elements move through both biotic (the biosphere) and abiotic compartments (the atmosphere, hydrosphere, and lithosphere) on earth. In addition to energy flows, biogeochemical cycles establish the relations among ecosystem compartments at local, regional and global scales. In this system of inputs, outputs, sources and sinks, elements are moved from one part of an ecosystem (e.g., ocean, soil, and atmosphere) where the element may temporarily accumulate to another, back and forth among organisms, and from living organisms to the abiotic environment and back again. Simply, in biogeochemical cycling, chemical elements are cycled and reused within and among earth's various compartments over and again (Manahan, 2004; Lin et al., 2010).

The biogeochemical cycles proceed via biological, geological and chemical interactions along hydrological, gaseous, and mineral (Pérez-Guzmán et al., 2010). Some of the most ecologically important and well known element cycling are for carbon, nitrogen, oxygen, phosphorus, sulfur, water, and iron (Pérez-Guzmán et al., 2010).

Sulfur cycling

Sulfur is very essential element for all living organisms. The biogeochemistry of S is of high interest due to its influence on many different biogeochemical cycles. Sulfur exists mainly in organic forms and partly in inorganic forms. It is transported by physical processes like wind, erosion by water, and geological events like volcanic eruptions. However, in its compounds such

as SO_2, H_2S, S^{2-} or organic S, it can be moved from the ocean to the atmosphere, to land and then to the ocean through rainfall and rivers. All of the possible inorganic S sources, including SO_4^{2-}, S^{2-}, and reactive intermediates such as polysulfide, and thiosulfate can be produced in natural environment by microbial processes, therefore microbial mediated oxidation, and reductive cycling control the biogeochemistry of S isotopes. The distribution of S is primarily controlled by dissimilatory bacterial SO_4^{2-} reduction (Canfield, 2001a). There are two basic pathways by which organic S is formed, the first pathway is assimilatory SO_4^{2-} reduction in which active uptake of SO_4^{2-} into cells occur, followed by its reduction to produce amino acids and other S requiring cellular components. This pathway represents a very small fraction, however the other major way of organic S formation is via incorporation of reduced S into OM during digenesis. In addition, S isotope distribution is controlled by sedimentary cycle of microbial sulfide oxidation, and subsequent disproportionation of intermediate phases of S (e.g., elemental S, and thiosulfate) (Habicht et al., 2001), which has discovered an explanation for the discrepancy between fractionation observed in nature, and those occurring experimentally during bacterial sulfate reduction.

a. **Mineralization:** This process involves conversion of organically bound S to inorganic forms of S such as SO_4^{2-}, and is assimilated by plants and microorganisms, especially for those who prefers SO_4^{2-} as an electron acceptors (e.g. SRBs). Insufficient mineralization of organically bound S will inhibit microbial growth affecting the sulfide mineral formation in bioremediation approach, where metal sulfide formation is a main goal.
b. **Immobilization:** It is a process of microbial mediated conversion of inorganic forms of S; SO_4^{2-}, SO_3^{2-}, S^{2-}, thiosulfate ($S_2O_3^{2-}$), trithionite compounds to organic S compounds. Organic S compounds are not bioavailable form rather then they are sequestered.

c. **Oxidation**: This process included oxidation of elemental S and inorganic S compounds like H_2S, SO_3^{2-} and $S_2O_3^{2-}$ to SO_4^{2-}. Oxidation of S can be beneficial in agriculture as it has ability to alter the pH. Micronutrients like K, Mg, Ca, and others can be solubilized and be accessible to plants. On the other hand, in contaminated soils, it can cause environmental disasters by mobilizing the harmful trace elements downstream.

d. **Reduction:** Dissimilatory bacterial reduction of dissolved sulfate is the primary means by which reduced sulfur (H_2S) is produced in the natural environment. Dissimilatory sulfate reduction is more favorable under anaerobic, and alkaline conditions. Primarily sulfur reducing bacterial community (*Desulfomonas, Desulfovibrio, Desulfatomaculum spp.*) plays role in reducing SO_4^{2-} to H_2S.

Iron cycling

Iron composes more than 30% of the earth's mass, and is a ubiquitous element found in the atmosphere, biosphere, lithosphere, and hydrosphere. It is one of the most abundant elements on earth and among the most important elements in the biosphere (Morgan, 1988). Iron is an essential element for numerous cellular processes and metabolic pathways in both eukaryotic and prokaryotic organisms. Despite its abundance, Fe can be in short supply for growing organisms as it changes its chemical form, in ways that controls its availability. It is a reactive metal in its pure state that oxidizes readily in the presence of oxygen. Iron exists in reduced form (Fe(II)), or oxidized form (Fe(III)) depending on the oxygen concentration, pH, and biological activities. The oxidized, and reduced form of Fe are abundant in Fe(II), and Fe(III) bearing minerals. The Fe cycle is highly influenced by natural processes, anthropogenic activities, and microbial communities, and is driven by the oxidation and reduction processes.

Under aerobic conditions, highly soluble ferrous ion is converted to insoluble Fe(III) ions, or by microbes under acidic pH. Under aerobic condition, Fe exists in Fe(III) oxy/hydroxides forms. On the other hand, under anaerobic conditions, Fe is abundant in the form of Fe(II)s ions. Under low Fe stress, microbes secrets chelating agent known as siderophores to form Fe(III)-siderophore complexes making insoluble Fe bioavailable (Barbeu et al., 2001). Iron can be transported to the ocean as dust or volcanic ash, among which coarser particle will sink rapidly, while smaller (colloidal) particles will travel further and stay in the surface ocean, increasing the amount of bioavailable Fe (Duggen et al., 2009; Thompson et al., 2006). In soil, microorganisms play important role in the transformations of Fe in following ways:

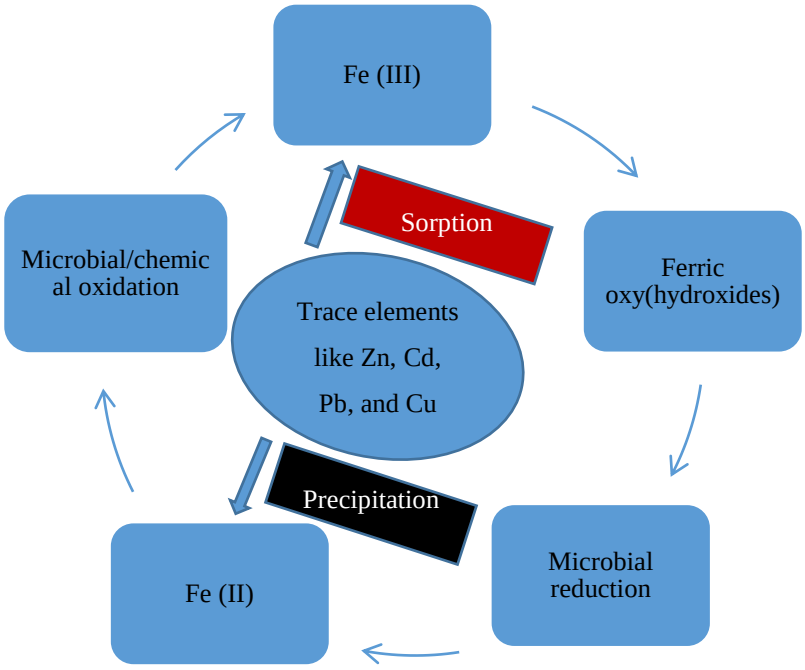

Figure 2-4: Biogeochemical cycling of Fe in soil.

Carbon cycling

Carbon biogeochemical cycling is one of the most significant global element cycling. The biogeochemical cycle of C comprises a sequence of events that are key to making the earth capable of sustaining life. It describes the movement of C as it is recycled and reused among the atmosphere, biota, soil organic carbon (SOC) and ocean (Janzen, 2004). Out of total, about 80% (8.06×10^7 Pg C) of organic, and inorganic C compounds are buried in earth that comprises 4000 Pg of OC held by fossil fuels and 4×10^4 Pg of inorganic C held by ocean surface that helps to buffer atmosphere CO_2 which comprises about 750 Pg (McCarl et al., 2007). On the other hand, soil represents the largest terrestrial pool as it constitutes 1500 Pg C which is about three times C storage in vegetation and two times in the atmospheric pool (Schlesinger, 1997). With the presence of different fractions of C, there is a continuous exchange of C among the pools. Over the long term, the C- cycle was balanced among different pools and being able to keep the earth's temperature relatively stable. However, with increased anthropogenic activities during the recent century altered the cycle via shifting C from one to another pool. For example, alterations that transferred more C into the atmosphere result in warmer temperatures on earth (Kleypas et al., 1999).

Soil OC is important because it is actively in flux with the atmosphere and as such, it is a potential feedback loop to climate change that is still not fully understood (Schmidt et al., 2011). Additionally, soil C is important for many soil properties such as pH buffering capacity, nutrient and water storage capacity, soil structure, and as a source of nutrients to organisms (Essington, 2004; Lal et al., 1999). Within soil, C goes through a sub-cycle that is part of the global C- cycle. Soil C has multiple pools of C; residue (deceased organisms), biomass (plant root, hyphae), humic substances, non humic substances, and inorganic C (carbonate minerals), however soil C

is represented via humic and non humic substances. Biomass C becomes residual C once the organisms die or release waste products which is broken down by microbes through enzymes that is excreted to begin digestion in soil matrix. The residue then becomes non humic substances (amino acids, peptides, sugars, etc) that is further transformed to humic substances via a series of biochemical reactions; known as humification (Essington, 2004). Humic substances can be divided into three main fractions: humic acids (HA), fulvic acids (FA) and humin, and are an operationally defined fraction of soil organic matter representing the largest pool of recalcitrant OC in the terrestrial environment (Essington, 2004).

Soil organic matter are increasingly emphasized in aquatic ecosystems or its geochemical and ecological roles. Organic matter in aqueous systems acts as a proton donor or acceptor and as a pH buffer, and affects the transport and degradation of pollutants. It also participates in mineral dissolution and precipitation reactions. Organic matter also influence the availability of nutrients, and serve as a carbon substrate for microbially mediated reactions. Dissolved organic carbon (DOC) comprises the vast majority of the organic matter in most water samples. (Weishar et al., 2003).

Mechanistic Understanding of Remediation Success

Synchrotron based X-ray analysis

Once element/contaminant enters into soil, it transforms into different forms depending on reactivity and biogeochemical properties of soils. Therefore it is required to measure the elemental distribution, and chemical speciation in relation to the minerals formed to characterize the soil properly. Provided the above information, understanding of mobility, bioavailability and toxicity can be measured especially on addition of fertilizers, pesticides, herbicides and introduction of contaminants into soils.

With the heterogeneity and complexity of soil, any single approach cannot characterize it with high precision; therefore an integrated approach is needed to obtain unique but complementary information for complete understanding of chemical environment (Fendorf and Sparks, 1996). There are several known analytical methods for elemental speciation that are restricted to fluid samples. Solid samples can be measured via these methods, only if the solid samples are dissolved without losing any species information, which can be very tedious and carry high errors (Welter, 2003). Traditionally, metal speciation in soils have been measured by sequential extraction that gives information on metal origin, its biological, and physico-chemical properties, bioavailability, mobilization, and transport. There are several limitation associated with this method as incomplete dissociation of target metals, removal of dissolved species, and change in states of redox-sensitive elements may occur (Nachtegaal et al., 2004). Therefore, the application of molecular-level spectroscopic techniques that are highly sensitive and non-destructive to sample integrity would provide definitive answers to complex environmental questions that has been supplied by X-ray based technique offered by several synchrotron sources (Rehr et al., 2000). X-ray absorption spectroscopy can be used to probe most phases of matter including crystalline or amorphous solids, liquids, and gases thus making XAS as one of the most versatile research tools to fully investigate the molecular nature of a wide variety of substances. (Miller et al., 2012).

Argonne National Laboratory located in IL, USA is one of the largest synchrotron facilities that offers different X-ray base techniques such as X-ray fluorescence (XRF), X-ray absorption spectroscopy (XAS) that includes X-ray absorption fine structure (XAFS) and X-ray absorption near edge structure (XANES), and X-ray diffraction (XRD) (Fendorf and Sparks, 1996). The principle of this technique is based on the X-ray absorption that occurs by

bombarding an element of interest with a beam of high energy particles from a synchrotron radiation source to excite, and eject electrons of particular element of interest from lower electron orbital with lower energy to the higher electron orbital with higher energy that are unoccupied or into continuum leaving core hole (Kelly et al., 2008). When the electron from outer-shell are expelled, they emit an energy called fluorescence which is collected, and measured by computer-controlled detectors. The data collected by the detector yield characteristic spectra providing an information on oxidation state, number and type of nearest neighboring atoms, coordination environment, and interatomic bond distances enhancing our understanding of the fate and transport of toxic elements in the environment (Miller et al., 2012). These X-ray based techniques can be used in soils from bulk to micro-scale level based on the need to meet specific objectives. The XAS can be measured at both bulk, and micrometer scale by focusing beam size in micro-XANES, and micro-XAFS (Liang, 2010). While soils are highly heterogeneous at a variety of size scales, the micro-scale studies can be beneficial in understanding the species composition at micro-scale level, and the mechanisms involved in their formations. It also helps identify the minor minerals formations that could be overlooked by bulk level XAS. Whereas bulk XAS has been proven to identify the overall speciation (Kelly et al., 2008; Stern et al., 2012; Miller et al., 2012).

Synchrotron based X-ray fluorescence (XRF) helps to study the elemental distribution, their relationship, and associations (Figure 2-3). In addition, it helps to identify the hotspots where, XAS can be collected. Therefore, XRF is known as a complementary technique for XAS analysis (Kelly et al., 2008).

The X-ray absorption is typically divided into two regimes: X-ray absorption near edge spectroscopy (XANES) and X-ray fine structure spectroscopy (XAFS). X-ray absorption near

edge spectroscopy is related to the edge energy. The absorption edge due to the excitation of core electrons to the continuum is very specific for every element. Small disturbance is due to change in redox state lead to a chemical shift of the edge position that depends on the oxidation state of the absorber atom available for excitation. That is why XANES can be used to identify the valence states and different oxidation states of elements present in soils. However, with the short distance based (small absorption edge) technique, it does not give more information from other shells. Therefore, employing XANES on the element with different oxidation states will be more useful to predict its bioavailability, toxicity and mobility in soils. For example, Fe is one of the most ubiquitous elements of particular interest as it forms highly reactive and often nanometer-sized Fe(III) oxy-hydroxides in the soil environment. Under reducing conditions, the oxy-hydroxides transform into Fe(II) minerals, so that redox processes can often be traced back by analyzing the Fe oxidation state of fine-grained Fe minerals (Prietzel et al., 2007). The XAFS region is the oscillation part in the X-ray spectrum that is found above the edge. It contains information on the local molecular bonding environment of the element of interest including type and number of atoms in coordination with the absorber, the distance between atoms and the degree of bonding disorder (Kelly et al. 2008). The XAFS portion of the spectra is best understood in terms of the wave behavior of the photoelectron, therefore it is required to transform the energy data to k-space or the wave number of the photoelectron ($\chi(k)$), referred to as the chi-function (Kelly et al., 2008).

In XAS analysis, an unknown sample spectra are compared to reference spectra with statistical analyses such as a linear combination fitting (LCF) or principle component analysis (PCA) to predict the mineralogical identification of the element (Beauchemin et al., 2002; Scheinost et al., 2002; Scheckel and Ryan, 2004). The results provide information on speciation

(chemical form or species) identifying its redox state and physicochemical characteristics that can be related to their bioavailability, thereby in conjunction with additional experiments, reactions of an element of interest under particular environment can be predicted (Miller et al., 2012).

The X-ray absorption spectroscopy (XAS) has been in use since 1970s in soil science, mineralogy, and geochemistry (Sayers et al., 1988). It is not very practical in soils due to its complexity; however it has been very useful in less complex system, or in crystallographic studies. Numerous studies have been done over the past two decades that had employed XAS to metal/metalloid adsorption complexation mechanisms at the soil or mineral/water interface, and has been proven to be very successful (sparks, 2003). A wide range of surface sorption processes have been investigated by this method, including surface precipitation (Chisholm-Brause et al., 1990), co-precipitation (Waychunas et al., 2003), surface redox reactions (Arai et al., 2003) and adsorption reactions (Randall, 1999). X-ray absorption spectroscopy has been used in many different studies to examine contaminants such as Pb in soils (Cotter-Howells et al., 1994, 1999; Ryan et al., 2001; Scheckel and Ryan, 2004). X-ray absorption spectroscopy is one of the only methods capable of providing direct molecular-scale speciation of Pb in natural geomedia. Several studies have employed XAS to probe Pb speciation in mine tailings (Ostergen et al., 1999; Brown et al., 1999; O-day et al., 1998). The particular importance of sorbed species in mine and smelter impacted soils has been highlighted (Morin et al., 1999). They revealed that most of the tailings were carbonate rich, and Pb was principally found in carbonate and sorbed phases (Ostergen et al., 1999; O'Day et al., 1998). In addition, Ostergen et al. (1999) used XAS techniques to quantitatively speciate Pb in three different types of mine tailings from Leadville, CO revealing dramatic variation in Pb speciation compared to chemical extraction, and more

conventional micro analytical techniques such as scanning electron microscopy and electron probe microanalysis, conducted in the laboratory. The importance of XAS technique has been emphasized by Scheckel (2004) especially for the amended soils where extractions are not very suitable unless supported by XAS data. There are several studies done in Zn speciation by using XAS technique (Manceau et al., 2000; Ford, and Sparks, 2000; Nachtegaal et al., 2005; and Voegelin et al., 2005). Nachtegaal et al. (2005) used XAS technique on smelter soils from Leadville, CO, and reported several slag-related Zn mineral phases, i.e. willemite, sphalerite, gahnite and hemimorphite, in the treated and non-treated soils by bulk and micro-focused EXAFS spectroscopy. Isaure et al. (2002) reported that the mentioned minerals were deposited on soil mainly by fall out from the chimney stack of the smelter, and sphalerite (ZnS) minerals as the remnants of the raw ore that by-passed the pyrometallurgical smelting process due to incomplete oxidation of ZnS (up to 20%), generating ZnS containing slags. They also revealed willemite (Zn_2SiO_4) as a high-temperature anhydrous silicate that originates from the smelting process. Likewise, hemimorphite ($Zn_4Si_2O_7(OH)2{\cdot}H2O$) and gahnite ($ZnAl_2O_4$) could have been formed in the smelting process.

For most systems the application of XRD, especially synchrotron based XRD and XAS technique in combination is complementary. The X-ray diffraction is one of the highly used techniques for characterizing abundant soil, which depends on long range ordering of atomic planes to probe crystalline structure at a length scale of approximately 50 Å or more. X-ray absorption spectroscopy probes the immediate environment of the selected element, within about 6 Å, and its theory and interpretation does not rely on any assumption of symmetry or periodicity. While both XRD and XAS can be used to determine distances between atoms, the information is derived from two very different X-ray interactions with the sample (Fendorf and Sparks, 1996).

Microarray Analysis

As soil sustains a huge diversity of microorganisms, of which about 99% is not cultureable. Using a culture-dependent technique would not be feasible to study the complex microbial community (Whitman, 1998). Owing to their extremely large diversity and their yet cultivable status microbial detection, quantification in the natural system is a great challenge especially on a large scale throughput (Fitter et al., 2005). There are several novel methods, most of which are based on rRNA and rDNA analyses and have been able to explore the soil microbial diversity to a larger extent; however, those techniques could be expensive based on the amount of data it provides, labor intensive and time-consuming. The next advancement in microbial ecology is to extract genomic, evolutionary and functional information from bacterial artificial chromosome libraries of the soil community genomes (metagenome), and sophisticated analyses that apply molecular phylogenetics, microarrays and *in situ* activity measurements. Microarray provides huge amounts of new data, potentially increasing our understanding that provide new insight into the relationship between phylogenetic and functional diversity (Torsvik et al., 2002; Sessitsch et al., 2006). Microarrays are miniaturized arrays of hundreds to thousands of discrete DNA fragments or synthetic oligonucleotides attached to a solid substrate such as glass or nylon membrane. Microarrays can be divided into two types; 1) DNA microarrays constructed with DNA fragments typically generated using polymerase chain reaction (PCR) (Schena et al., 1995), 2) oligonucleotides microarrays are constructed with shorter 10 to 120-mer sequence that are specified to be complementary to specific coding regions of interest. Oligonucleotides are often used in detecting mutation and polymorphisms whereas DNA microarray has wider applications. Microarrays are widely accepted functional genomics technology for large-scale genomic analysis (Schena et al., 1998; Schena, 2003). Recently, the potential research

applications of microarray technology to studies in microbial ecology have been explored (Zhou and Thompson, 2002; Zhou, 2003). GeoChip constructed with 50-mer oligonucleotides probes have evolved over several generations. GeoChip 4.2 relevant to this thesis work, is a functional gene array targeting 740 functional genes, and 95847 probes involved in the biogeochemical processes and functional activities of microbial communities important to human health, ecosystem management, agriculture, energy, global climate change, and environmental cleanup and restoration including N-, C-, S- and P- cycling, metal reduction and resistance, and organic contaminants degradation (Van Nostrand et al., 2011; Tu et al., 2014).

Microarray hybridization is based on the association of a single stranded molecule that is labeled with a fluorescent tag, with its complementary molecule, which is attached to the microarray slide. The specific gene profile is generated by an unknown experimental sample is compared with control (reference) pattern. The fluorescein labeled DNA in solution is considered as the target, and the DNA strand fixed on the microarray slide is referred as probes. Since the sequence of the arrayed molecule is usually known, it is used to investigate the unknown target molecule. The technical advancements have enabled microarray-based genomic technologies to revolutionized biological systems (Zhou et al., 1998). Adapting microarray technology in environmental samples hold several challenges in term of probe design, the coverage of gene sequences, specificity, sensitivity and quantitation (Wu et al., 2006). One of the greatest challenges in using FGAs for detecting functional genes and/or microorganisms in the environmental samples is to design oligonucleotide probes specific to the target genes/ microorganisms of interest as sequences of particular functional genes are highly homologous and/or incomplete (He et al., 2007), however GeoChip 4.0 has been considered as the most-comprehensive functional gene array to study the functional diversity, composition, structure and

dynamics of microbial communities, and to link their structure to environmental factors and ecosystem functioning (Tu et al., 2014). Several studies have been done to study the microbial community structure in the metal contaminated sites, and have observed the role of microbes in metal reduction (Brodie et al., 2003; He et al., 2007; Van Nostrand et al., 2009; 2011; Wu et al., 2012; Brodie et al., 2003). These studies have observed the microbial community structure changes with the role of SRBs in metal reduction.

Colloidal Bound Trace Element Mobilities

Colloidal material is defined as sub-micro meter mineral particle or bacterial cell that has at least one dimension between 1 nm and 1 μm, and are too small to withstand gravitational settings (Lead et al., 1997; Weber et al., 2009). Due to its higher surface area, and a large number of potentially reactive functional groups exposed to the solution, the colloidal fraction can sorb large fraction of trace components, and thereby act as a potential carrier of poorly soluble contaminants in the subsurface environment (Lead et al., 1997; Thompson et al., 2006; and Weber et al., 2009). Colloidal particles are mainly minerals with amphoteric surface (e.g. iron, aluminum and manganese oxides, carbonates) and fixed charge surfaces (phyllosilicates faces) including OM coatings on mineral phases and bacteria. The basic mechanism involved in association of contaminants with colloidal particles are surface complexation, ion exchange, and hydrophobic partitioning. Basically, abundance of colloidal particles, and their dispersion depends upon their characteristics at solid/liquid interfaces, which in turn depend on environmental variables such as pH, salinity, presence of other competitive and/or complexing cations or anions, temperature, bedrock geology/mineralogy, suspended particulate content and water velocity (Kretzschmar et al., 1999).

The fate of contaminants and eventually their impact on the groundwater quality depends on the nature, and behavior of potentially mobile colloids and their size, and connectivity of pores, and stability (De Jong et al., 2002). Colloids show tendency to remain in suspension due to their very small size, and surface charge characteristics, however their stability in suspension is determined by the solution chemistry, ionic strength, number of particles and their size distribution, and mixing conditions (Thompson et al., 2006). In fact, the above-mentioned factors that control the colloidal stability in suspension are themselves influenced by the dynamic shifts in redox status of the environment (Sposito, 2004). Changing redox status has a strong impact on Fe chemistry; therefore, the interaction of Fe redox processes with colloidal chemistry is complex. This complexity is further accentuated by the fact that soil microbes catalyze at least the reduction portion of the Fe redox cycle. Thus, concentrations of electron donors, electron acceptors and microbial population dynamics significantly influence colloidal stability in soils through biogeochemical pathways (Lovely et al., 2004).

Colloidal assisted transport has been commonly observed in river basins, and flood plains (Voegelin et al., 2007), however it has hardly been studied in reduced environment (Weber et al., 2009). In SO_4^{2-} rich environment, it is traditionally assumed that metals are effectively immobilized by getting sequestered in metal sulfides under reduced conditions (Kirk, 2004). The newly precipitated colloidal metal sulfide clusters are highly resistant to oxidation and may significantly enhance the metal mobility under reduced conditions (Luther et al., 2005; Borch et al., 2009). Copper-rich sulfide colloids or in template with bacterial membrane were reported to contribute in Cu, Pb and Cd mobilization in rivers under periodic SO_4^{2-} reducing environment (Weber et al., 2009). In addition, there are column studies that reported dispersion of mercury sulfide from mine tailings indicating sulfide colloids can also be mobile in porous media (Lowry

et al., 2004). Repeated cycling between Fe reduction and oxidation have a cumulative impact on colloidal stability as well. Reduction of ferric oxides under suboxic conditions can promote colloid dispersion by dissolving Fe-oxide cements that hold aggregates together (Thompson et al., 2006; Banfield, 2004; Elimelech et al., 2002).

Moreover, bacteria can also dramatically accelerate the transport of heavy metals in groundwater. Šimůnek et al. (2006) conducted both batch and column experiments to investigate adsorption of cadmium (Cd) onto *Bacillus subtilis* spores or *Escherichia coli* vegetative cells and Cd transport in alluvial gravel aquifer media in the presence of these bacteria and they have found that Cd traveled 17 to 20 times faster when it traveled with mobile bacteria.

Role of Microbes

Microorganisms are ubiquitous in every habitable environment on earth. They are provided with metabolic processes that exclusively affects chemistry, and physical properties of surroundings (Newman, 2002). Microbes have changed the universe in several different ways. They have altered the chemistry of the atmosphere via photosynthesis, nitrogen fixation, carbon sequestration. They have changed the composition of oceans, rivers, and pore fluids via control of mineral weathering rates, and/ or by inducing mineral precipitation. An alteration of chemical speciation, and mobilities of almost all the elements (Falkowski et al., 2008) in soil, and sediments have been possible by releasing complexing agents and by catalyzing redox reactions enzymatically. In addition microbes have help sustain higher trophic level organisms via primary production, and remineralizing OC even under extreme environments (Newman, 2002). All the microbial metabolic processes that are evolved to perform those functions are the fundamental component of biogeochemical cycles (Gadd, 2002). The microbial ability to effect and/or mediate mobilization or immobilization processes depends upon their ability to influence metal

distribution among soluble and insoluble phases (McLean et al., 2002). Most of the metal-microbes interactions have been studied as means for contaminant removal, immobilization, and detoxification of metal or radionuclide pollutants (Eccles, 1999). Therefore, microbiological processes have potential applications in bioremediation. The chemistry of life, however, is based on redox reactions, i.e., successive transfers of electrons and protons from a relatively limited set of chemical elements (Williams et al., 1996).

Microbially mediated mobilization and immobilization of trace elements

The microbially mediated mobilization of metals are possible via the metabolic processes; autotrophic and heterotrophic leaching, chelation by microbial metabolites and siderophores, and methylation that may result in volatilization process. All the mentioned processes can cause dissolution of insoluble metal compounds and minerals, including oxides, phosphates, sulfides and more complex mineral ores, and desorption of metal species from exchange sites on, e.g., clay minerals or OM in the soil resulting in mobility of metals in the environment. The heterotrophic leaching often occurs when microorganisms acidify their environment by proton efflux through plasma membrane H^+-ATPases in order to maintain charge balance, or may occur as a result of respiratory carbon dioxide accumulation. With acidification, metals are released via competition between protons and the metal in a metal-anion complex or in sorbed form, efflux of organic acids and siderophores. Microbially mediated mobilization have been effectively used in leaching of a variety of wastes and low-grade minerals, soils and muds, filter dust/oxides, lateritic ores, copper converter slag, fly ash and electronic waste materials (Gadd, 2002). The most autotrophic-leaching of metals is carried out by chemolithotrophic, acidophilic bacteria. They fix carbon dioxide and obtain energy from the oxidation of Fe(II) or reduced S compounds resulting in the solubilization of metals (Schippers et

al., 1999). Leaching of metals sulfides by using *Thiobacillus species* and other acidophilic bacteria is well established for industrial scale bio-mining (Rawlings, 1999).

Microbially mediated metals immobilization help metals to be transformed into insoluble, and chemically stable, therefore, it can be employed in bioremediation to minimize their spread, and leaching to groundwater. The main drivers of metal immobilization are redox reactions coupled with precipitations and sorption by microorganisms, organic substrate, and Fe hydroxides. The mechanisms through which metal immobilizations occur are: biosorption, metal precipitation by sulfate reduction, redox transformation, methylation, and plant-microbe interaction (Kosolapov et al., 2004).

Metal precipitation is one of the significant processes involved in the long term retention of metals in artificial and natural wetlands. Such processes may be accompanied by other indirect reductive metal precipitation method which includes dissimilatory sulfate reduction and the subsequent precipitation of metal sulfides (Finneran et al., 2002). Since metal sulfides are more resistant to oxidation. Even less to moderate sulfide formations can help bring contamination to the permissible level as solubility is very low.

Dissimilatory sulfate reduction also help form FeS and FeS_2, among which the systems with FeS_2 formation are more resistant to solubilization of metals (Huerta-Diaz et al., 1998). There are several studies reporting dissimilatory sulfate reduction as a major mechanism in immobilizing metals. The natural communities of sulfur reducing bacteria (SRB) generated ZnS deposits from dilute groundwater solutions supporting biogenic form of many low-temperature metal sulfide formations (Labrenz et al., 2000). In addition, recent evidence indicates that hyperthermophillic and mesophilic dissimilatory Fe(III)-reducing bacteria and archaea can precipitate Au^0 via oxidation of hydrogen to reduce Au^{3+}. Similarly, hyperthermophillic

microorganisms can reduce metals leading to the formation of magnetite (Fe_3O_4) and uraninite (UO_2) ore deposits at ~100 °C in coupled with oxidation of hydrogen or organics (Kashefi et al., 2001). Similarly, uranium ((U(VI)) can be reduced to U(IV) by certain Fe(III) reducing bacteria such as *Geobacter metallireducens* (Finnerman et al., 2002). Vanadium (V) has been shown to be reduced to blue colored V(IV), and then to black colored V(III), reduction of Hg^{2+} to less toxic Hg^0 (Kosolapov, 2004; Wiatrowski, 2006), and reduction of Cr(VI) to Cr(IV), and Cr(III) has been reported via dissimilatory sulfate reduction by SRBs; *Desulfovibrio desulfuricans* that is also reported in reduction of toxic Pd(II) to Pd(0). Sulfur reducing bacteria biofilm reactors are reported to entrap or precipitate metals such as Cd and Cu (White, and Gadd, 2000). In addition, oxidation of Fe(II), and Mn(II) is another mechanism that is common in bioremediation, oxidation of reduced Fe and Mn are driven by both abiotic reaction forming Fe(III), which is further precipitated as Fe (oxy)hydroxides. This mechanism is very common in metal contaminated environments such as acid mine drainage, tailings piles, drainage pipes, sediments, bogs, and plant rhizosphere. The precipitated hydroxides of Fe, and Mn can strongly absorb other heavy metals such as Cu, Ni, Pb, Co, Cr, and others playing significant role in bioremediation (Gadd, 2004).

Effect of heavy metal contamination on microbial community structure

It is well known that microbes can grow under extreme environments (Gadd, 2002); however, the long term exposure to a complex mixture of hydrocarbons (HCs) and/or heavy metals may be challenging to maintain diversified community structure, and microbial function, which is often crucial for any application of remediation strategies. Studies have shown that microbial community structure changes with long term exposure to contaminants depending upon the concentration of contaminants (Shi et al., 2005). The influence of soil heavy metals

pollution on soil microbial biomass, enzyme activity, and community composition near a copper smelter soil was also observed by Wang et al. (2007).

Sulfate reducing bacteria

Sulfate-reducing bacteria (SRB) may be one of the primitive forms of life on earth that can be traced back billions of years in the geologic rock record when oxygen concentrations in earth's atmosphere were low. The SRBs left their first mark on their environment in pyrite minerals (FeS_2) as old as 3400 million years (Ohmoto et al., 1993). Presently SRBs are ubiquitous in both marine and terrestrial environments. Provided by the ability to adapt to extreme physical and chemical conditions, they have very significant role in biogeochemical cycles. Their role in ore deposits formation have been proven by Labrenz et al. (2000). Their study showed the SRBs that can form ZnS mineral precipitate under very low oxygen environment. In addition, several studies have reported that SRBs are active in acidic sulfide-rich mine tailings and sediments impacted by mining activities; however, it varies under fluctuating in situ physico-chemical conditions. There is a strong correlation between C and S cycle due to microbial metabolisms, therefore, S cycle is highly influenced by SRBs activities (Schidlowski et al., 1983). There is a lack of information regarding the activity of SRB in more neutral pH sulfide-rich mine tailings despite the fact that these represent very favorable conditions (in terms of pH) for bacterial growth. Dissimilatory sulfate-reducing bacteria use sulfate mainly as an electron acceptor in the anaerobic oxidation of inorganic or organic substrates such as $H_2 + CO_2$, lactate, acetate, and propionate accumulating a large amount of sulfide. Further, the large amount of sulfide ions combine with available metal ions to form insoluble products resulting in the production and transformation of natural mineral deposits (Vasconcelos et al., 2000). Thus, the role played by sulfate-reducing bacteria in natural

processes is undoubtedly very important under anoxic or oxygen-free conditions. The role of SRBs has been successfully used in bioremediation of contaminated groundwater and soils. Both microbially mediated Fe and SO_4^{2-} reduction are being investigated as potential processes that are capable of combating acidity and promoting contaminant metal precipitation in mining environments (Sen and Johnson, 1999, Wendt-Potthoff et al., 2002; Winch et al., 2008b).

References

Adriano, D. C. 2001. Trace elements in terrestrial environments: Biogeochemistry, bioavailability, and risks of metals. Springer- Verlag, New York.

Arai, Y.; Lanzirotti, A.; Sutton, S.; Davis, J. A.; Sparks, D. L. 2003. Arsenic speciation and reactivity in poultry litter. Environmental Science and Technology. 37:4083-4090.

Agency for Toxic Substances and Disease Registry (ATSDR). 2005. Toxicological profile for Zinc. Atlanta, GA: U.S. Department of Health and Human Services, Public Health Service.

Agency for Toxic Substances and Disease Registry (ATSDR). (2007). Toxicological profile for Lead (Update). Atlanta, GA: Department of Health and Human Services, Public Health Service.

Agency for Toxic Substances and Disease Registry (ATSDR). 2012. Toxicological profile for Cadmium. Atlanta, GA: Department of Health and Human Services, Public Health Service.

Beyer, W., Dalgarn, J., Dudding, S., French, J., Mateo, R., and Miesner, J. 2004. Zinc and lead poisoning in wild birds in the Tri-State mining district (Oklahoma, Kansas, and Missouri). Archives of Environmental Contamination and Toxicology. 48:108-117.

Borch, T., Kretzschmar, R., Kappler, A., Cappellen, P. V., Ginder-Vogel, M., and Voegelin, A. 2009. Biogeochemical redox processes and their impact on contaminant dynamics. Environmental Science and Technology. 44:15-23.

Brodie, E. L., Desantis, T. Z., Joyner, D. C., Baek, S. M., Larsen, J. T., Andersen, G. L. 2006. Application of a high-density oligonucleotide microarray approach to study bacterial population dynamics during uranium reduction and reoxidation. Applied and Environmental Microbiology. 72:6288-6298.

Centers for Disease Control and Prevention (CDC). 2012. Fourth National Report on Human Exposure to Environmental Chemicals. Updated Tables. http://www.cdc.gov/exposurereport/.

Chaney, R. L., Malik, M., Li, Y. M., Brown, S. L., Brewer, E. P., and Angle, J. S. 1997. Phytoremediation of soil metals. Current Opinion in Biotechnology. 8:279-284.

Clemente, J. S., and Fedorak, P. M. 2005. A review of the occurrence, analyses, toxicity, and biodegradation of naphthenic acids. Chemosphere. 60:585-600.

Cunningham, S., Shann, J., Crowley, D. E., and Anderson, T. A. 1997. Phytoremediation of contaminated water and soil. ACS Symposium Series. 664:2-19.

Clark, M. W., McConchie, D., Lewis, D., and Saenger, P. 1998. Redox stratification and heavy metal partitioning in Avicennia-dominated mangrove sediments: A geochemical model. Chemical Geology. 149:147-171.

De Jong, L. W., Moldrup, P, and Jacobsen, O. H. 2002. International workshop on colloids and colloidal facilitated transport of contaminants in soils and sediments, Sept. 19–20, Tjele, Denmark, 2002. DIAS Report, Plant production, vol. 80.

Du Laing, G., Rinklebe, J., Vandecasteele, B., Meers, E., and Tack, F. 2009. Trace metal behaviour in estuarine and riverine floodplain soils and sediments: A review. Science of the Total Environment. 407:3972-3985.

Eccles, H. 1999. Treatment of metal contaminated waste : why select a biological process ? Metal accumulation in intertidal marshes : Role of sulphide precipitation. Wetlands, 28:735-746.

Edwards, K. J., Bond, P. L., Druschel, G. K., McGuire, M. M., Hamers, R. J., and Banfield, J. F. 2000. Geochemical and biological aspects of sulfide mineral dissolution: Lessons from iron mountain, California. Chemical Geology. 169:383-397.

Elimelech M, and Ryan, J. N. 2002. In: Huang PM Bollag J-M, Senesi Nicola, editors. Interactions between soil particles and microorganisms: impact on the terrestrial ecosystem. New York' John Wiley and Sons.

Essington, M. E. 2004. Soil and water chemistry: an integrative approach. CRC press, 2004.

Falkowski, P. G., Fenchel, T., and Delong, E. F. 2008. The microbial engines that drive earth's biogeochemical cycles. Science (New York, N.Y.). 320:1034-1039.

Fendorf, S. E., and Li, G. 1996. Kinetics of chromate reduction by ferrous iron. Environmental Science and Technology. 30:1614-1617.

Fitter, A., Gilligan, C., Hollingworth, K., Kleczkowski, A., Twyman, R., and Pitchford, J. 2005. Biodiversity and ecosystem function in soil. Functional Ecology. 19:369-377.

Fendorf, S., Wielinga, B. W., and Hansel, C. M. 2000. Chromium transformations in natural environments: The role of biological and abiological processes in chromium (VI) reduction. International Geology Review. 42:691-701.

Finneran, K. T., Anderson, R. T., Nevin, K. P., and Lovley, D. R. 2002. Potential for bioremediation of uranium-contaminated aquifers with microbial U (VI) reduction. Soil and Sediment Contamination: An International Journal. 11:339-357.

Fosmire, G. J. 1990. Zinc toxicity. American Journal of Clinical Nutrition. 51:225-227.

Fuhrman, J. A. 2009. Microbial community structure and its functional implications. Nature. 459:193-199.

Habicht, K. S., and Canfield, D. E. 2001. Isotope fractionation by sulfate-reducing natural populations and the isotopic composition of sulfide in marine sediments. Geology. 29:555-558.

Hettiarachchi, G. M., and Pierzynski, G. M. 2002. In situ stabilization of soil lead using phosphorus and manganese oxide. Journal of Environmental Quality. 31:564-572.

Hettiarachchi, G., Pierzynski, G., and Ransom, M. 2001. In situ stabilization of soil lead using phosphorus. Journal of Environmental Quality. 30:1214-1221.

Huerta-Diaz, M. A., Tessier, A., and Carignan, R. 1998. Geochemistry of trace metals associated with reduced sulfur in freshwater sediments. Applied Geochemistry. 13:213-233.

Gadd, G. M., Sayer, J. A. 2000. Fungal transformations of metals and metalloids. Geochemistry In: Lovley, D. R. (Ed.), Environmental Microbe–Metal Interactions. Am. Soc. Microbiol, Washington. p. 237-256.

Gadd, G. M. 2002. Interactions between microorganisms and metals/radionuclides: the basis of bioremediation. In: Keith-Roach, M. J., Livens, F. R. (Eds.), Interactions of Microorganisms with Radionuclides. Elsevier, Amsterdam. p. 179-203.

Gadd, G. M. 2004. Microbial influence on metal mobility and application for bioremediation. Geoderma. 122:109-119.

Gadd, G. M. 2010. Metals, minerals and microbes: Geomicrobiology and bioremediation. Microbiology (Reading, England). 156:609-643.

Gray, C. W., Dunham, S. J., Dennis, P. G., Zhao, F. J., and McGrath, S. P. 2006. Field evaluation of in situ remediation of heavy metal contaminated soil using lime and red-mud. Environmental Pollution. 142:530-539.

Griffiths, B., Ritz, K., Ebblewhite, N., and Dobson, G. 1998. Soil microbial community structure effects of substrate loading rates. Soil Biology and Biochemistry. 31:145-153.

He, Z., Gentry, T. J., Schadt, C. W., Wu, L., Liebich, J., and Chong, S. C. 2007. GeoChip: A comprehensive microarray for investigating biogeochemical, ecological and environmental processes. The ISME Journal. 1:67-77.

Hettiarachchi, G. M., G. M. Pierzynski, G. M., and Ransom, M.D. 2001. In situ stabilization of soil lead using phosphorus. Journal of Environmental quality. 30:1214-1221.

Hettiarachchi, G. M., and Pierzynski, G.M. 2002. Insitu stabilization of soil lead using phosphorus and manganese oxide: Influence on plant growth. Journal of Environmental quality. 31:564-572.

Hsiang, Jack, and Elva Díaz. 2011. Lead and developmental neurotoxicity of the central nervous system. Current Neurobiology. 2:35-42.

Johnson, D. B., and Hallberg, K. B. 2005. Acid mine drainage remediation options: A review. Science of the Total Environment. 338:3-14.

Kansas Geological Survey (KGS). 2001. Public outreach. http://www.kgs.ku.edu/Publications/pic17/pic17_2.html

Kashefi, K., Tor, J. M., Nevin, K. P., and Lovley, D. R. 2001. Applied Environmental Microbiology. 67:3275-3279.

Kelly, S. D., Hesterberg, D., and Ravel, B. 2008. In (Ed.), Analysis of soils and minerals using X-ray absorption spectroscopy in methods of soil analysis, part 5- mineralogical methods (A. L. Ulery and L. R. Drees.

Isaure, M., Laboudigue, A., Manceau, A., Sarret, G., Tiffreau, C., and Trocellier, P. 2002. Quantitative Zn speciation in a contaminated dredged sediment by μ-PIXE, μ-SXRF, EXAFS spectroscopy and principal component analysis. Geochimica Et Cosmochimica Acta. 66:1549-1567.

Kadlec, R., and Knight, R. 1996. Treatment wetlands, Lewis, Boca Raton, 893.

Kirk, G. 2004. The biogeochemistry of submerged soils. John Wiley and Sons, Chichester.

Kleypas, J. A., Buddemeier, R. W., Archer, D., Gattuso, J. P., Langdon, C., and Opdyke, B. N. 1999. Geochemical consequences of increased atmospheric carbon dioxide on coral reefs. Science (New York, N.Y.). 284:118-120.

Kosolapov, D., Kuschk, P., Vainshtein, M., Vatsourina, A., Wiessner, A., and Kästner, M. 2004. Microbial processes of heavy metal removal from Carbon-Deficient effluents in constructed wetlands. Engineering in Life Sciences. 4:403-411.

Kretzschmar, R.; Borkovec, M.; Grolimund, D.; and Elimelech, M. 1999. Mobile subsurface colloids and their role in contaminant transport. Advances in Agronomy. 66:121-193.

Kleikemper, J., Schroth, M. H., Sigler, W. V., Schmucki, M., Bernasconi, S. M., and Zeyer, J. 2002. Activity and diversity of sulfate-reducing bacteria in a petroleum hydrocarbon-contaminated aquifer. Applied and Environmental Microbiology. 68:1516-1523.

Kosolapov, D., Kuschk, P., Vainshtein, M., Vatsourina, A., Wiessner, A., Kästner, M. 2004. Microbial processes of heavy metal removal from Carbon-Deficient effluents in constructed wetlands. Engineering in Life Sciences. 4:403-411.

Labrenz, M., and Banfield, J. 2004. Sulfate-reducing bacteria-dominated biofilms that precipitate ZnS in a subsurface circumneutral-pH mine drainage system. Microbial Ecology. 47:205-217.

Lal, R. 1999. Global carbon pools and fluxes and the impact of agricultural intensification and judicious land use. In prevention of land degradation, enhancement of carbon sequestration, and conservation of biodiversity through land use change and sustainable land management with a focus on Latin America and the Caribbean. World Soil Resources Report, FAO, Rome, Italy. 86:45-52.

Lead, J., Hamilton-Taylor, J., Davison, W., and Harper, M. 1999. Trace metal sorption by natural particles and coarse colloids. Geochimica Et Cosmochimica Acta. 63:1661-1670.

Le Peltier, F., Didillon, B., Jumas, J., and Olivier-Fourcade, J. 2003. Supported bimetallic catalyst with a strong interaction between a group viii metal and tin, and its use in a catalytic reforming process.

Lindsay, W. L. 1979. Chemical equilibria in soils. Wiley, New York, NY.

Lothenbach, B., Krebs, R., Furrer, G., Gupta, S. K., and Schulin, R. (1998). Immobilization of cadmium and zinc by Al- montmorillinite and gravel sludge. European Journal of Soil Science. 49:141-148.

Long, X., Yang, X., and Ni, W. 2002. Current situation and prospect on the remediation of soils contaminated by heavy metals. The Journal of Applied Ecology. 13:757-762.

Lothenbach, B., Krebs, R., Furrer, G., Gupta, S., and Schulin, R. 1998. Immobilization of cadmium and zinc in soil by Al-montmorillonite and gravel sludge. European Journal of Soil Science. 49:141-148.

Lovley, D. R. 1995. Bioremediation of organic and metal contaminants with dissimilatory metal reduction. Journal of Industrial Microbiology. 18:161-195.

Lovley, D. R., Holmes, D. E., and Nevin, K. P. 2004. Dissimilatory Fe(III) and Mn(IV) reduction. Journal of Industrial Microbiology. 14:85-93.

Lowry, G. V., Shaw, S., Kim, C. S., Rytuba, J. J., and Brown, G. E. Jr. 2004. Macroscopic and microscopic observations of particle-facilitated mercury transport from New Idria and Sulphur Bank mercury mine tailings. Environmental Science and Technology. 38:5101-5111.

Lu, Z., Deng, Y., Van Nostrand, J. D., He, Z., Voordeckers, J., Zhou, A. 2012. Microbial gene functions enriched in the deepwater horizon deep-sea oil plume. The ISME Journal. 6: 451-460.

Luther III, G. W., and Rickard, D. T. 2005. Metal sulfide cluster complexes and their biogeochemical importance in the environment. Journal of Nanoparticle Research. 7: 389-407.

Machemer, S. D., and Wildeman, T. R. 1992. Adsorption compared with sulfide precipitation as metal removal processes from acid mine drainage in a constructed wetland. Journal of Contaminant Hydrology. 9:115-131.

Marchand, L., Mench, M., Jacob, D., and Otte, M. 2010. Metal and metalloid removal in constructed wetlands, with emphasis on the importance of plants and standardized measurements: A review. Environmental Pollution. 158:3447-3461.

Mays, P., and Edwards, G. 2001. Comparison of heavy metal accumulation in a natural wetland and constructed wetlands receiving acid mine drainage. Ecological Engineering. 16:487-500.

Mendie, U. 2005. The nature of water. The Theory and Practice of Clean Water Production for Domestic and Industrial use.Lagos: Lacto-Medals Publishers. p. 1-21.

Morgan, E. 1988. Membrane transport of non-transferrin-bound iron by reticulocytes. Biochimica Et Biophysica Acta (BBA)-Biomembranes. 943: 428-439.

Murray-Gulde, C. L., Bearr, J., and Rodgers, J. H. 2005. Evaluation of a constructed wetland treatment system specifically designed to decrease bioavailable copper in a wastestream. Ecotoxicology and Environmental Safety. 61:60-73.

McLean, E. J., Robinson, R. I., Teat, S. J., Wilson, C., and Woodward, S. 2002. Transformation of sulfur dioxide to sulfate at a palladium centre. Journal of the Chemical Society, Dalton Transactions. 18:3518-3524.

McLean, L., Pray, T., Onstott, T., Brodie, E., Hazen, T., and Southam, G. 2007. Mineralogical, chemical and biological characterization of an anaerobic biofilm collected from a borehole in a deep gold mine in South Africa. Geomicrobiology Journal. 24:491-504.

Manahan, S. E. 2004. Environmental chemistry. CRC press.

Manceau, A., Schlegel, M., Musso, M., Sole, V., Gauthier, C., Petit, P. 2000. Crystal chemistry of trace elements in natural and synthetic goethite. Geochimica Et Cosmochimica Acta. 64: 3643-3661.

Martin, T., Oswald, O., and Graham, I. A. 2002. Arabidopsis seedling growth, storage lipid mobilization, and photosynthetic gene expression are regulated by carbon: Nitrogen availability. Plant Physiology. 128:472-481.

McMahon, P. B., Dennehy, K. F., Bruce, B. W., Gurdak, J. J., and Qi, S. L.(2007. Water-quality assessment of the high plains aquifer, 1999-2004 US Department of the Interior, US Geological Survey.

Morin, G, Ostergren, J. D., Juillot, F., Ildefonse, P., Calas G, and Brown, G. E. 1999. XAFS determination of the chemical form of lead in smelter-contaminated soils and mine tailings: Importance of adsorption processes. Am. Mineral. 84:420-434.

Mulligan, C. N, Yong, R. N., and Gibbs, B. F. 2001. Remediation technologies for metal-contaminated soils and groundwater: an evaluation Engineering Geology. 60:197-201.

Muyzer, G., and Stams, A. J. 2008. The ecology and biotechnology of sulphate-reducing bacteria. Nature Reviews Microbiology. 6:441-454.

Nachtegaal, M., and Sparks, D. L. 2004. Effect of iron oxide coatings on zinc sorption mechanisms at the mineral/water interface. J. Colloid Interface Science. p. 276.

Nachtegaal, M., Marcus, M., Sonke, J., Vangronsveld, J., Livi, K., van Der Lelie, D. 2005. Effects of in situ remediation on the speciation and bioavailability of zinc in a smelter contaminated soil. Geochimica Et Cosmochimica Acta. 69:4649-4664.

Newman, D. K., and Banfield, J. F. 2002. Geomicrobiology: How molecular-scale interactions underpin biogeochemical systems. Science (New York, N.Y.). 296:1071-1077.

Nriagu, J.O. 1984. Formation and stability of base metal phosphates in soils and sediments. In J.O. Nriagu and P. B. Moore (eds.) Phosphate Minerals. Springer-Verlag, Berlin, Germany.

O'Day, P. A., Carroll, S. A., and Waychunas, G. A. 1998. Rock-water interactions controlling zinc, cadmium, and lead concentrations in surface waters and sediments, US Tri-State mining district. 1. Molecular identification using X-ray absorption spectroscopy. Environmental Science Technology. 32:943-955.

Ostergren, J. D., Brown, G. E., Parks, G. A., and Tingle, T. N. 1999. Quantitative speciation of lead in selected minetailings from leadville, co. Environmental Science and Technology. 33:1627-1636.

Pérez-Guzmán, L., Bogner, K., and Lower, B. 2012. Earth's ferrous wheel. Nature Education Knowledge. 3-32.

Pérez-López, R., Nieto, J. M., López-Cascajosa, M. J., Díaz-Blanco, M. J., Sarmiento, A. M., and Oliveira, V. 2011. Evaluation of heavy metals and arsenic speciation discharged by the industrial activity on the tinto-odiel estuary, SW Spain. Marine Pollution Bulletin. 62:405-411.

Pierzynski, G. M., and Vaillant, G. C. 2006. Remediation to reduce ecological risk from trace element contamination: A decision case study. Journal of Natural Resources and Life Sciences Education. 35:85-94.

Pierzynski, G. M., and Gehl, K. A. 2004. An alternative method for remediating lead-contaminated soils in residential areas: A decision case study. Journal of Natural Resources and Life Sciences Education. 33:63-69.

Pivetz, B. E. 2001. Phytoremediation of contaminated soil and groundwater at hazardous waste sites United States Environmental Protection Agency, Office of Research and Development, Office of Solid Waste and Emergency Response: Superfund Technology Support Center for Ground Water, National Risk Management Research Laboratory.

Plekhanova, I., and Bambusheva, V. 2010. Extraction methods for studying the fractional composition of heavy metals in soils and their comparative assessment. Eurasian Soil Science. 43:1004-1010.

Plum, L. M., Rink, L., and Haase, H. 2010. The essential toxin: Impact of zinc on human health. International Journal of Environmental Research and Public Health. 7:1342-1365.

Ponnamperuma, F. 1972. The chemistry of submerged soils Academic Press NY and London.

Prietzel, J., Thieme, J., Eusterhues, K., and Eichert, D. 2007. Iron speciation in soils and soil aggregates by synchrotron-based X-ray microspectroscopy (XANES -XANES).

Pope, L. M. 2005. Assessment of contaminated stream bed sediment in the Kansas part of the historic Tri-State lead and zinc mining district, Cherokee County, USGS Scientific Investigations Report. p. 5251.

Randall, S. R., Sherman, D. M., Ragnarsdottir, K. V., and Collins, C. R. 1999. The mechanism of cadmium surface complexation on iron oxyhydroxide minerals Geochimica Et Cosmochimica Acta. 63:2971-2987.

Ravel, A., and Newville, M. 2005. Athena, Artemis, Hephaestus: Data analysis for X-ray absorption spectroscopy using IFEFFIT. Journal of Synchrotron Radiation. 12:537-541.

Rehr, J. J., and Albers, R. C. 2000. Theoretical approaches to X-ray absorption fine structure. Rev. Mod. Phys. 72:621-654.

Ruby, M. V., Davis, A. and Nicholson, A. 1994. In situ formation of lead phosphates as a method to immobilize lead. Environmental Science and Technology. 28:646-654.

Ruby, M. V. 2004. Bioavailability of soil-borne chemicals: Abiotic assessment tools. Human and Ecological Risk Assessment. 10:647-656.

Ryan, J. A., Zhang, P., Hesterberg, D., Chou, J., and Sayers, D. E. 2001. Formation of chloropyromorphite in a lead-contaminated soil amended with hydroxyapatite. Environmental Science and Technology. 35:3798-3803.

Salt, D. E., Blaylock, M., Kumar, N. P., Dushenkov, V., Ensley, B. D., and Chet, I. 1995. Phytoremediation: A novel strategy for the removal of toxic metals from the environment using plants. Nature Biotechnology. 13:468-474.

Scheckel, K. G., and Ryan, J. A. 2004. Spectroscopic speciation and quantification of lead in phosphate-amended soils. Journal of Environmental Quality. 33:1288-1295.

Scheckel, K. G., and Ryan, J. A. 2002. Effects of aging and pH on dissolution kinetics and stability of chloropyromorphite. Environmental Science and Technology. 36:2198-2204.

Shi, W., Becker, J., Bischoff, M., Turco, R. F. and Konopka, A. E. 2002. Association of microbial community composition and activity with lead, chromium, and hydrocarbon contamination. Applied Environmental. Microbiology. 68:3859-3866.

Schreier, C. G., and Reinhard, M. 1994. Transformation of chlorinated organic compounds by iron and manganese powders in buffered water and in landfill leachate, Chemosphere. 29:1743-1753.

Schaider, L. A., Senn, D. B., Brabander, D. J., McCarthy, K. D., and Shine, J. P. 2007. Characterization of zinc, lead, and cadmium in minewaste: Implications for transport, exposure, and bioavailability. Environmental Science and Technology. 41:4164-4171.

Sessitsch, A., Hackl, E., Wenzl, P., Kilian, A., Kostic, T., and Stralis-Pavese, N. 2006. Diagnostic microbial microarrays in soil ecology. New Phytologist. 171:719-736.

Šimůnek, J., He, C., Pang, L., and Bradford, S. 2006. Colloid-facilitated solute transport in variably saturated porous media. Vadose Zone Journal. 5:1035-1047.

Sparks, D. L., Page, A. L., Helmke, P. A., Loeppert, R. H., Soltanpour, P. N., and Tabatabai, M. A. 1996. Methods of soil analysis Part 3-{Chemical} methods. Publisher and source.

Sparks, D. L. 2003. Environmental soil chemistry. 2nd ed. Academic Press, San Diego, CA.

Sposito, G., Barry, D., and Kabala, Z. 1991. Stochastic differential equations in the theory of solute transport through inhomogeneous porous media. Advance Porous Media. 1:295-309.

Stein, O. R., Borden-Stewart, D. J., Hook, P. B., and Jones, W. L. 2007. Seasonal influence on sulfate reduction and zinc sequestration in subsurface treatment wetlands. Water Research. 41:3440-3448.

Stern, E. A., and Heald, S. M. 1979 X-ray filter assembly for fluorescence measurements of X-ray absorption file structure. Rev. Science Instrum. 50:1579-1583.

Thompson, A., Chadwick, O. A., Rancourt, D. G., and Chorover, J. 2006. Iron-oxide crystallinity increases during soil redox oscillations. Geochimica Et Cosmochimica Acta. 70:1710-1727.

Toevs, G. R., Morra, M. J., Polizzotto, M. L., Strawn, D. G., Bostick, B. C., and Fendorf, S. 2006. Metal (loid) diagenesis in mine-impacted sediments of lake coeur d'alene, idaho. Environmental Science and Technology. 40:2537-2543.

Torsvik, V., and Øvreås, L. 2002. Microbial diversity and function in soil: From genes to ecosystems. Current Opinion in Microbiology. 5:240-245.

Tu, Q., Yu, H., He, Z., Deng, Y., Wu, L., and Nostrand, J. D. 2014. GeoChip 4: A functional gene-array-based high-throughput environmental technology for microbial community analysis. Molecular Ecology Resources. 14:914-928.

U.S. EPA. 1993. Subsurface flow constructed wetlands for wastewater treatment. Environmental Protection Agency Report EPA 832-R-93-008.

U.S. EPA. 1997. EPA Superfund Record of Decision: Cherokee County, Kansas. U. S. Environmental Protection Agency Report EPA/ROD/R0797/073.

Vallee, B. L., and Falchuk, K. H. 1993. The biochemical basis of zinc physiology. Physiol. Rev. p. 79-118.

Van Nostrand, J. D., Wu, W., Wu, L., Deng, Y., Carley, J., and Carroll, S. 2009. GeoChip-based analysis of functional microbial communities during the reoxidation of a bioreduced uranium-contaminated aquifer. Environmental Microbiology. 11:2611-2626.

Van Nostrand, J. D., Wu, L., Wu, W. M., Huang, Z., Gentry, T. J., and Deng, Y. 2011. Dynamics of microbial community composition and function during in situ bioremediation of a uranium-contaminated aquifer. Applied and Environmental Microbiology. 77:3860-3869.

Vega, F. A., Covelo, E. F., and Andrade, M. 2006. Competitive sorption and desorption of heavy metals in mine soils: Influence of mine soil characteristics. Journal of Colloid and Interface Science. 298:582-592.

Wan, J., Tokunaga, T. K., Brodie, E., Wang, Z., Zheng, Z., and Herman, D. 2005. Reoxidation of bioreduced uranium under reducing conditions. Environmental Science and Technology. 39:6162-6169.

Wang, Y., Shi, J., Wang, H., Lin, Q., Chen, X., and Chen, Y. 2007. The influence of soil heavy metals pollution on soil microbial biomass, enzyme activity, and community composition near a copper smelter. Ecotoxicology and Environmental Safety. 67:75-81.

Waychunas, G. A., Rehr, J. J., and Fuller, C. C, and Davis, J. A. 2003. Surface complexation and precipitate geometry for aqueous Zn (II) sorption on ferrihydrite: {II}. XANES analysis and simulation: Geochimica et Cosmochimica Acta. 67:1,031-1,043.

Weber, F., Voegelin, A., Kaegi, R., and Kretzschmar, R. 2009. Contaminant mobilization by metallic copper and metal sulphide colloids in flooded soil. Nature Geoscience. 2:267-271.

White, C., and Gadd, G. 2000. Copper accumulation by sulfate-reducing bacterial biofilms. FEMS Microbiology Letters. 183:313-318.

Woulds, C., and Ngwenya, B. T. 2004. Geochemical processes governing the performance of a constructed wetland treating acid mine drainage, central Scotland. Applied Geochemistry. 19:1773-1783.

Wu, L. 2001. Development and evaluation of functional gene arrays for detection of selected genes in the environment. Applied Environmental. Microbiology. 67:5780-5790.

Yergeau, E., Kang, S., He, Z., Zhou, J., and Kowalchuk, G. A. 2007. Functional microarray analysis of nitrogen and carbon cycling genes across an Antarctic latitudinal transect. The ISME Journal. 1:163-179.

Zhang, P., and Ryan, J. A. 1999. Transformation of Pb (II) from cerrusite to chloropyromorphite in the presence of hydroxyapatite under varying conditions of pH. Environmental Science and Technology. 33:625-630.

Zhang, H., Zao, F. J., Sun, B., Davison, W., and McGrath, S. P. 2001. A new method to measure effective soil solution concentration predicts copper availability to plants. Environmental Science and Technology. 32:704-710.

Zhang, S., Xue, X., Liu, R., and Jin, Z. 2005. Current situation and prospect of the comprehensive utilization of mining tailings [J]. Mining and Metallurgical Engineering. 3: 44-48.

Zhou, J., and Thompson, D. K. 2002. Challenges in applying microarrays to environmental studies. Current Opinion in Biotechnology. 13:204-207.

Zhou, J., Kang, S., Schadt, C., and Garten Jr, C. 2008. Spatial Scaling of Functional Gene Diversity Across various Microbial Taxa. Proceedings of National Academy of Sciences, USA. 105:7768-7773.

Chapter 3 - Biogeochemical Transformations of Trace Elements in a Contaminated Minewaste Materials under Reduced Conditions

Abstract

The milling and mining operation of metal ores are one of the major sources of trace metal contamination in the earths' surface due to exposure of unstable sulfides present in minewaste to oxygen-rich waters. The spring river and its tributaries in southeast Kansas are contaminated with lead (Pb), zinc (Zn), and cadmium (Cd), due to historic mining activities conducted in the Tri-State mining district. Trace metal transformations and cycling in minewaste/soils could greatly influence ecosystem and human health. It has been hypothesized, if mine waste materials are disposed in the flooded subsidence pits; these metals can be transformed back into their sulfide forms under reduced conditions limiting their mobility, and toxicity. However, the existing mine tailings are low in OC and S. The objective of this study was to examine the effect of OC and S addition on the biogeochemical transformations of Pb, Zn and Cd in these minewaste materials. Short-, medium- and long-term saturated column experiments were conducted in order to study the effect of redox induced biogeochemical transformation of Pb, Zn and Cd over time. A reduction in dissolved organic carbon (DOC) along with sulfate-S reduction and estimated redox potentials indirectly indicated sulfide formation via dissimilatory sulfate reduction. Scanning electron microscopy-energy dispersive X-ray analysis conducted on darker patches that appeared in the columns after ~70 days of submergence showed colocalization of Pb, Cd or Zn with S, indirectly suggesting metal sulfide formation. Further, SEM-EDXA conducted on colloids retained on 0.45 µm- and 15 nm-membranes used on column effluent provided evidence that about <1% of total Cd and total Pb were transported as freely dispersed, or in-association with the bacterial membranes, during the

initial 32-day of submergence. Retention filters may be needed in subsurface treatment systems in order to avoid colloidal assisted escape of metals, and to ensure compliance with the maximum concentration limits for Pb and Cd in groundwater.

Introduction

The milling and mining operations of metal ores are one of the major sources of heavy metal contamination on the earth's surface, in particular, the generation of sulfide rich tailings has a heavy impact on neighboring water bodies (Edwards et al., 2000; Baker et al., 2003; Navarro et al., 2008). Acid mine drainage resulting from the exposure of sulfide rich minerals to oxygen rich water leads to leaching of several contaminants that may impact groundwater quality (Johnson et al., 2005; Vega et al., 2006). Thus, metal contamination and acid mine drainage are high priority environmental concerns, particularly where minewaste materials rich in metal-sulfides are abandoned without any mitigation provisions in place (Nordstorm et al., 1999; Concas et al., 2006).

The Tri State mining district located in parts of southeast Kansas, southwest Missouri and northeast Oklahoma was one of the largest Pb and Zn producers in the world, beginning operation around 1848 and continuing until around 1970. The district has a large quantity of minewaste on the surface as chat and tailings which contain trace levels of sulfide minerals such as pyrite (FeS2), galena (PbS), sphalerite (ZnS), and others (Newfields, 2003). The movement of soluble metals and metal-laden sediments from the landscape into surface waters via surface runoff are the primary ecological concerns for both aquatic and terrestrial organisms (Pierzynski and Vaillant, 2006). The USEPA has suggested subsurface disposal (i.e., minewaste disposal in flooded subsidence pits) as a remediation strategy for the highly contaminated and abandoned minewaste materials. The assumption is that these metals can be transformed back into their

sulfide forms under reducing conditions, limiting mobility and toxicity. However, there are several challenges associated with this strategy. The mine waste is inherently low in DOC and this could slow the reduction processes (Zhang et al., 2005; Hayes et al., 2006; Borch et al., 2009) as OC is the driver of biogeochemical cycling of major and trace elements (Evans et al., 2006; Borch et al., 2010). Insufficient S content in minewaste could also limit sulfide formation, and promote carbonate precipitation, depending on pH and carbonate concentration (Falkowski et al., 2000; Toevs et al., 2007). High carbonate concentration in the Tri-State minewaste materials continues to buffer pH, thereby keeping the pH of the materials elevated (KGS, 2010). The alkaline pH and carbonate concentration may favor the formation of metal carbonates that are not as stable as sulfide minerals (Lindsay, 1979; Toevs et al., 2007; Du Liang et al., 2009). In addition, subsurface submergence of minewaste materials may result in seepage of leachate with high concentrations of metals into groundwater. Another challenge would be acquiring sufficient clean soil for capping, and long term continuous monitoring could make this remedial action expensive (USEPA, 2010).

With the addition of OC and S to minewaste, these metals can be transformed back into their sulfide forms under reduced conditions thereby limiting their mobility and toxicity (Brookins, 1986; 1988). A typical sulfate reduction reaction using organic matter (OM) as an electron donor is:

SO_4^{2-}+ OM (2C) +$2H_2O$→ H_2S+ $2HCO_3^-$ (pH<7.0) (Stein et al., 2007)

At high metal concentration, metals tend to precipitate as metal sulfides at pH<7.0, as the rate of H_2S formation increases at pH of 7.0 and is at the maximum at 8.0 (Morris et al., 1972; Nielsen et al., 1988; Burton et al., 2008).

$H_2S+M^{2+}\rightarrow MS + 2H^+$

In low metal concentration environments, metals tend to coprecipitate and/or adsorb on Fe sulfides (Morse et al., 1993; Rickard et al., 1995). Sulfate reduction does not occur at higher redox levels when other more favorable electron acceptors are available (Adriano et al., 2001; Stein et al., 2007). Under sulfate-reducing conditions, chalcophile metal contaminants such as Pb, Cu, Cd, Zn, Fe and Ni are generally believed to be effectively immobilized as metal sulfides (Labrenz and Banfield, 2004; Toevs et al., 2006; Weber, 2009).

High-resolution SEM-EDXA analysis is a powerful tool that can be used as an indirect approach to determine the colocalization of Pb, Zn, and Fe with S, and semi-quantification of elemental distribution (Seaman et al., 1997; Moral et al., 2005; Reith et al., 2009). However, poor sensitivity of this technique and a lower concentration of elements could limit use of this technique (Hettiarachchi et al., 2009).

The rates of sulfate reduction in wetlands are extremely variable and depend on many factors such as pH, redox potential, type of organic matter, and the ratio of OC to S (Lyew and Sheppard, 1999; Stein et al., 2007; Pester et al., 2012). Newly precipitated colloidal metal sulfide clusters may significantly enhance the metal mobility in reduced conditions (Weber et al., 2009; Borch et al., 2010). Metal-rich sulfide colloids or metals associated with bacterial membrane were found contributing in Cu, Pb and Cd mobilization in rivers. Colloids (sub micrometer mineral particle or bacterial cells) that are small enough to withstand gravitational settling can act as a potential carrier of poorly soluble contaminants in the subsurface environment posing the risk to river and groundwater quality (Luther et al., 2005; Weber et al., 2009). Therefore, remediation planning that involves subsurface wetlands needs to consider possible colloidal assisted trace elements movement as a consequence of this treatment strategy. There may be a multitude of biochemical transformations and physical processes responsible for such transport.

Studies combining both physico- and biogeochemical processes concurrently happening in these systems are needed for a better understanding of metal transformations and dynamics essential to design and improve effective remediation and mitigation strategies. The objectives of this experiment were to study solution chemistry, and understand the role(s), and mechanisms of biogeochemical redox transformations of Pb, Zn and Cd, and their dynamics under submerged conditions over time.

Materials and Methods

Highly contaminated minewaste material was collected from a secured repository area in Baxter Springs, KS; a part of the Tri-State mining district that has a history of 120 years of Pb- and Zn-ore mining related activities. Three series of column experiments; short-, medium- and long-term were conducted based using a completely randomized, two-way factorial experiment (factor 1: organic C with two levels, 0 and 10.7 mM L^{-1}; factor 2: sulfur with two levels, 0 and 253 mg Kg^{-1}). The minewaste, sieved to 2-mm size, was homogenized and air-dried. About 0.5 g of sample was digested using the aqua-regia reflux tube soil digestion method in order to determine the background concentrations of elements of interest (Zarcinas et al., 1996). Based on the sum of background elemental concentration, Na_2SO_4 solution was added to the minewaste at 253 mg S Kg^{-1} for the S addition treatment. The required amount of Na_2SO_4 was calculated based on the ratio of 1: 2 mM of Σ metals (Pb, Zn, Cd, Mn, Fe and S): mM of S. The S treated minewaste material was equilibrated for 10 days at room temperature on reciprocating shaker (6010, Eberbach Corporation, Ann Arbor, MI) at 192 reciprocations/min for 3 days, and at 98 reciprocations/min afterwards. The treated and equilibrated minewaste was further leached under vacuum with deionized (DI) water until a target of <2 mS cm^{-1} of electrical conductivity was achieved, and air dried. The aqua-regia digestion on post leached samples indicated about 50%

recovery of S from the treatment. Both S treated and untreated minewaste materials were inoculated with 5 g kg^{-1} of soil slurry with the purpose of inoculating materials with sulfate reducing bacteria. This soil slurry (Ivan, Kennebec, and Kahola silt loams) material was collected from the North Agronomy farm closer to the creek at Kansas State University, Manhattan, KS. Prior to its addition to the minewaste, the serial dilution of soil slurry was cultured on the petridish using postgate's medium (BP1420500) and incubated overnight at 34 ºC in an anaerobic jar (AG0025A used with an oxygen absorber; OXAN0025A, Fisher Scientific, USA). The black patches observed on petridish indirectly confirmed the presence of sulfur reducing bacteria (SRBs) in the soil slurry. The method used for SRBs culture was adapted from Luptakova et al. (2005). The minewaste materials non-treated or treated with S and properly mixed with soil slurry, was used to pack the Plexiglas columns (20 cm length, 3.2 cm ID with 3 windows milled at 2.8 cm, 9.8 cm, and 16.94 cm from the top of the column) to achieve bulk density of about 1.7 g cm^{-3}. The packed columns were saturated slowly with DI water using a mariotte's bottle that delivers a constant rate of flow, and the columns were equilibrated overnight before they were supplied with eluent. The eluent consisted of a base of simulated groundwater (1 mM NaCl, 1mM $MgCl_2$, 1 mM KCl, 1 mM $CaCl_2$ adjusted to pH 7.2) with or without 10.7 mM Na-lactate (32 mM OC). This provided four treatments for the columns designated C0S0, C1S0, C0S1, and C1S1 where C0 designates simulated groundwater without OC, C1 with OC, S0 designates simulated groundwater applied to columns without added S, and S1 designates simulated groundwater applied to columns with added S. The eluent solutions were supplied using a syringe pump (78-8210, KDS LEGATO 210, KD scientific Inc., Holliston, MA) at the rate of 13 mm day^{-1} simulating slow groundwater discharge rate. Groundwater composition and supply rate was adapted from Wan et al. (2005).

Samples collection and handling

Effluent samples were collected every 3rd, 7th and 15th day, for short-, medium- and long-term experiments respectively. The collected samples were filtered via 0.2 µm nylon filter (SF020N, Environmental express, Charleston, SC), and separated in to several aliquots. The sample aliquots for DOC and anion measurements were frozen at -20 °C, and samples for total element analysis were acidified and stored at 4 °C until used for measurement. At the end of each column experiment eluent supply was stopped, and columns were left overnight for draining out an excess water. About 20 g samples were collected inside an anaerobic chamber at 1.2- 3.2 cm depth, from the port located at the height of 18 cm (far end). The collected samples were stored in an air tight vials, and frozen at -40 °C until sample preparations were done for SEM-EDXA analysis. Appropriately preserved samples were also used for synchrotron X-ray based spectroscopy analysis and microarray analysis and for further details related to these analyses refer Karna et al. (2014b) (Chapter 4) and Karna et al. (2014c) (Chapter 5).

Solution chemistry analysis

The pH, and redox potential (Eh) measurements were done inside the anaerobic glove box chamber immediately after sample collection by using $Ag/AgCl_2$ electrodes (pH glass body filled combination, model 300731.0; and ORP (redox) combination electrode, model 300746.0, Orion, Cole-Palmer, USA). Colorimetric determination of Fe^{2+} was done by using the phenanthroline method (phen method) that was tested for its capability of quantifying ferrous and total iron with less errors by Anastàcio et al. (2008), and the color developed via this method was measured on a DU 800 series (Beckman Coulter Inc., Fullerton, CA). The DOC concentration was measured using a TOC analyzer (TOC-L, Shimadzu, Japan) after purging inorganic carbon with 1 mol L^{-1} HCl. In order to characterize dissolved OM, the dissolved

organic matter (DOM) quality measurement was done using a fluorometer (UV-visible spectrophotometer (Shimadzu UV-1601, Kyoto, Japan) (Figure 6). The anions (F^-, Cl^-, Br^-, NO_2^-, NO_3^-, $SO_4^{2-}$and PO_4^{3-}) were measured using ion chromatography (Dionex ICS-1000, Sunnyvale, CA, USA). The total dissolved concentrations of Pb, Zn, Cd, Fe, Mn, S, Mg, Ca, Na, K and Cu were measured on inductively coupled plasma optic emission spectroscopy (ICP-OES) or graphite Furnace atomic absorption spectroscopy (GF-AAS; Varian Inc., USA). The quality assurance, and quality control (QA/QC) was maintained by running duplicates of each sample, measuring the recovery of spiked samples, and using the SRM water sample NIST 1643e (National Institute of Standards and Technology, Gaithersburg, MD).

Scanning electron microscopy- Energy dispersive X-ray (SEM-EDXA)

The stored soil samples were gently ground while frozen in the glovebox under anaerobic conditions and a thin smear was prepared on a 12 mm OD aluminum stubs affixed with C-adhesive tape; Pelco Tabs™ (Ted Pella Inc., Redding, CA) to image and analyze the samples at micro-scale. Imaging and elemental analysis were performed using a high resolution field emission scanning electron microscope; Nova NanoSEM 430 (FEI, Hillsboro, OR) equipped with energy dispersive spectroscopy (EDS) silicon drift detector (SDD: 80 mm2) (Oxford Instruments, Bucks, United Kingdom). For EDS, the primary electron beam energy was 15 KeV, the spot size was 4, and data were collected over 120s for minimum 3 spots per sample under vacuum of 0.45 torr to obtain quality images. Copper was used for quantity optimization of the EDS. The weight percent (Wt %) of elements were directly calculated and given by the Nova NanoSEM 430 system when analyzing the samples. The weight percent were converted into mM for better comparison of elements with different molecular weights.

To trace the colloidal bound trace elements mobility, SEM-EDXA was conducted on the residues retained on 0.45 µm- nylon membrane (HNWP02500, Millepore, Billerica, MA), and 15 nm- polycarbonate membrane (110601, Whatman, Piscataway, NJ) at the sampling points of 14, 32, 64, 119 and 252-day. The colloids retained on filters were mounted on 12 mm OD aluminum stubs affixed with C- adhesive tape; Pelco Tabs^{TM} (Ted Pella Inc., Redding, CA) to image and analyze the samples. Imaging and elemental analysis were performed in a similar way as mentioned above. As supportive evidence, effluent filtered through 0.45 µm-, and 15 nm-membrane were also analysed using ICP-OES unless a lower detection limit was necessary in which case GF-AAS was used instead. Use of GF-AAS might have prevented us from estimating accurate concentrations of colloidal bound trace metals as GF-AAS gives truly dissolved metal concentrations, whereas ICP-OES gives total metal concentrations including atomized nanoparticles (Barrett and McBride, 2007; De Livera et al., 2011). In addition, synchrotron based micro-scale X-ray analysis ((X-ray fluorescence (XRF) followed by X-ray absorption spectroscopy (XAS) and bulk- scale XAS (Karna et al., 2014b (Chapter 4)) were conducted. The microarray analysis using geochip 4.2 (He et al., 2007) was also conducted (Karna et al., 2014c (Chapter 5)) in order to support our solution chemistry results.

Results and Discussions

The data presented in this section were collected on the homogenized minewaste of <2 mm size. The particle size distribution (PSD) was done by following the modified method developed by Kilmer et al. (1949). The mine waste contained 85% sand (2000 to 50 µm), 11.3% silt (50 to 2 µm), and 3.4% clay (<2 µm). The total N and total C concentrations were 0.03 g kg^{-1} and 1.56 g kg^{-1}, respectively. The pH of the water extract (1: 2 minewaste: DI Water mass ratio) was 7.2, and the electric conductivity was 2.31 mS cm^{-1}. The major element composition of

minewaste obtained through aqua-regia digestion is listed in Table 3-1. The SRM 2711a (National Institute of Standards and Technology, Gaithersburg, MD) was digested along with minewaste as a QA/QC sample in order to assure the recovery percentage of each analyte.

The Eh measurements did indicate sub-oxic conditions (Figure 2a). This could be because of challenges associated with disturbance of the sample due to release or absorption of gases such as O_2, H_2S and reactions at the liquid junction of the reference electrode (such precipitation of heavy metal sulfides or the effect of suspended matter). Additionally, low exchange current densities, and the predominance of mixed potentials could give less consistent results that were also observed by Whitfield (1974); Lindberg and Runnells (1984); Chapelle et al. (1996), and Sigg (2000). Due to inherent weaknesses associated with redox measurements, researchers tended to calculate the redox status of the system directly by using redox couples such as Fe^{3+}/ Fe^{2+}, HS^-/ SO_4^{2-}, NH_4^+/ NO_3^-, NO_2^-/ NO_3^-, CH_4^+ (aq)/ HCO_3^- (Lindberg and Runnells, 1984). We did redox calculation using Fe^{3+}/ Fe^{2+} redox couples that revealed our system to be more reduced compared to what redox potential probe measurement results indicated. Nordstorm (1979) and Lindberg, and Runnells (1984) observed similar results in acid mine drainage water and normal groundwater from diversified areas. The pH of our system mostly remained alkaline (>7.2) in both treated, and non-treated materials throughout submergence. Similar results were observed by Newfields (2003) in the mining district, and this could be due to higher carbonate concentrations in minewaste materials. Dissolution of calcite provides buffering capacity to maintain circumneutral pH favoring carbonate mineral formations that subsequently could influence trace metals mobility (Komárek, 2004). In the current study, an alkaline pH should also have helped in reducing Pb, Zn and Cd concentration in effluent samples. This result can be supported by earlier studies reporting immobility, and low

bioavailability of Pb, Zn and Cd at alkaline pH as fewer H^+ ions are available to compete with cations for binding sites (Hettiarachchi et al., 2004; Peréz Lopéz et al., 2011; Khaokaew et al., 2012). At alkaline pH values, with initial higher Zn concentrations, the precipitation of $Zn(OH)_2$, $Zn(CO_3)_2$, and $ZnFe_2O_4$ may control Zn solubility, and $PbCO_3$ may control Pb solubility (Manceau et al., 2000; Roberts et al., 2002). Alkaline pH could have a substantial impact on sorption/desorption, dissolution/precipitation, complexation, and oxidation/reduction processes influencing metal mobilities as observed by Wang et al. (2006) and Violante et al. (2010).

At circumneutral pH and above, Fe primarily exists as insoluble, solid phase minerals in the Fe(II) and Fe(III) oxidation states. However the solubility of Fe(III) increases and Fe(II) primarily exists as an aqueous species even in the presence of oxygen with decreasing pH. Reductive dissolution of Fe results in the formation of freshly precipitated Fe(hydr)oxides that have ten times higher adsorption capacity for metals compared to aged oxides and it also enhances cation exchange capacity by 10 fold thereby immobilizing contaminants trace elements (Zn>Pb) at circumneutral pH (Shun et al., 1977; Christian et al., 2008). Thus, repeated iron cycling observed in the current study (Figure 2c) explains the transformation between Fe(II) and Fe(III) minerals influencing Pb and Zn mobility. Similar results were found by Thompson et al. (2006) and Stein et al. (2007) who observed that metal mobility was reduced after repeated soil iron redox cycling in treatment wetlands.

In the current study, effluent concentration of Pb, Cd and Zn decreased rapidly, and mostly remained low and stable in C1S1 compared to C1S0, C0S1, and C0S0 under medium-, and long -term submergence (Figures 3-1 and 3-3). Lead, Zn and Cd have faster water exchange reaction kinetics than Fe^{2+} that results in more metal sulfides formation prior to FeS formation, and subsequent pyrite formation (Morse et al., 1999). The metal reduction results can be further

supported by the observed dynamics of DOC and sulfate-S in our system. An initial DOC concentration in eluent (~32 mM) were consumed earlier in C1S1 compared to C1S0 (figure 3-2b) indicating enhanced dissimilatory sulfate reduction via enhanced OC consumption due to higher microbial growth and activities upon OC plus S addition. Meanwhile, the effluent sulfate-S concentration was reduced with OC plus S addition from 574 mg L^{-1} to 437 mg L^{-1} under medium-term submergence (Figure 3-2a). These results are supported by previous work that reported metal sulfide formations via dissimilatory sulfate reduction comprising microbial respiration of electron acceptors by following the classical sequence of redox reactions observed in submerged soils (Sposito, 1991; Fendorf, 2000; Kim et al., 2005). During this sequence of redox reactions in S rich environments, the heterotrophic dissimilatory sulfur reducing bacteria (SRBs) use organic C (Na-lactate provided in this study) as an electron donor in order to reduce inorganic sulfate or other oxidized S forms (Fortin et al., 1997; Elias et al., 2004). Similar results have been found by Luther III (1999), Finneran et al. (2002), Stein et al. (2007), and Banfield (2013) in organic rich environments with sufficient available sulfate under reduced conditions.

The extent of DOC metabolism largely depends on the biochemical composition of the DOM (Benner, 2003), which is essential to interpret its' biogeochemical role in ecosystems (Hood, 2010). Because of this reason, change in fluorescence of effluent samples collected at 28, 112, and 210-day were analyzed. The visual inspection of EEMs or 'peak picking' of fluorescence peaks (Coble, 1996) indicated peak T (Tryptophan like) as a commonly detected peak (Figure 3-9). In addition, Peak A (humic acid like), Peak B (Tryosine like) were also detected although they are not clearly visible on EEMs due to the background color. The peaks T and B represent microbially derived DOM giving indirect evidence of enhanced microbial activities upon OC and S addition over time (Figure 3-9, Table 3-3). Similarly, humic acid like

(Peak A) showed increasing trend of humic acid formation over time in OC and S treated columns (Table 3). The matured DOM might be indicative of enhanced C-cycling by microorganism in OC added systems and they may also ultimately be playing a role in an effective mobilization of trace elements by providing adsorption sites (Shi et al., 2013).

Scanning Electron Microscopy-Energy dispersive X-ray Analysis (SEM-EDXA)

Darker regions indicating a microenvironment with higher microbial activity formed in submerged soils were observed in C1S1 after 70 days of submergence. Similar dark patches or active microsites are commonly observed in submerged soil (Kanazawa et al., 1974; Subba Rao et al., 1976). This was a clear indication of the heterogeneous nature of redox reactivity in these systems. In order to understand its biogeochemistry, SEM-EDXA mapping was conducted on at least 3 spots per sample and those indicated enhanced colocalization of Pb, Zn and Fe with S (Figure 3-4). We conducted comparative SEM-EDXA on the starting minewaste materials and treated and non-treated minewaste submerged for 252-day. The results indicated similar colocalization of Pb with S in all samples (Figure 3-5) suggesting the presence of Pb-S association in the starting materials as well. These results provide indirect evidence for the immobilization of metals via sulfide formation. The effluent chemistry results were also supported by synchrotron based X-ray analysis; X-ray absorption near edge structure (XANES); and X-ray absorption fine structure (XAFS) spectroscopy. The micro-scale Pb and Zn XAS (XAFS/XANES) indicated enhanced PbS, and ZnS formation with OC plus S treatment (C1S1) under long term submergence (Figures 3-7 and 3-8) that was further supported by bulk Pb- and Zn-XAS analysis (Karna et al., 2014b, (Chapter 4)). In addition, micro-scale Pb- and Zn-XAS indicated enhanced metal sulfide formation even under medium-term submergence indicating higher redox reactivity at isolated microenvironments. The observed relationship between Pb, Zn

and Cd immobility with metal sulfide formations has been strengthened by the results obtained from microbial analysis conducted using functional gene arrays (FGA); GeoChip 4.2. The microarray results indicated enhanced SRB genes (Karna et al., 2014c, (Chapter 5)) in OC plus S added columns (C1S1), indicating sulfide precipitation as a dominant mechanism controlling their solubility. SRBs mediated dissimilatory sulfate reduction rate is highly variable depending on the pH, redox potential, type of organic matter, and the ratio of OC to S (Lyew and Sheppard, 1999; Stein et al., 2007; Pester et al., 2012). This above variability could be due to factors influencing SRB activities such as availability of more efficient electron acceptors at higher redox levels, and competition with methane producing bacteria (MPB) at low redox levels due to altered C: S ratios. The alteration of C: S ratio may occur due to OC load via microbial consumption of oxygen (Stein and Hook, 2005).

Scanning electron microscopy-energy dispersive X-ray conducted on residues collected on 0.45 µm- and ~15 nm-membranes at different time points exhibited both bacterial associated, and/or dispersed colloidal bound trace element mobility more commonly observed in control (C0S0) compared to treated (C1S1) (Figure 3-6). Larger size colloid (>0.45 µm) seems to be highly involved in Cd and Pb mobility compared to smaller colloids (<15 nm). This result was further supported with Pb and Cd concentration measurements in the effluent samples filtered through 0.45 µm- and 15 nm- nylon membranes (Table 3-2). About 445 µg L^{-1} of larger and 260 µg L^{-1} of smaller colloids associated Cd transport, respectively, was observed in C0S0 compared to 20 µg L^{-1} of larger and 3 µg L^{-1} of smaller colloids associated Cd transport, respectively, observed in C1S1. Similarly 280 µg L^{-1} of larger colloids associated Pb mobility was observed in C0S0 only, whereas none was observed in C1S1. The Pb and Cd mobility was about 1% of their total concentration (Figure 3-6; Table 3-2). The results indicated that the biogenic sulfide formation

occurred with OC and S addition thereby helping to reduce further leaching of sequestered contaminants. We suspect iron oxides and other possibly sulfide, carbonate, and silicate minerals as the main possible carriers. The colloids assisted metal transport results from the current study are in agreement with Weber et al. (2009). Both bacterial and dispersed colloids assisted metal transport were observed during initial submergence that were associated with newly precipitated sulfides (Weber et al. 2009). The cycling event may cause wide shifts in the concentration of colloidal and dissolved material due to either Fe mineral dissolution or pH shifts associated with changes in oxidation state of Fe. The colloidal assisted metals mobility were relevant in current study, however considering the % metal escape, it may not be a concern as escaped metals could get diluted once mixed with groundwater over time. In any case, a retention filter and other engineering controls may be needed to meet the USEPA groundwater MCL for Cd ($<5 \mu g L^{-1}$) and Pb ($<15 \mu g L^{-1}$).

Conclusions

The solution chemistry data from our current study indicated that metals were effectively immobilized under both medium- and long-term submergence in all the treatments. However, C1S1 showed an enhanced effect. Metal immobilization effects observed in this study was supported by SEM-EDXA analysis that indicated colocalization of metals with S. This was further confirmed via synchrotron based X-ray analysis provided direct evidence of enhanced sulfide formation with the C1S1 treatment, and the microarray analysis indicated enhanced sulfur reducing bacteria (SRB) genes involved in sulfide formation. Scanning electron microscopy-energy dispersive X-ray analysis conducted on colloids in the effluent water retained on 0.45 µm- or 15 nm-membranes suggested that only about <1% of total Cd and Pb were transported as freely dispersed, and in association with the bacterial membrane during initial 32-day of submergence. While still indicating a loss of metals, these would readily be diluted in groundwater. Retention filters maybe needed in the subsurface treatment systems in order to avoid colloidal assisted escape of metals. Uncertainty of the fate of sequestered metals in wetland treatment systems under varying redox conditions needs to be studied.

Acknowledgements

We acknowledge Kansas State University Research and Extension, Kansas State University, Manhattan, KS for providing financial support for conducting this experiment. We also acknowledge Drs. Dan Boyle, Natalie Mladenov, and Matthew Kirk for assisting with SEM-EDXA, DOM, and Geochem workbench, and soil chemistry group and lab assistants especially Dorothy Menefee for helping me with experimental set up.

References

Adriano, D. C. 2001. Trace elements in terrestrial environments: Biogeochemistry, bioavailability, and risks of metals. Springer- Verlag, New York.

Anastácio, A. S., Harris, B., Yoo, H., Fabris, J. D., and Stucki, J. W. 2008. Limitations of the ferrozine method for quantitative assay of mineral systems for ferrous and total iron. Geochimica Et Cosmochimica Acta. 72:5001-5008.

Baker, B. J., and Banfield, J. F. 2003. Microbial communities in acid mine drainage. FEMS Microbiology Ecology. 44:139-152.

Benner, R., and Kaiser, K. 2003. Abundance of amino sugars and peptidoglycan in marine particulate and dissolved organic matter. Limnology and Oceanography. 48:118-128.

Borch, T., Kretzschmar, R., Kappler, A., Cappellen, P. V., Ginder-Vogel, M., Voegelin, A., and Campbell, K. 2009. Biogeochemical redox processes and their impact on contaminant dynamics. Environmental Science and Technology. 44:15-23.

Brookins, D. G. 1986. Geochemical behavior of antimony, arsenic, cadmium and thallium: Eh-pH diagrams for 25° C, 1-bar pressure. Chemical Geology. 54:271-278.

Brookins, D. G. 1988. Copper. Eh-pH diagrams for geochemistry, Springer- Verlag, New York. 60-63.

Burton, E. D., Bush, R. T., Sullivan, L. A., and Mitchell, D. R. 2008. Schwertmannite transformation to goethite via the fe (II) pathway: Reaction rates and implications for iron-sulfide formation. Geochimica Et Cosmochimica Acta. 72:4551-4564.

Chapelle, F. H., Bradley, P. M., Lovley, D. R., O'Neill, K., and Landmeyer, J. E. 2002. Rapid evolution of redox processes in a petroleum Hydrocarbon-Contaminated aquifer. Ground Water. 40:353-360.

Chen, K. Y., and Morris, J. C. 1972. Kinetics of oxidation of aqueous sulfide by oxygen. Environmental Science and Technology. 6:529-537.

Coble, P. G. 1996. Characterization of marine and terrestrial DOM in seawater using excitation-emission matrix spectroscopy. Marine Chemistry. 51:325-346.

Concas, A., Ardau, C., Cristini, A., Zuddas, P., and Cao, G. 2006. Mobility of heavy metals from tailings to stream waters in a mining activity contaminated site. Chemosphere. 63:244-253.

Edwards, K. J., Bond, P. L., Druschel, G. K., McGuire, M. M., Hamers, R. J., and Banfield, J. F. 2000. Geochemical and biological aspects of sulfide mineral dissolution: Lessons from iron mountain, California. Chemical Geology. 169:383-397.

Evans, M., Warburton, J., and Yang, J. 2006. Eroding blanket peat catchments: Global and local implications of upland organic sediment budgets. Geomorphology. 79:45-57.

Falkowski, P., Scholes, R. J., Boyle, E., Canadell, J., Canfield, D., Elser, J. 2000. The global carbon cycle: A test of our knowledge of earth as a system. Science (New York, N.Y.). 290:291-296.

Fellman, J. B., Hood, E., and Spencer, R. G. 2010. Fluorescence spectroscopy opens new windows into dissolved organic matter dynamics in freshwater ecosystems: A review. Limnology and Oceanography. 55:2452-2462.

Fendorf, S., Wielinga, B. W., and Hansel, C. M. 2000. Chromium transformations in natural environments: The role of biological and abiological processes in chromium (VI) reduction. International Geology Review. 42:691-701.

Finneran, K. T., Anderson, R. T., Nevin, K. P., and Lovley, D. R. 2002. Potential for bioremediation of uranium-contaminated aquifers with microbial U (VI) reduction. Soil and Sediment Contamination: An International Journal. 11:339-357.

Fortin, D., and Beveridge, T. 1997. Microbial sulfate reduction within sulfidic mine tailings: Formation of diagenetic Fe sulfides. Geomicrobiology Journal. 14:1-21.

Hayes, J. M., and Waldbauer, J. R. 2006. The carbon cycle and associated redox processes through time. Philosophical Transactions of the Royal Society of London.Series B, Biological Sciences. 361:931-950.

He, Z., Gentry, T. J., Schadt, C. W., Wu, L., Liebich, J., Chong, S. C., Jardine, P. 2007. GeoChip: A comprehensive microarray for investigating biogeochemical, ecological and environmental processes. The ISME Journal. 1:67-77.

Hettiarachchi, G. M., and Pierzynski, G. M. 2004. Soil lead bioavailability and in situ remediation of lead-contaminated soils: A review. Environmental Progress. 23:78-93.

Jambor, J. L., Nordstrom, D. K., and Alpers, C. N. 2000. Metal-sulfate salts from sulfide mineral oxidation. Reviews in Mineralogy and Geochemistry. 40:303-350.

Johnson, D. B., and Hallberg, K. B. 2005. Acid mine drainage remediation options: A review. Science of the Total Environment. 338:3-14.

Kansas Geological Survey (KGS). 2001. Public outreach. http://www.kgs.ku.edu/Publications/pic17/pic17_2.html

Khaokaew, S., Landrot, G., Chaney, R. L., Pandya, K., and Sparks, D. L. 2012. Speciation and release kinetics of zinc in contaminated paddy soils. Environmental Science and Technology. 46:3957-3963.

Kim, G., Hyun, M., Chang, I., Kim, H., Park, H., Kim, B., and Weightman, A. 2005. Dissimilatory Fe (III) reduction by an electrochemically active lactic acid bacterium phylogenetically related to enterococcus gallinarum isolated from submerged soil. Journal of Applied Microbiology. 99:978-987.

Labrenz, M., and Banfield, J. 2004. Sulfate-reducing bacteria-dominated biofilms that precipitate ZnS in a subsurface circumneutral-pH mine drainage system. Microbial Ecology. 47:205-217.

Lindberg, R., and Runnels, D. 1984. Ground water redox reactions: An analysis of equilibrium state applied to Eh measurements and geochemical modeling. Science. 225:925-927.

Luther III, G. W., and Rickard, D. T. 2005. Metal sulfide cluster complexes and their biogeochemical importance in the environment. Journal of Nanoparticle Research. 7:389-407.

Lyew, D., and Sheppard, J. D. 1997. Effects of physical parameters of a gravel bed on the activity of sulphate-reducing bacteria in the presence of acid mine drainage. Journal of Chemical Technology and Biotechnology. 70:223-230.

Manceau, A., Schlegel, M., Musso, M., Sole, V., Gauthier, C., Petit, P., and Trolard, F. 2000. Crystal chemistry of trace elements in natural and synthetic goethite. Geochimica Et Cosmochimica Acta. 64:3643-3661.

Morse, J. W., and Arakaki, T. 1993. Adsorption and coprecipitation of divalent metals with mackinawite (FeS). Geochimica et Cosmochimica Acta. 57:3635-3640.

Morse, J., and Luther I, G. 1999. Chemical influences on trace metal-sulfide interactions in anoxic sediments. Geochimica Et Cosmochimica Acta. 63:3373-3378.

Nordstrom, D. K., and Alpers, C. N. 1999. Negative pH, efflorescent mineralogy, and consequences for environmental restoration at the iron mountain superfund site, California. Proceedings of the National Academy of Sciences of the United States of America. 96:3455-3462.

Navarro, M., Pérez-Sirvent, C., Martínez-Sánchez, M., Vidal, J., Tovar, P., and Bech, J. 2008. Abandoned mine sites as a source of contamination by heavy metals: A case study in a semi-arid zone. Journal of Geochemical Exploration. 96:183-193.

Pérez-López, R., Nieto, J. M., López-Cascajosa, M. J., Díaz-Blanco, M. J., Sarmiento, A. M., Oliveira, V., and Sánchez-Rodas, D. 2011. Evaluation of heavy metals and arsenic speciation discharged by the industrial activity on the tinto-odiel estuary, SW Spain. Marine Pollution Bulletin. 62:405-411.

Pester, M., Knorr, K. H., Friedrich, M. W., Wagner, M., and Loy, A. 2012. Sulfate-reducing microorganisms in wetlands - fameless actors in carbon cycling and climate change. Frontiers in Microbiology. 3:72-78.

Pierzynski, G. M. and Vaillant, G. C. 2006. Remediation to reduce ecological risk from trace element contamination: A decision case study. Journal of Natural Resources and Life Sciences Education. 35:85-94.

Pope, L. M. 2005. Assessment of contaminated stream bed sediment in the Kansas part of the historic Tri-State lead and zinc mining district, Cherokee county, 2004. USGS Scientific Investigations Report. p. 5251.

Rickard, D., Schoonen, M. A., and Luther, G. 1995. Chemistry of iron sulfides in sedimentary environments. ACS Symposium Series. 612:168-193.

Roberts, D. R., Scheinost, A., and Sparks, D. 2002. Zinc speciation in a smelter-contaminated soil profile using bulk and microspectroscopic techniques. Environmental Science and Technology. 36:1742-1750.

Sigg, L. 2000. Redox potential measurements in natural waters: Significance, concepts and problems. Redox, Springer- Verlag, New York, 1-12.

Sposito, G., Barry, D., and Kabala, Z. 1991. Stochastic differential equations in the theory of solute transport through inhomogeneous porous media. Advance Porous Media. 1:295-309.

Stein, O. R., Borden-Stewart, D. J., Hook, P. B., and Jones, W. L. 2007. Seasonal influence on sulfate reduction and zinc sequestration in subsurface treatment wetlands. Water Research.41:3440-3448.

Stein, O. R., and Hook, P. B. 2005. Temperature, plants, and oxygen: How does season affect constructed wetland performance? Journal of Environmental Science and Health. 40:1331-1342.

Stumm, W., and Morgan, J. 1996. Aquatic chemistry, chemical equilibria and rates in natural waters. 3rd edition. Wiley, New York, USA. p. 684-685.

Thompson, A., Chadwick, O. A., Rancourt, D. G., and Chorover, J. 2006. Iron-oxide crystallinity increases during soil redox oscillations. Geochimica Et Cosmochimica Acta. 70:1710-1727.

Vega, F. A., Covelo, E. F., and Andrade, M. 2006. Competitive sorption and desorption of heavy metals in mine soils: Influence of mine soil characteristics. Journal of Colloid and Interface Science. 298:582-592.

Violante, A., and Pigna, M. 2002. Competitive sorption of arsenate and phosphate on different clay minerals and soils. Soil Science Society of America Journal. 66:1788-1796.

Wan, J., Tokunaga, T. K., Brodie, E., Wang, Z., Zheng, Z., Herman, D., Sutton, S. R. 2005. Reoxidation of bioreduced uranium under reducing conditions. Environmental Science and Technology. 39:6162-6169.

Wang, Y., Morin, G., Ona-Nguema, G., Menguy, N., Juillot, F., Aubry, E and Brown Jr, G. E. 2008. Arsenite sorption at the magnetite–water interface during aqueous precipitation of

magnetite: EXAFS evidence for a new arsenite surface complex. Geochimica Et Cosmochimica Acta. 72:2573-2586.

Weber, F., Voegelin, A., Kaegi, R., and Kretzschmar, R. 2009. Contaminant mobilization by metallic copper and metal sulphide colloids in flooded soil. Nature Geoscience. 2:267-271.

Whitfield, M. 1974. The hydrolysis of ammonium ions in sea water-a theoretical study. Journal of the Marine Biological Association of the United Kingdom. 54:565-580.

Zarcinas, B. A., McLaughlin, M. J., and Smart, M. K. 1996. The effect of acid digestion technique on the performance of nebulization systems used in inductively coupled plasma spectrometry. Communications in Soil Science and Plant Analysis. 27:1331-1354.

Zhang, S., Xue, X., Liu, R., and Jin, Z. 2005. Current situation and prospect of the comprehensive utilization of mining tailings. Mining and Metallurgical Engineering. 3:44-48.

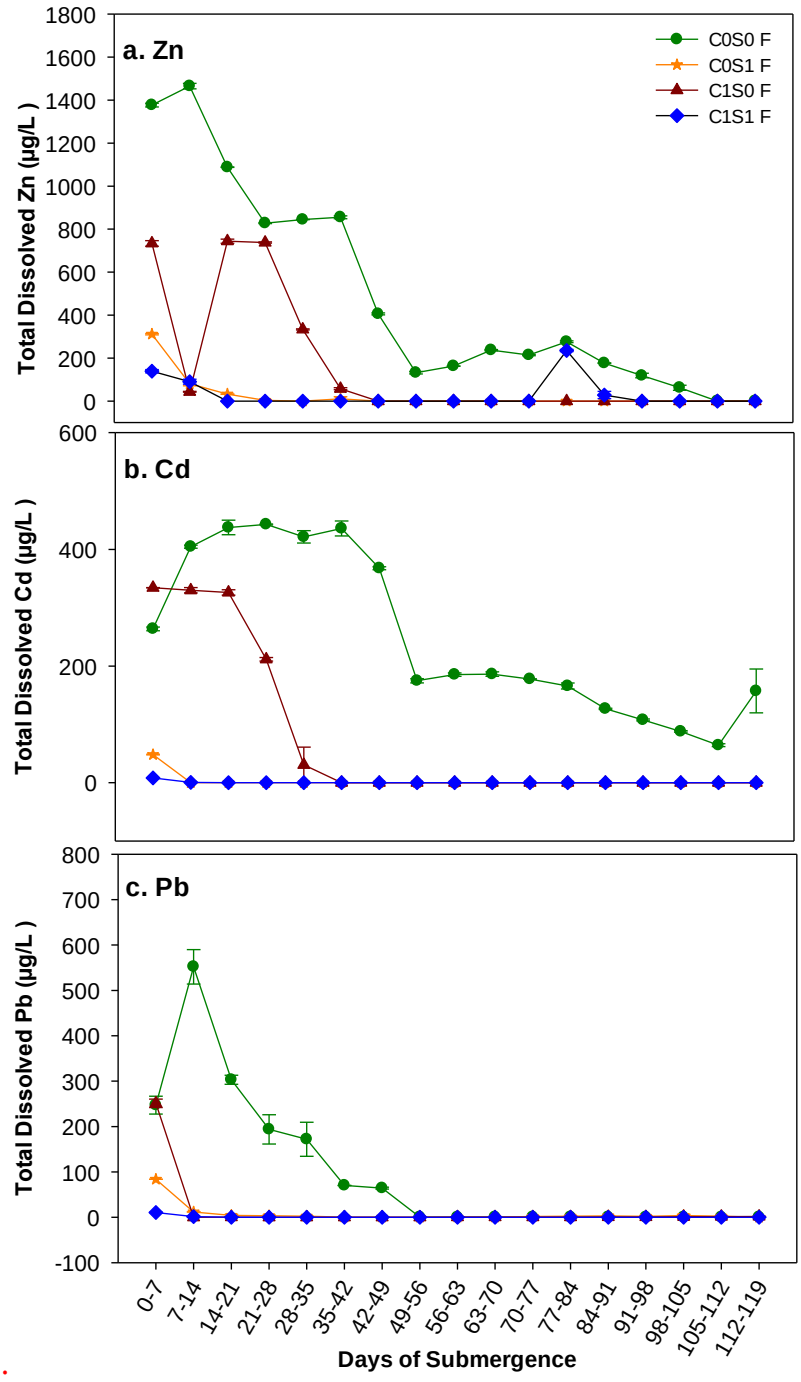

Figure 3-1: Pb, Zn and Cd concentration observed in effluent samples under medium-term (119-day) submergence in control (C0S0), S treated (C0S1), organic C treated (C1S0), and OC plus S treated (C1S1) samples.

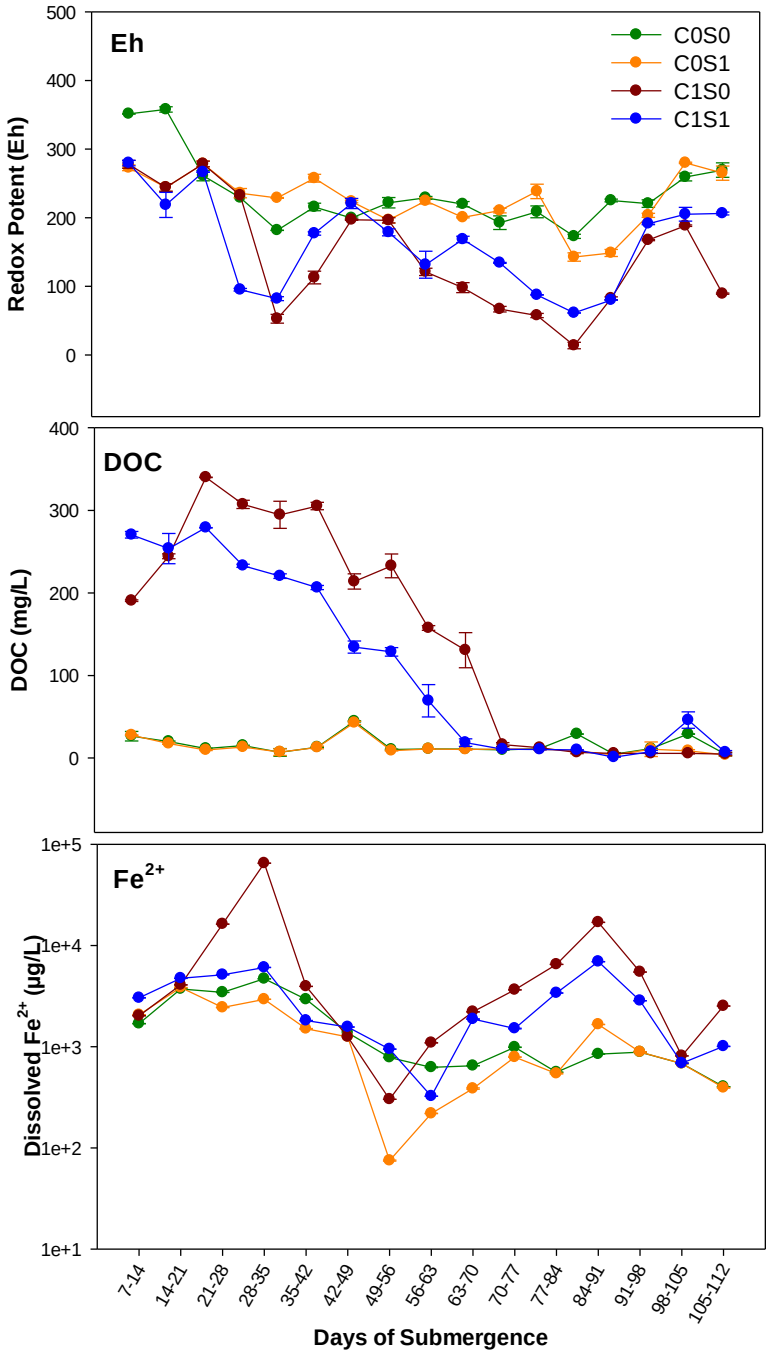

Figure 3-2: Sulfate-S, DOC concentration and ferrous ion cycling observed in effluent samples under medium-term (119-day) submergence in control (C0S0), S treated (C0S1), organic C treated (C1S0), and OC plus S treated (C1S1) samples.

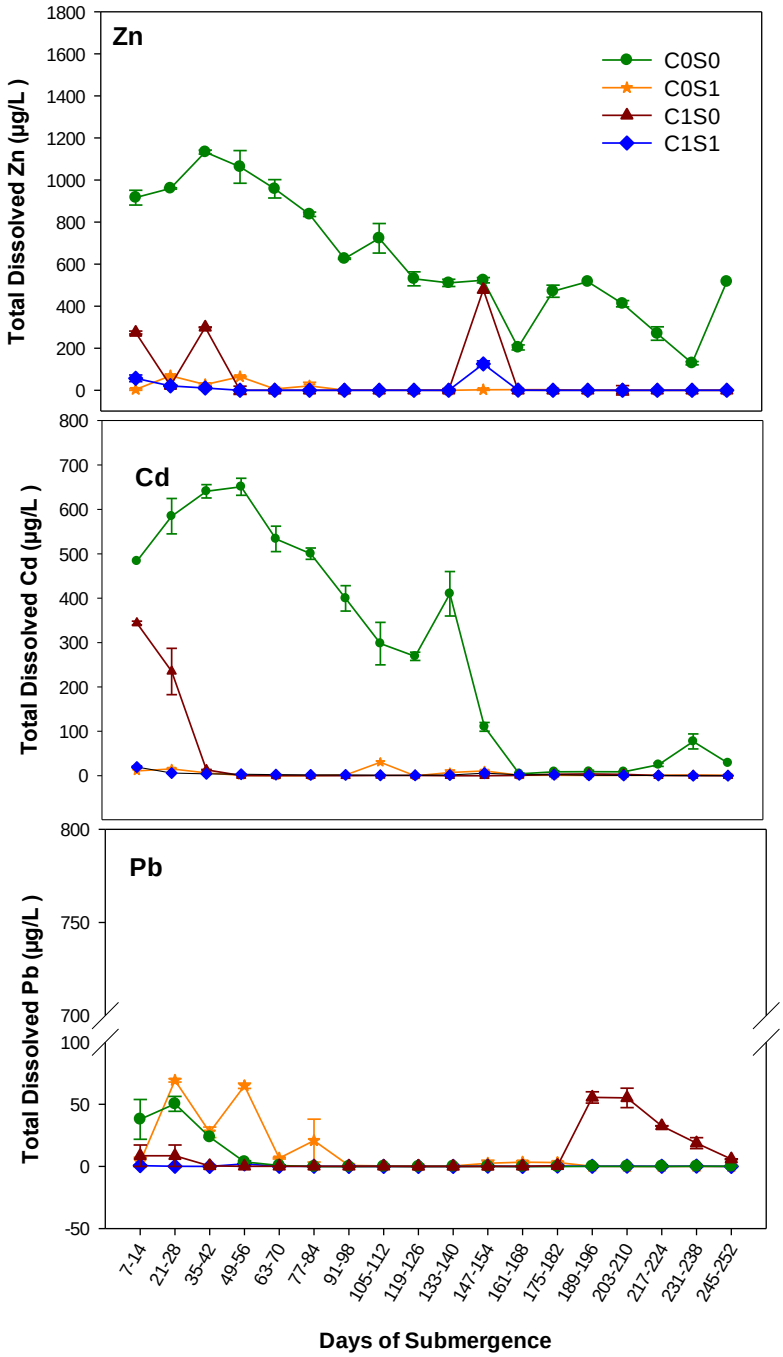

Figure 3-3: Pb, Zn and Cd concentration observed in effluent samples under long-term (252-day) submergence in control (C0S0), S treated (C0S1), organic C treated (C1S0), and OC plus S treated (C1S1) samples.

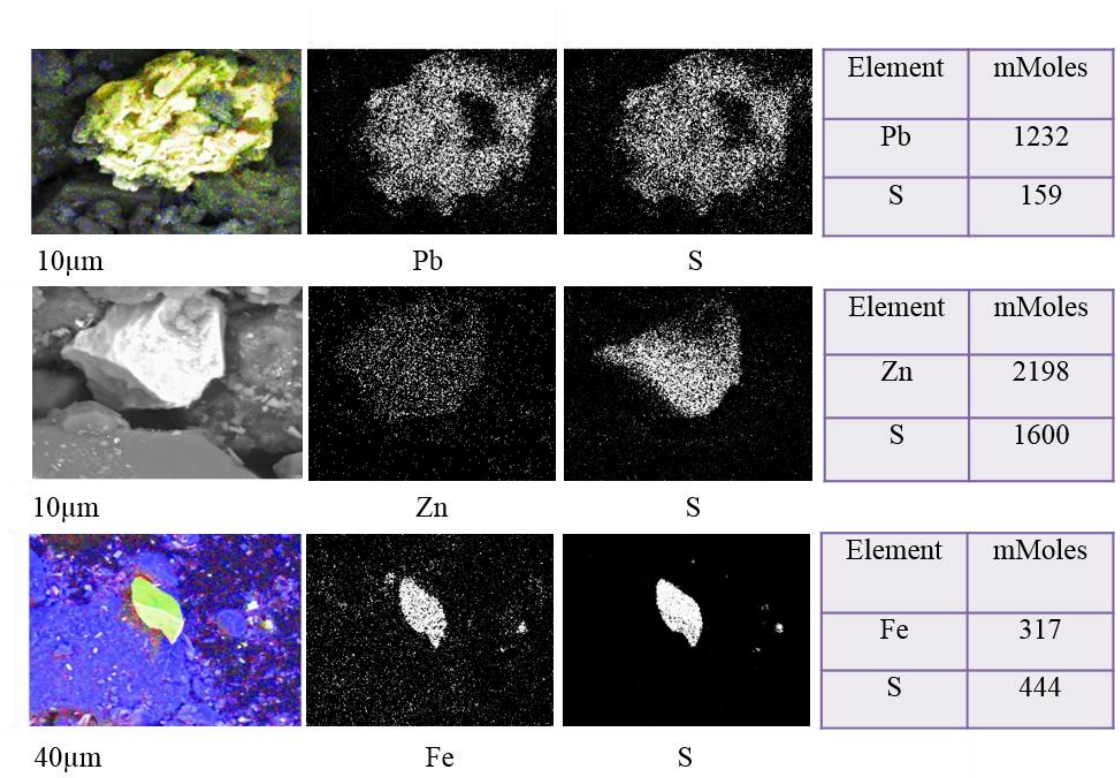

Element	mMoles
Pb	1232
S	159

Element	mMoles
Zn	2198
S	1600

Element	mMoles
Fe	317
S	444

Figure 3-4: Scanning electron microscopy (SEM) secondary electron image, and SEM-EDXA mapping analysis for Pb, Zn, Fe, and S, showing elemental distribution, and colocalization of Pb, Zn, and Fe with S in the microsites formed in OC plus S treated (C1S1) samples under medium term (119-day) submergence.

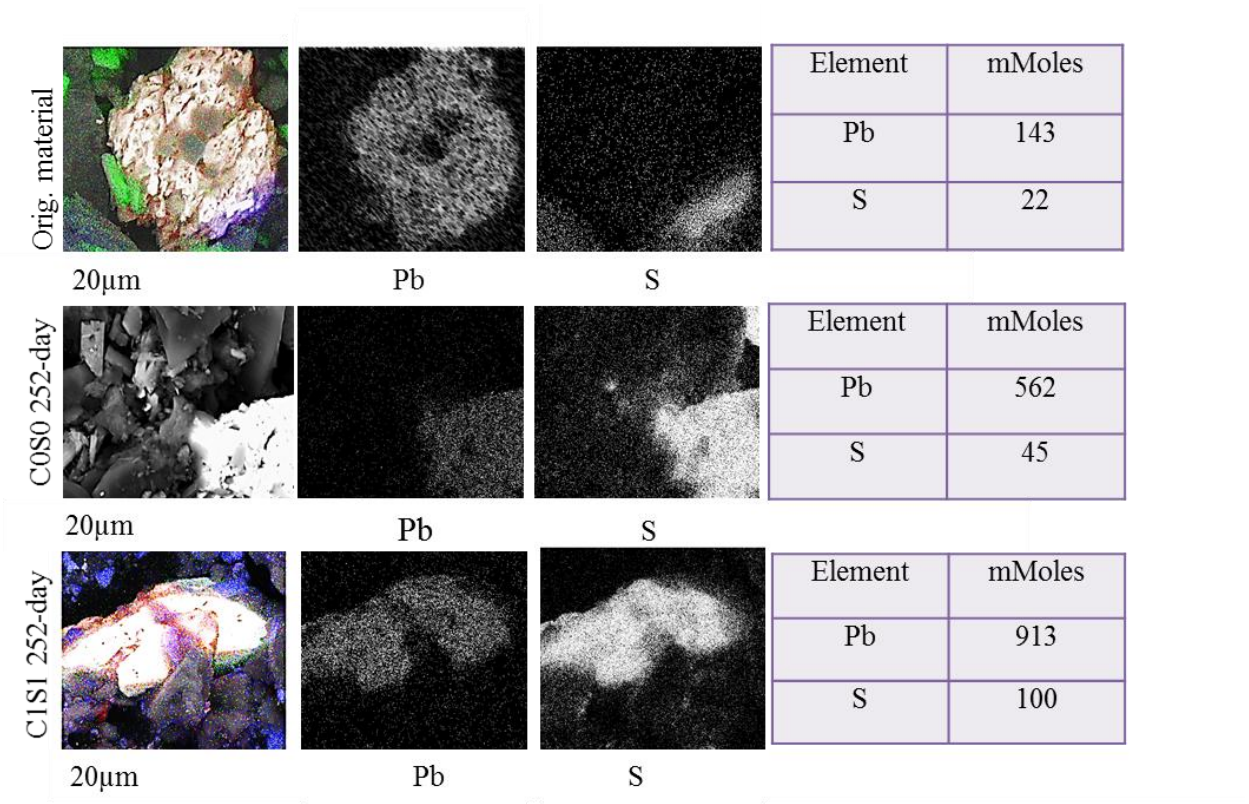

Element	mMoles
Pb	143
S	22

Element	mMoles
Pb	562
S	45

Element	mMoles
Pb	913
S	100

Figure 3-5: Scanning electron microscopy (SEM) secondary electron image, and SEM-EDXA mapping analysis for Pb and S, showing elemental distribution, and colocalization of Pb with S in starting material, positive control (C0S0) and OC plus S treated columns (C1S1) under long-term (252-day) submergence.

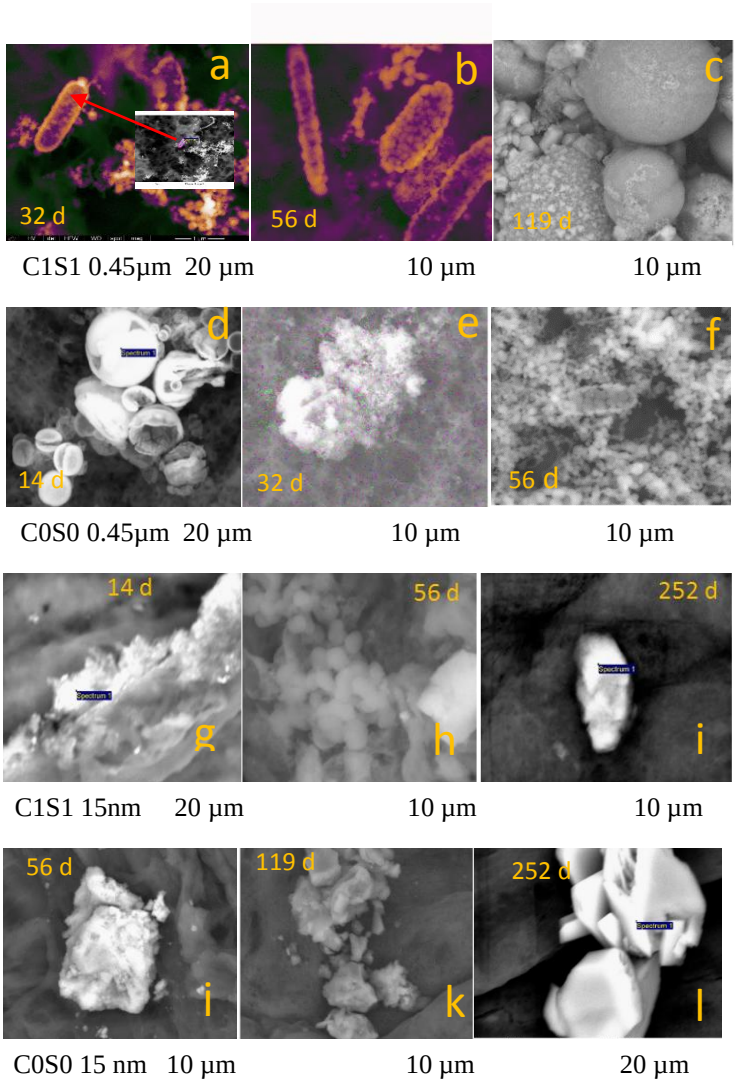

Element	14 d	32 d	56 d	119 d
Fe	1214	1187	751	118
S	6	31	56	175
Zn	44	-	15	27
Cd	20	19	6	-
Pb	7	-	-	4

Element	14 d	32 d	56 d	119 d
Fe		340	1656	1176
S	53	25	31	
Zn	361	477	265	123
Cd	122	93	4	14
Pb	48	14	1.5	2

Element	14 d	32 d	56 d	119d	252 d
Fe	1542	11	93	-	5
S	143	2991	365	384	19
Zn	50	3	17	8	-
Cd	3	-	-	-	3
Pb	12	-	-	-	2

Element	14 d	32 d	56 d	119d	252 d
Fe	40	-	2547	69	19
S	6	-	319	-	3925
Zn	3	-	-	15	-
Cd	-	2	-	2	-
Pb	1	-	15	3	15

Figure 3-6: SEM-EDXA showing bacterial associated and freely dispersed colloidal bound trace elements mobility observed on residue retained on 0.45 µm, and 15 nm pore size membranes at different time points. The elemental analyses are presented in the attached table. The letter ‘d’ in the attached table represents for day.

Table 3-1: Total element concentration in minewaste collected from the Tri-State mining district.

Element	Cd	Pb	Zn	Fe	Mn	S
mg kg^{-1}	67	5048	23468	6834	97	9458

Table 3-2: Cd and Pb concentration in effluent samples filtered through 0.45 µm, and 15 nm pore size membrane showing colloidal bound Cd and Pb mobility at different time points.

	<0.45 µm	**<15 nm**	**<0.45 µm**	**<15 nm**
Samples	**Cd(µgL^{-1})**	**Cd(µgL^{-1})**	**Pb(µgL^{-1})**	**Pb(µgL^{-1})**
C0S0 14-d	264	260	280	<DL
C0S0 32-d	445	103	198	<DL
C0S0 64-d	178	57	<DL	<DL
C0S0 119-d	171	84	<DL	<DL
C0S0 252-d	64	4	<DL	<DL
C1S1 14-d	20	3	<DL	<DL
C1S1 32-d	11	1.0	<DL	<DL
C1S1 64-d	2	<DL	<DL	<DL
C1S1 119-d	1	<DL	<DL	<DL
C1S1 252-d	<DL	<DL	<DL	<DL

*DL corresponds to detection limit. Detection limit of 0.6 for Cd, and 0.7 µgL^{-1} for Pb was determined. The letter ‘d’ represents for day on which effluent samples were collected.

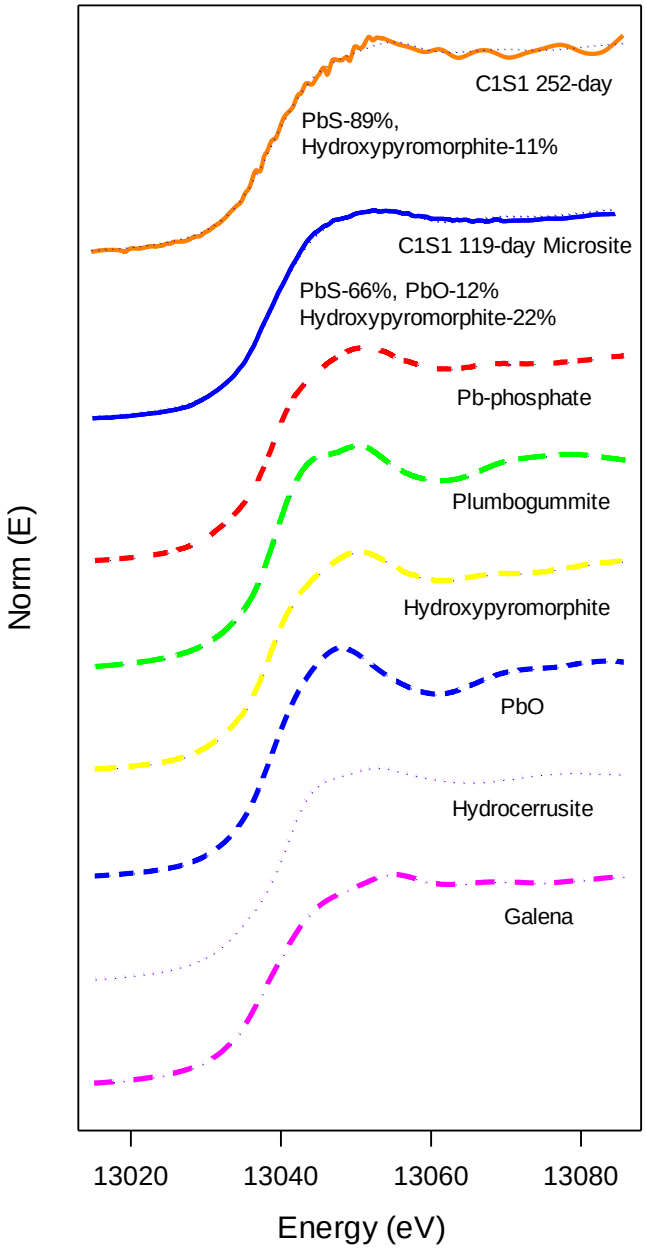

Figure 3-7: Representative Pb L(III)-edge µ-XANES spectra in OC plus S treated (C1S1) sample. Solid lines represent the normalized spectra and the dotted lines represent the best fits obtained using statistical analyses; principal component analysis (PCA), and linear combination fitting (LCF).

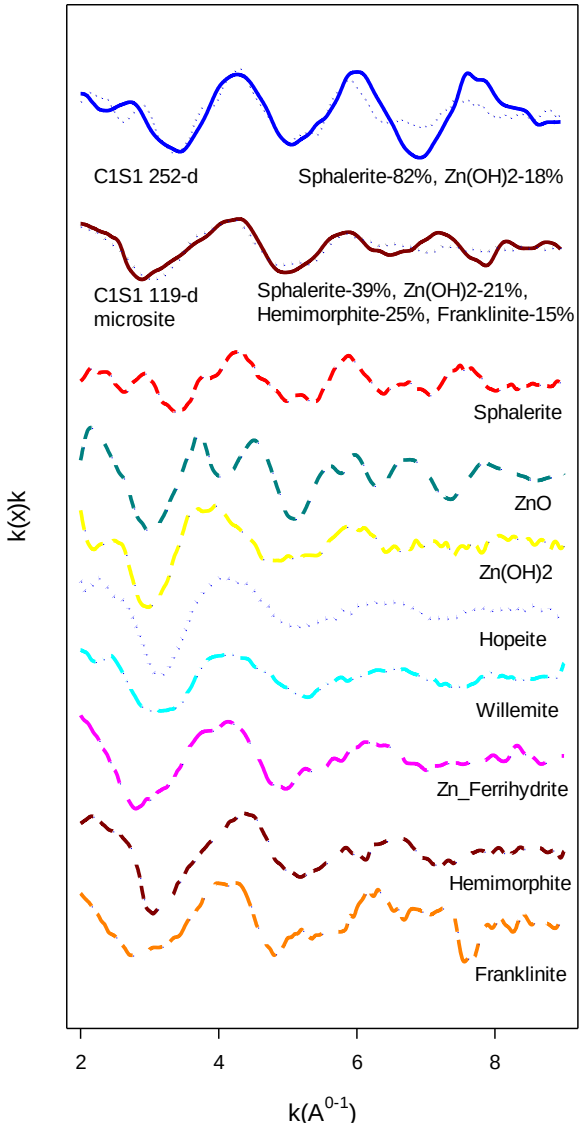

Figure 3-8: Representative Zn kα-edge μ-XANES spectra showing enhancement of metal sulfide formation over time with OC plus S treatment (C1S1). Solid lines represent the normalized spectra and the dotted lines represent the best fits obtained using statistical analyses; principal component analysis (PCA), and linear combination fitting (LCF).

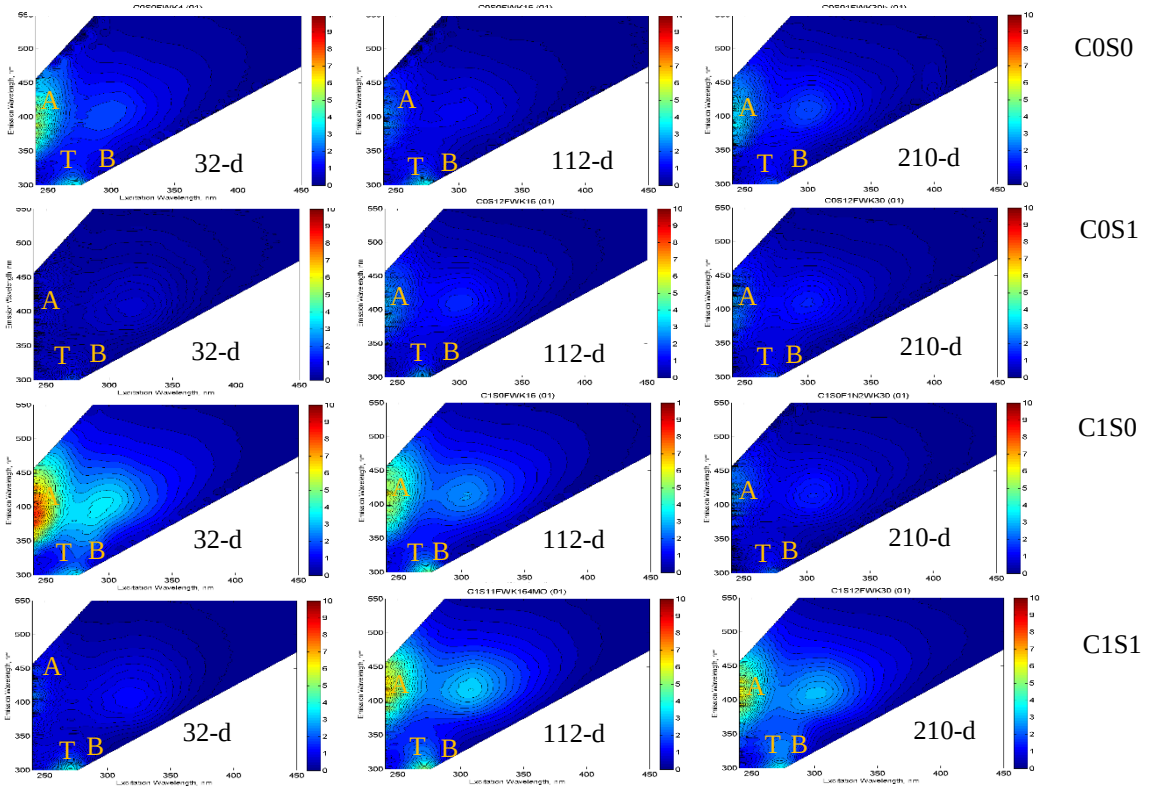

Figure 3-9: Flourescence dissolved organic matter (DOM) excitation and emission measurement (EEM) for control (C0S0), S treated (C0S1), OC treated (C1S0), and OC plus S treated (C1S1) samples collected at 32-day, 112-day, and 210-day. The EEM measurement show the positions for peak A, T, and B detections.

Table 3-3: Fluorescence Index for DOM peaks detected. Peak 'T' stands for tryptophan, peak 'B' for tryosine, and peak 'A' for humic acid.

Treatments	Peak T	Peak B	Peak A
C0S0 32-d	1.42	1.61	0.80
C0S0 112-d	1.13	0.99	0.72
C0S0 210-d	0.13	1.29	0.68
C0S1 32-d	0.50	0.95	0.85
C0S1 112-d	0.97	1.72	0.67
C0S1 210-d	0.95	1.48	0.70
C1S0 32-d	2.36	2.62	0.75
C1S0 112-d	2.61	2.85	0.97
C1S0 210-d	1.44	2.44	0.65
C1S1 32-d	0.86	2.71	1.10
C1S1 112-d	0.91	3.49	3.99
C1S1 210-d	1.81	3.61	4.23

Chapter 4 - Understanding Subsurface Transformation and Dynamics of Lead and Zinc in Contaminated Minewaste Materials using Synchrotron based X-Ray Analysis

Abstract

Metal contamination due to milling and mining operations of metal ores are of great concern in the world. The Spring River and its tributaries in southeast Kansas are contaminated with lead (Pb), and Zinc (Zn) due to long-term historic mining activities conducted in the Tri-State mining district in parts of southeast Kansas, southwest Missouri and northeast Oklahoma. Trace metals cycling in minewaste materials with low organic carbon (OC) and sulfur (S) could greatly influence plant productivity, the ecosystem, and human health. It has been hypothesized that if these mine waste materials are disposed of in the flooded subsidence pits; metals can be transformed back into their sulfide forms under reduced conditions limiting their mobility and toxicity. The objective of this study was to examine the effect of OC and S addition on the biogeochemical transformations of Pb, Zn and Cd in minewaste containing microcosms. Advanced molecular spectroscopic techniques were used in this study to understand the effect of redox induced biogeochemical transformation of Pb and Zn over time. Microscopically focused synchrotron-based XRF (μ-XRF) was used to map elemental distribution in the minewaste materials. Results showed a higher correlation of Pb and Zn with Fe and Mn during initial stages of submergence. Micro-scale X-ray absorption near edge structure (XANES) and X-ray absorption fine structure (XAFS) results were unable to give an average Pb and Zn speciation, however μ-XAS helped to identify the presence of minor mineral. Bulk XAFS results showed enhanced metal sulfide formations with OC and S addition. After integrating these results with our previous effluent solution chemistry data and microarray data we conclude that aided-metal

sulfide formations through treatment addition is possible in minewaste materials when disposed of in flooded mine pits. The mechanistic understanding gained in this study is also relevant for remediation of any other waste material rich in Pb, Zn or any similar metals using subsurface wetland systems.

Introduction

One of the main sources of heavy metal contamination at the earth's surface are milling and mining operations, especially those associated with sulfide rich tailings, which can have a heavy impact on the nearby water bodies (Edwards et al., 2000; Baker et al., 2003; Bhattacharya et al., 2006). The acid mine drainage resulting from the exposure of sulfide rich minerals to oxygen rich water leads to the leaching of several contaminants that can also affect groundwater quality (Johnson et al., 2005; Vega et al., 2006). Thus, metal contamination and possible associated acid mine drainage are significant environmental concerns globally (Nordstrom et al., 1999; Concas et al., 2006).

The Tri-State mining district situated in parts of southeast Kansas, southwest Missouri, and northeast of Oklahoma has a 120 year history of Pb- and Zn-ore mining activities. The extensive mining left a huge quantity of chat and tailings minewaste on the surface which contain trace levels of various sulfide minerals such as pyrite (FeS_2), galena (PbS), sphalerite (ZnS), and others (Newfields, 2003). The movement of soluble metals and metal-laden sediments from the landscape into surface waters via surface runoff are the primary ecological concerns for both aquatic and terrestrial organisms (Pierzynski and Vaillant, 2006). The USEPA has considered the disposal of minewaste materials in flooded subsidence pits (i.e., wetland treatment) as a remediation strategy for the highly contaminated minewaste materials with the hypothesis that under reduced conditions in sulfate-rich environments, these metals can be

transformed back into their sulfide forms, limiting their mobility, and toxicity. However, there are several challenges associated with this strategy. The minewaste materials are inherently low in dissolved OC and that could have significant impact on redox processes (Zhang et al., 2005; Hayes et al., 2006; Stein et al., 2007) as OC is the driver of biogeochemical cycling of major and trace elements (Evans et al., 2006; Borch et al., 2010). Sulfur is relatively mobile element compared to trace elements such as Pb and Zn, therefore, insufficient S content remaining in minewaste could limit sulfide formation, and promote carbonate precipitation instead, depending on pH and carbonate concentration (Falkowski et al., 2000; Toevs et al., 2007). As the Tri-State mining district has limestone parent material, higher pH and abundant $CaCO_3$ are expected (KGS, 2010), and that may enhance carbonate precipitation which is not stable as sulfides (Toevs et al., 2006). Additionally, subsurface submergence of minewaste may result in seepage of leachate with high concentrations of Pb and Zn into groundwater regardless of liners/barriers. Further, the requirement of a large volume of clean soil for capping and long term continuous monitoring could make this remedial action expensive (USEPA, 2010).

The mobility of metals depends on speciation that is highly controlled by a dynamic interplay of physical, chemical, and biological processes in wetlands (Adriano et al., 2001; Gadd et al., 2004; Toevs et al., 2006). Microbial sulfate reduction for metal remediation requires reduction of metals via biogenic sulfide formations (Labrenz et al., 2000; Finneran et al., 2002; Banfield et al., 2013). It requires multiple approaches to understand underlying mechanisms of metal sequestration and to confirm sulfide formation in a heterogeneous environment (Banfield, 2013). X-ray absorption spectroscopy is a promising and powerful tool as it is element specific and can provide information on metals in a variety of physical states: amorphous or crystalline compounds, as well as dissolved species (Nachtegaal et al., 2005). Synchrotron based X-ray

fluorescence (XRF) allows to obtain elemental maps at micro-scale resolution that provide information such as relative concentrations of elements, their spatial distribution, and correlations with other elements. Such approaches may help understand underlying mechanisms of trace element transformations. X-ray absorption spectroscopy (XAS) such as X-ray absorption near edge structure (XANES) or extended X-ray absorption fine structure (EXAFS) spectroscopy can be done in bulk and at micro-scale. Bulk XAS gives overall speciation information in studied systems whereas micro-scale spatially resolved XAS would help elucidating underlying mechanisms (Roberts et al., 2002). Analysis of bulk XAS demands a library of reference spectra in order to perform linear combination fitting that estimates a single average spectrum collected from a large spot (Manceau et al., 2000). We hypothesized that it is essential to treat these minewaste materials with OC and S to induce metal transformation back to their sulfide forms under reduced conditions thereby limiting their mobility and toxicity. Our objective of this experiment was to study the biogeochemical transformations of Pb and Zn by identification and semi quantification of the dominant forms of Pb and Zn in submerged columns using various OC and S treatments. Mechanistic information will be obtained via micro-scale spatially-resolved measurements to understand the dominant interfacial processes such as mineral dissolution, precipitation/co-precipitation, and sorption/desorption that determine the long-term fate of Pb and Zn minerals.

Materials and methods:

Highly contaminated minewaste material was collected from a secured repository area in the Tri-State mining region near Baxter Springs, KS. The material was sieved to 2-mm size, homogenized, and air-dried. A 0.5 g sample was digested in triplicate following the aqua-regia reflux tube soil digestion method in order to determine the background concentrations of selected

elements (Zarcinas et al., 1996). Particle size analysis was performed using the method of Kilmer et al. (1949). A Na_2SO_4 solution was added to the minewaste material to provide S at a ratio of 1: 2 mM of Σ metals: mM sulfur. The metals used in the summation were Pb, Cd, Zn, Fe and Mn. The treated materials were equilibrated for 10 days at room temperature on a reciprocating shaker (6010, Eberbach Corporation, Ann Arbor, MI) at 192 reciprocates/min for 3 days, and at 92 reciprocates/min for the rest 7 days. The treated and equilibrated minewaste was leached with deionized (DI) water until a target electrical conductivity of <2 mS cm^{-1} was achieved and then the materials were air-dried. Both S treated and untreated minewaste materials were inoculated with 0.5 g $100g^{-1}$ of soil slurry (Ivan, Kennebec, and Kahola silt loams) collected from the North Agronomy farm closer to the creek at Kansas State University, Manhattan, KS. Prior to its addition to the minewaste, the serial dilution of soil slurry was cultured on the petridish using postgate's medium (BP1420500), and incubated overnight at 34 ºC in an anaerobic jar (AG0025A used with oxygen absorber; OXAN0025A, Fisher Scientific, USA). The black patches observed on the plate indirectly confirmed the presence of sulfur reducing bacteria (SRBs) in the soil slurry. After inoculation, the minewaste was carefully packed in Plexiglas columns (20cm length, 3.2 cm ID with 3 windows milled at 2.8 cm, 9.84 cm, and 16.94 cm.) to achieve bulk density of about 1.7 g cm^{-3}. The packed columns were saturated slowly with DI water using a Mariotte's bottle that delivers a constant rate of flow, and the columns were equilibrated overnight before they were supplied with simulated groundwater.

The eluent consisted of a base of simulated groundwater (1 mM NaCl, 1mM $MgCl_2$, 1 mM KCl, 1 mM $CaCl_2$ adjusted to pH 7.2) with or without 10.7 mM Na-lactate (32 mM OC). This provided four treatments for the columns designated C0S0, C1S0, C0S1, and C1S1 where C0 designates simulated groundwater (Wan et al., 2005) without OC, C1 with OC, S0 designates

simulated groundwater applied to columns without added S, and S1 designates simulated groundwater applied to columns with added S. The eluent was supplied from the bottom of columns in order to avoid gravity influenced water movement. Solutions were delivered using a syringe pump (78-8210, KDS LEGATO 210, KD scientific Inc., Holliston, MA) at a rate of 13 mm day^{-1} simulating slow groundwater discharge rate as described by Wan et al. (2005). Three series of column experiments were conducted: short-, medium- and long-term using a completely randomized design with a two-way factorial combination of treatments (factor 1: organic C with two levels, 0 and 10.7 mM L^{-1}; factor 2: S with two levels, 0 and 252.7 mg Kg^{-1}). At the end of each column experiments, 20 g minewaste samples were collected at 1.2- 3.2 cm depth, from the port located at the height of 18 cm (far end). The collected samples were frozen at -40 °C until sample preparations were done for synchrotron based X-ray analysis.

Micro X-ray fluorescence and X-ray absorption spectroscopy

The micro X-ray fluorescence (μ-XRF), and micro X-ray absorption spectroscopy (μ-XAS) was conducted at sector 20-ID-B and 13-ID-E (given synchrotron facility). The 13-ID-E beamline source is a 3.6 cm period undulator optimized to provide a tunable energy as low as 2.4 KeV to 27.5 KeV. This beamline has an unfocused beam size of 3 mm x 1 mm and a focused beam size down to 2 μm x 2 μm with a greater X-ray flux. It has solid 13-element solid state Ge detector and a double crystal monochromator (DCM); Si (111) and Si (311), and two mirrors downstream DCM. Similarly, 20-ID-B utilizes a similar undulator, DCM, and detector as 13-ID-E, and has an energy range of 3-50 KeV. A week before analysis, the minewaste were dried in an anaerobic chamber, gently ground to homogenize, and embedded in electrical resin (Epotek, 401, Epoxy Technology, USA) on quartz slides following the modified procedure developed by Arai (2003).

For XAS, the angle of the incident X-ray beam was ~45^{o} with respect to the sample surface. Elemental maps were generated at ambient temperature for Pb, Zn and Fe over an area varying from 200 µm x 200 µm to 500 µm x 500 µm with 2 µm steps. Using the XRF maps, five points of interest (POIs) (high relative concentrations) for Pb and Zn and 3 POIs for Fe were identified and used for more detailed spectroscopic investigations. Micro-XAFS spectra were collected from 100 eV below the absorption edge to 300 eV beyond the absorption edge with increments varying from 0.05 to 10 eV. About 4-5 successful scans were collected at each selected POI at the Pb LIII-edge and Zn K-edge, and 3 scans at the Fe K-edge in fluorescence mode. Due to a high level of background noise (a common issue in micro-scale XAFS due to the very small amount of sample are being exposed to X-rays), only the XANES region of Pb were used for Pb data analysis, however, useable Zn XAFS data were collected and the XAFS (2 to 9 in *k*-space) region was used for Zn data analysis. Spectra were processed using the IFEFFIT software package (Ravel and Newville, 2005). During processing, replicated spectra were aligned and merged, the background was removed and then normalized. A minimal smoothing was done using IFEFFIT software by applying four point smoothing algorithm while comparing carefully with the unsmoothed spectra. The data were then converted to *k* space (*k* is the photoelectron wavenumber), and weighted with k^1 to compensate for the dampening of XAFS amplitude with increasing *k.* Zn-XAFS processed spectra were analyzed in a two-step process using labview software (ALS beamline 10.3.2, Lawrence-Berkeley National Laboratory, Berkeley, CA) for principal component analysis (PCA), and the IFEFFIT software package for linear combination fitting (LCF) (Ravel, and Newville, 2005). The standards used for micro Zn-XAS LCF were Zn-ferrihydrite, hydrozincite ($Zn_5(CO_3)_2(OH)_6$), franklinite ($Zn_{0.6}Mn_{0.32}^{+}Fe_{0.12}^{+}Fe_{1.53}^{+}Mn_{0.53}^{+}O_4$), hemimorphite ($Zn_4Si_2O_7(OH)_2.H_2O$), smithsonite ($ZnCO_3$),

sphalerite (ZnS),$Zn(SO_4)$, ZnAl -layered double hydroxide (ZnAl-LDH), and $Zn(OH)_2$ to get the consistent fit. Similarly, for micro Pb-XAS LCF, lead nitrate ($PbNO_3$), galena (PbS), anglesite ($PbSO_4$), cerussite ($PbCO_3$), lead chloride ($PbCl_2$), hydrocerussite ($Pb_3(CO_3)_2(OH)_2$), leadhillite ($Pb_4(SO_4)(CO_3)_2(OH)_2$), plumboferrite ($Pb_2Mn_{0.2}Mg_{0.1}Fe_{10.6}O_{18.4}$), plumbonacrite $Pb_{10}(CO_3)_6O(OH)_6$, and plumbogummite ($PbAl_3(PO_4)_2(OH)_5 \cdot H_2O$ were used. The spoil values are provided in the supplementary information SI (Table 1). The LCF fittings in combination with the lowest χ^2 and R-factor close to 1 were considered as the most likely set of components in our experimental spectra and were used for the data interpretations.

Bulk X-Ray Absorption Spectroscopy (Bulk-XAS)

Due to the practical limitations of μ-XAS in determining overall speciation (need large numbers of μ-XAS spectra per sample), bulk XAS was also conducted at sector 5-BM-D of DND-CAT to obtain overall elemental transformations and/or mineral formation at each submergence interval. A week before analysis, the collected samples were dried in an anaerobic chamber and gently ground to homogenize using an agate mortar and pestle. Samples were packed inside the Plexiglas sample holders with slots (1900 μm x 600 μm x 150 μm: L x W x D), and were sealed with X-ray transparent Kapton® tape. This beamline has an energy range of 4.5-25 KeV and a Si (111) double crystal monochromator that has a focused beam size of 15000 μm x 500 μm and unfocused beam size of 12 mm x 3 mm. A Canberra 13-element Ge solid state detector was used. Two Al foil (0.1 mm) layers were placed on the detector to reduce the low energy fluorescence emissions from Fe in the samples. The energy was calibrated using Pb-metal foil standard. The angle of the incident X-ray beam was ~45^o with respect to the sample surface. The samples were analyzed by using the unfocused beam of 12 mm x 3 mm under a continuous flow of the X-stream^{TM} cryogenic crystal cooler (Rigaku company, Tokyo, Japan). X-stream^{TM}

was used to minimize any beam induced elemental transformations and help maintain the integrity of redox-sensitive samples. Bulk-Pb LIII-edge and Zn K-edge spectra were collected with 6 scans per sample and were processed by following the steps as previously mentioned under µ-XAS analysis. The Pb- and Zn-XAFS region (2 to 10 in *k*-space) were used for data analysis. The LCF was conducted using the set of standards with lower spoil value provided in appendix A (supplementary information (SI) Table 1 and 2).

Results and Discussions

The mine waste material consisted of 85% sand (2000 to 50 µm), 11.3% silt (50 to 2 µm), and 3.4% clay (<2 µm). The total N and total C concentrations were 0.03 g kg^{-1}, and 1.56 g kg^{-1} respectively. The pH of a water extract (water: minewaste ratio of 2:1) was 7.2 and the electrical conductivity was 2.31 mS cm^{-1}. Select elemental concentrations of the minewaste are given in Table 1.

Micro-X-ray fluorescence and -X-ray absorption spectroscopy (Micro- XRF and -XAS)

Synchrotron based µ-XRF allows mapping of elements in thin sections/samples with higher sensitivity, better detection limits, and certainty thereby facilitating better understanding of elemental distributions and their relationships (Jassogne et al., 2009). The collection of S µ-XRF maps was not possible at the time of data collection at any of these hard X-ray beamlines. The µ-XRF maps collected on the C0S0 and C1S1 samples are presented in (Figures 4-1 and 4-2). In each map, the brightest color (white) represents the highest concentration (high fluorescence signal) of an element, while the darkest color (black) represents the lowest concentration of an element (low-fluorescence signal), although the shading is relative across

each map. The P1-Pn spots indicated on the µ-XRF maps for C0S0 revealed that Pb is more (colocalized) with Fe and Mn at short-term submergence which further remained same even under medium-term submergence. Whereas, Zn showed less correlation with Fe and Mn compared to Pb under short-term submergence that was slightly enhanced under medium-term submergence in C0S0 (Figure 4-1). It was apparent in C1S1 treatment where Pb seemed to be more associated with Fe and Mn compared to Zn over short-term submergence (Figure 4-2). This correlation was decreased over medium- and long-term submergence. The above explanations on elemental distribution and their relationship were given based on µ-XRF maps, and correlation maps provided in appendix A (SI Figure 1, 2, 3, 4, 5, 6) indicating metals' immobility was driven by adsorption, and co-precipitation of metals with Mn, and Fe(hydr)oxides under short- and medium-term submergence as a first stage in redox driven cycling. Similar results were observed for Pb and Zn reporting influence of pH and ageing Fe(hydr)oxides on metal adsorption (Kinniburgh et al., 1976; Kuo et al., 1979; Agbenin et al., 2000). During initial stages of reducing conditions, reductive dissolution of Fe results in formation of freshly precipitated Fe(hydr)oxides that has ten times higher adsorption capacity compared to aged oxides. These reactions product enhance cation exchange capacity (CEC) by 10 fold thereby immobilizing trace elements (Zn>Pb) at circumneutral pH. Cation exchange capacity (CEC) reduces as it becomes more crystalline over time (Shun et al., 1977).

An attempt was made to select five points of interest (POIs) (P1-Pn) to collect Pb and Zn-XAS, and 3 POI for Fe-XAS, however the µ-XAS data collected from all POIs were not useable. Among the useable data, two spectra of Pb and Zn were selected based on the lower χ^2 value, R-factor, and the fitting quality provided in appendix A (SI Table 3 and 4). Based on the comparison of µ-XAS results for Pb and Zn with the corresponding bulk-XAS data, it was clear

that collected μ-XAS data from few selected points were not able to provide the overall Pb and Zn speciation in all short-, and medium-term submerged samples. On the other hand, more representative micro-XAS data was observed over the long-term submergence (Figure 4-3, 4-4, 4-11a, 4-11b 4-12b, 4-12c). This could possibly be explained by significantly more heterogeneous Pb speciation/distribution during initial stages of submergence thereby providing poorly representative μ-XAS data. Micro-XAS however, was able to provide some minor Pb species formed in micro-environments such as hydroxypyromorphite, lead phosphates, and plumboferrite (Figure 4-3, 4-4, 4-11a, 4-11b 4-12b, 4-12c). A possible explanation for lead phosphates minerals formations could be due to enhanced P solubility that can be expected under reduced conditions. Similar results have been reported in several earlier studies where pyromorphite formation was observed due to enhanced P solubility under anaerobic conditions (Zhang and Ryan, 1999; Basta et al., 2004; Cao et al., 2008). The lack of agreement in micro- and bulk-XAS data is common in highly heterogeneous soil environment. Many other researchers reported that μ-XAS was unable to give average metal speciation, however was able to identify minor species due to heterogeneous metal chemistry (Manceau et al., 2000; Nachtegaal et al., 2005). Similarly, μ-XAS data for Zn was also unable to provide an average picture of Zn speciation during short- and medium-term submergence, whereas the data collected for samples submerged for long-term provided comparatively better representative Zn speciation indicating more heterogeneous nature of Zn speciation/distribution during initial stages of submergence (4-6a, 4-12b, 4-12c).

Bulk-X-ray Absorption Spectroscopy (Bulk-XAS)

Bulk Pb-XAS linear combination fitting results did not give any galena (PbS) formation in C0S0 under all short-, medium- and long-term submergence. It clearly showed that Pb

speciation in non-treated control system was dominated by Pb-carbonates (cerrusite, and hydrocerrusite) over time. This could be associated with the alkaline pH due to high carbonate concentration in minewaste materials. Dissolution of calcite provides buffering mechanism to maintain circumneutral pH that favors carbonate mineral formations. Calcite dissolution may also cause trace elements mobility and/or redistribution (Komárek, 2004). Other researchers also observed Pb-carbonates formation under alkaline pH conditions (Chen et al., 1997; Komárek, 2004; Toevs et al., 2007; Boynton et al., 2009). At alkaline pH, Pb-carbonate is the most stable Pb mineral controlling Pb solubility (Lindsay, 1979). Galena (PbS) formation was evident in C1S0 samples, and it seems that C1S0 is capable of overcoming dominating nature of carbonates in these systems through enhanced microbial activities (especially S-reducing bacteria) without any additional S additions. However, carbonates may potentially become dominating Pb mineral controlling the Pb solubility due to enhanced pH and S insufficiency in the long run. Similar observation was reported in the study conducted by Toevs et al. (2006) indicating metal carbonates controlling metals solubility at alkaline pH.

Bulk Zn-XAFS results showed that Zn appeared to be mostly transformed as silicate (hemimorphite, and willemite) when there was no OC and S addition (4-9a, 4-12a,). Hemimorphite was highly abundant in the mining district as it is extracted along with Pb and Zn ores (Boni et al., 1998; Shu et al., 2001). Further, in contrast to Pb, Zn was only partially transformed to sulfide in the OC plus S treated (C1S1) systems (4-10b, 4-12a). This could be explained by the lower affinity of Zn to S, compared to Pb. The relative affinity of free metal cation increases with the tendency of cation to form strong bonds, i.e., inner sphere complexes (Randall et al., 2001; Stein et al., 2007). Similar results were reported by Brennan and Lindsay (1996). Additionally, sphalerite (ZnS), and FeS_2 (pyrite) precipitate at similar pe+pH, Zn^{2+}

activity cannot be depressed significantly by the formation of sphalerite (ZnS) as redox will be poised by the transformation of iron oxides to FeS_2 (pyrite). Since soil contains more Fe than Zn, sufficient S is required to make labile Fe oxides to form pyrite and drop pe+pH thereby allowing sphalerite (ZnS) to control Zn solubility (Lindsay, 1979). This may be why we observed sphalerite (ZnS) formation only in C1S1 treatment where sufficient S was available. Overall, galena (PbS) formation in both C1S0 and C1S1 indicated that adding OC to these minewaste would make these transformations more efficient. On the other hand, treatment with only S addition may not be conducive and/or sufficient for stabilization of Pb, and Zn in the long run, as sufficient labile OC must be available for sulfate reduction and is a key rate-limiting factor of metal sulfide formation (Morse et al., 2002; Ku et al., 2008).

Considering the long-term consequences via minerals transformations observed in all treatments, adding OC plus S for metal sulfide formation may be a more promising option for managing minewaste materials disposed of in flooded subsidence mine pits. Trace metal sulfides are more stable than carbonates at wide range of pH and are highly resistant to desorption effects of chlorides (Zn, Cu and Cd), hydroxides and bicarbonates (Zn) under anoxic conditions (Du Liang et al., 2009). Precipitation of metal sulfides can act as a sink for trace metal contaminants (Nordstrom, 1999). Metals such as Pb, Zn, Cu can adsorb to or co-precipitate with iron mono-sulfide and they can also precipitate directly as discrete phases (Billon et al., 2001). However, challenges associated with this strategy would be exposure to oxygen rich waters causing sulfide oxidation that could constitute a secondary source of trace metal contamination. Another challenge would be maintaining enough sulfate concentration. For sulfide formation to happen, sulfate concentration should be at least 30 μM or methanogenic bacteria could out-compete sulfate reducers for substrate. Despite these challenges, careful application of OC plus S

treatment with agronomic and engineering control would be the best among available options as long as the minewaste are submerged in the subsidence pits.

Conclusions

It is clear from the current study that the addition of OC and S promoted metal sulfide formation. These observations were also supported by the solution chemistry data (Karna et al., 2014a (Chapter 3)) indicating effective immobilization of Pb and Zn under both medium- and long-term submergence, and the microarray results indicating enhanced sulfur reducing bacteria (SRBs) genes on OC plus S addition playing role in dissimilatory sulfate reduction thereby forming metal sulfides under a long-term submergence (Karna et al., 2014c (Chapter 5)). This study shows that the disposal of minewaste materials high in Pb and Zn in flooded subsidence pits could be an effective way of reducing ecological risk associated with leaving Pb and Zn risk minewaste materials aboveground.

Acknowledgements

We acknowledge Kansas State University Research and Extension, Kansas State University, Manhattan, KS for conducting this experiment. We highly acknowledge Advanced Photon Source, Chicago, IL supported by U.S. DOE under Contract # DE-AC02-06CH11357 for providing us beam time to conduct synchrotron based X-ray analysis. We also acknowledge Matt Newville at Sector 13-ID E, Chen Jung Shun at Sector 20-ID B, and Qing Ma at Sector 5-BMD, APS, Chicago, IL for assisting us with XAS data collections, and soil chemistry group and lab assistants especially Dorothy Menefee for helping me with experimental set up.

References

Adriano, D. C. 2001. Trace elements in terrestrial environments: Biogeochemistry, bioavailability, and risks of metals. Springer- Verlag, New York.

Arai, Y.; Lanzirotti, A.; Sutton, S.; Davis, J. A.; and Sparks, D. L. 2003. Arsenic speciation and reactivity in poultry litter. Environmental Science and Technology. 37:4083-4090.

Agbenin, J. O., and Olojo, L. A. 2004. Competitive adsorption of copper and zinc by a bt horizon of a savanna alfisol as affected by pH and selective removal of hydrous oxides and organic matter. Geoderma. 119:85-95.

Baker, B. J., and Banfield, J. F. 2003. Microbial communities in acid mine drainage. FEMS Microbiology Ecology. 44:139-152.

Basta, N., and McGowen, S. 2004. Evaluation of chemical immobilization treatments for reducing heavy metal transport in a smelter-contaminated soil. Environmental Pollution. 127:73-82.

Borch, T., Kretzschmar, R., Kappler, A., Cappellen, P. V., Ginder-Vogel, M., and Voegelin, A. 2009. Biogeochemical redox processes and their impact on contaminant dynamics. Environmental Science and Technology. 44:15-23.

Boynton, W. V., Ming, D. W., Kounaves, S. P., Young, S. M., Arvidson, R. E., and Hecht, M. H. 2009. Evidence for calcium carbonate at the mars phoenix landing site. Science (New York, N.Y.). 325:61-64.

Brennan, E., and Lindsay, W. 1996. The role of pyrite in controlling metal ion activities in highly reduced soils. Geochimica Et Cosmochimica Acta. 60:3609-3618.

Cao, X., Ma, L. Q., Singh, S. P., and Zhou, Q. 2008. Phosphate-induced lead immobilization from different lead minerals in soils under varying pH conditions. Environmental Pollution. 152:184-192.

Chen, X., Wright, J. V., Conca, J. L., and Peurrung, L. M. 1997. Effects of pH on heavy metal sorption on mineral apatite. Environmental Science and Technology. 31:624-631.

Concas, A., Ardau, C., Cristini, A., Zuddas, P., and Cao, G. 2006. Mobility of heavy metals from tailings to stream waters in a mining activity contaminated site. Chemosphere. 63:244-253.

Edwards, K. J., Bond, P. L., Druschel, G. K., McGuire, M. M., Hamers, R. J., and Banfield, J. F. 2000. Geochemical and biological aspects of sulfide mineral dissolution: Lessons from iron mountain, California. Chemical Geology. 169:383-397.

Evans, C. D., Chapman, P. J., Clark, J. M., Monteith, D. T., and Cresser, M. S. 2006. Alternative explanations for rising dissolved organic carbon export from organic soils. Global Change Biology. 12: 2044–2053.

Falkowski, P., Scholes, R. J., Boyle, E., Canadell, J., Canfield, D., Elser, J. 2000. The global carbon cycle: A test of our knowledge of earth as a system. Science (New York, N.Y.). 290:291-296.

Finneran, K. T., Anderson, R. T., Nevin, K. P., and Lovley, D. R. 2002. Potential for bioremediation of uranium-contaminated aquifers with microbial U (VI) reduction. Soil and Sediment Contamination: An International Journal. 11:339-357.

Gadd, G. M. 2004. Microbial influence on metal mobility and application for bioremediation. Geoderma. 122:109-119.

Hayes, J. M., and Waldbauer, J. R. 2006. The carbon cycle and associated redox processes through time. Philosophical Transactions of the Royal Society of London. Series B, Biological Sciences. 361:931-950.

Kinniburgh, D., Jackson, M., and Syers, J. 1976. Adsorption of alkaline earth, transition, and heavy metal cations by hydrous oxide gels of iron and aluminum. Soil Science Society of America Journal. 40:796-799.

Labrenz, M. 2000. Formation of sphalerite (ZnS) deposits in natural biofilms of sulfate-reducing bacteria. Science. 290:1744-1747.

Labrenz, M., and Banfield, J. 2004. Sulfate-reducing bacteria-dominated biofilms that precipitate ZnS in a subsurface circumneutral-pH mine drainage system. Microbial Ecology. 47:205-217.

Manceau, A., Schlegel, M., Musso, M., Sole, V., Gauthier, C., and Petit, P. 2000. Crystal chemistry of trace elements in natural and synthetic goethite. Geochimica Et Cosmochimica Acta. 64:3643-3661.

Moreau, J. W., Webb, R. I., and Banfield, J. F. 2004. Ultrastructure, aggregation-state, and crystal growth of biogenic nanocrystalline sphalerite and wurtzite. American Mineralogist. 89:950-960.

Nachtegaal, M., Marcus, M. A., Sonke, J. E., Vangronsveld, J., and Van Der Lelie, D. 2005. Effects of in situ remediation on the speciation and bioavailability of zinc in a smelter contaminated soil. Geochimica.Et Cosmochimica Acta. 69:4649-4664.

Nordstrom, D. K., and Alpers, C. N. 1999. Negative pH, efflorescent mineralogy, and consequences for environmental restoration at the iron mountain superfund site, California.

Proceedings of the National Academy of Sciences of the United States of America. 96: 3455-3462.

Randall, S. R., Sherman, D. M., and Ragnarsdottir, K. V. 2001. Sorption of as (V) on green rust (Fe 4 (II) Fe 2 (III)(OH) 12SO4• 3H2O) and lepidocrocite (gamma-FeOOH): Surface complexes from EXAFS spectroscopy. Geochimica Et Cosmochimica Acta. 65:1015-1023.

Roberts, D. R., Scheinost, A., and Sparks, D. 2002. Zinc speciation in a smelter-contaminated soil profile using bulk and microspectroscopic techniques. Environmental Science and Technology. 36:1742-1750.

Shu, W., Ye, Z., Lan, C., Zhang, Z., and Wong, M. 2001. Acidification of lead/zinc mine tailings and its effect on heavy metal mobility. Environment International. 26:389-394.

Shuman, L. 1977. Adsorption of Zn by Fe and al hydrous oxides as influenced by aging and pH. Soil Science Society of America Journal. 41:703-706.

Vega, F. A., Covelo, E. F., and Andrade, M. 2006. Competitive sorption and desorption of heavy metals in mine soils: Influence of mine soil characteristics. Journal of Colloid and Interface Science. 298:582-592.

Zhang, M., and Gorski, W. 2005. Electrochemical sensing platform based on the carbon nanotubes/redox mediators-biopolymer system. Journal of the American Chemical Society. 127:2058-2059.

Zhang, S., Xue, X., Liu, R., and Jin, Z. 2005. Current situation and prospect of the comprehensive utilization of mining tailings. Mining and Metallurgical Engineering. 3:44-48.

Figures and Tables

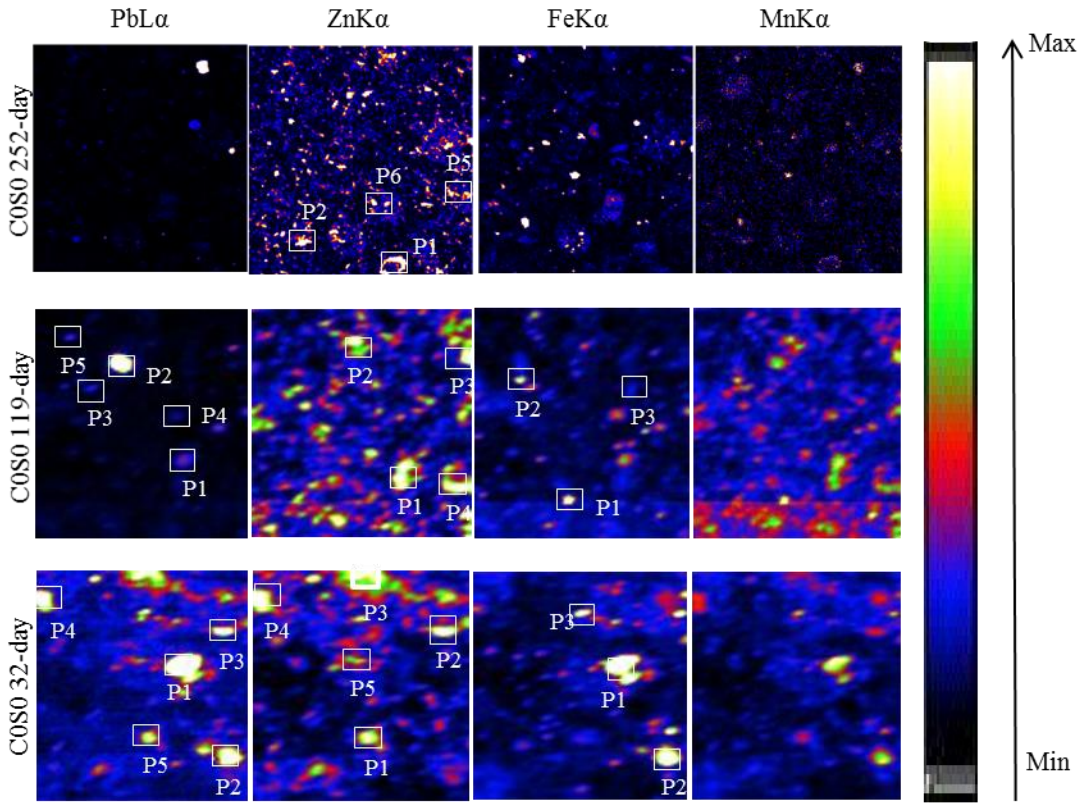

Figure 4-1: Micro-XRF maps, showing the elemental distribution of lead (Pb), zinc (Zn), iron (Fe), and manganese (Mn) in control (C0S0) samples under short (32-day), medium-term (119-day) and long-term (252-day) submergence. The µ-XRF map for control (C0S0) submerged for 252-day could not be collected. In each map, the brightest color (white) represents the highest fluorescence signal or highest concentration of an element, while the darkest color represents the lowest fluorescence signal or lowest concentration of an element.

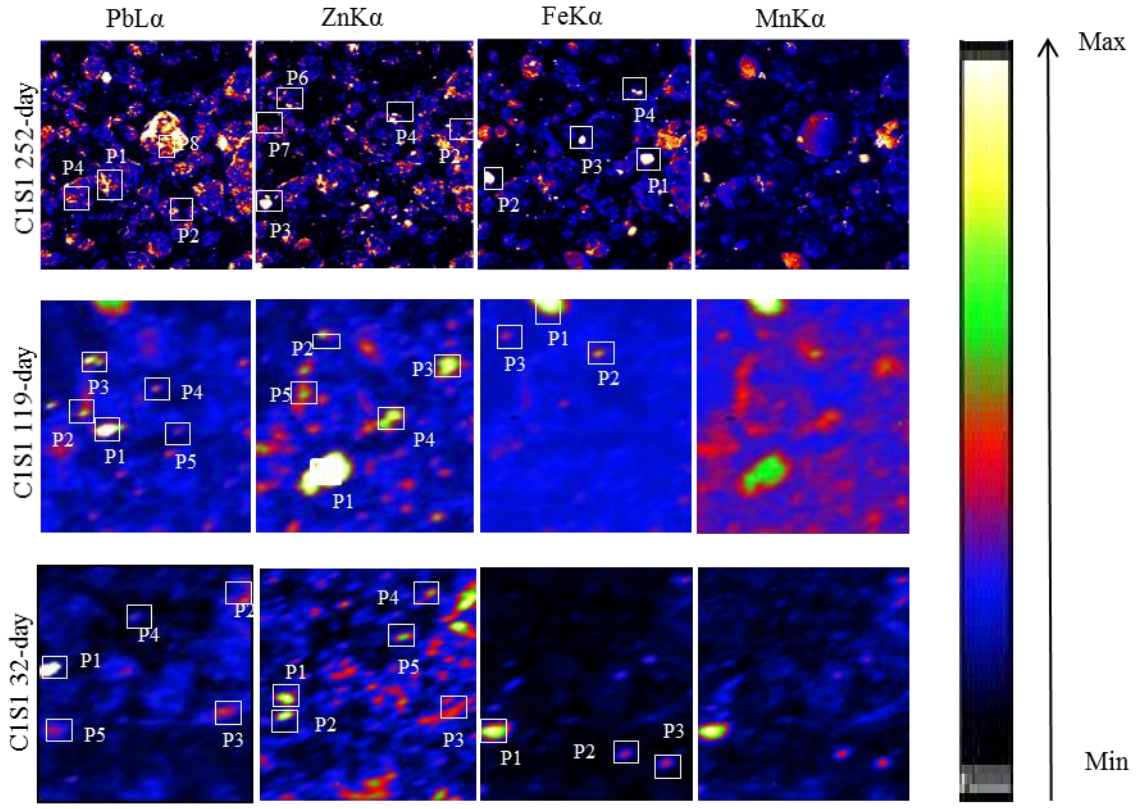

Figure 4-2: Micro-XRF maps, showing the elemental distribution of lead (Pb), zinc (Zn), iron (Fe), and manganese (Mn) in OC plus S treated (C1S1) samples under short (32-day), medium (119-day) and long-term (252-day) submergence. In each map, the brightest color (white) represents the highest fluorescence signal or highest concentration of an element, while the darkest color represents the lowest fluorescence signal or lowest concentration of an element.

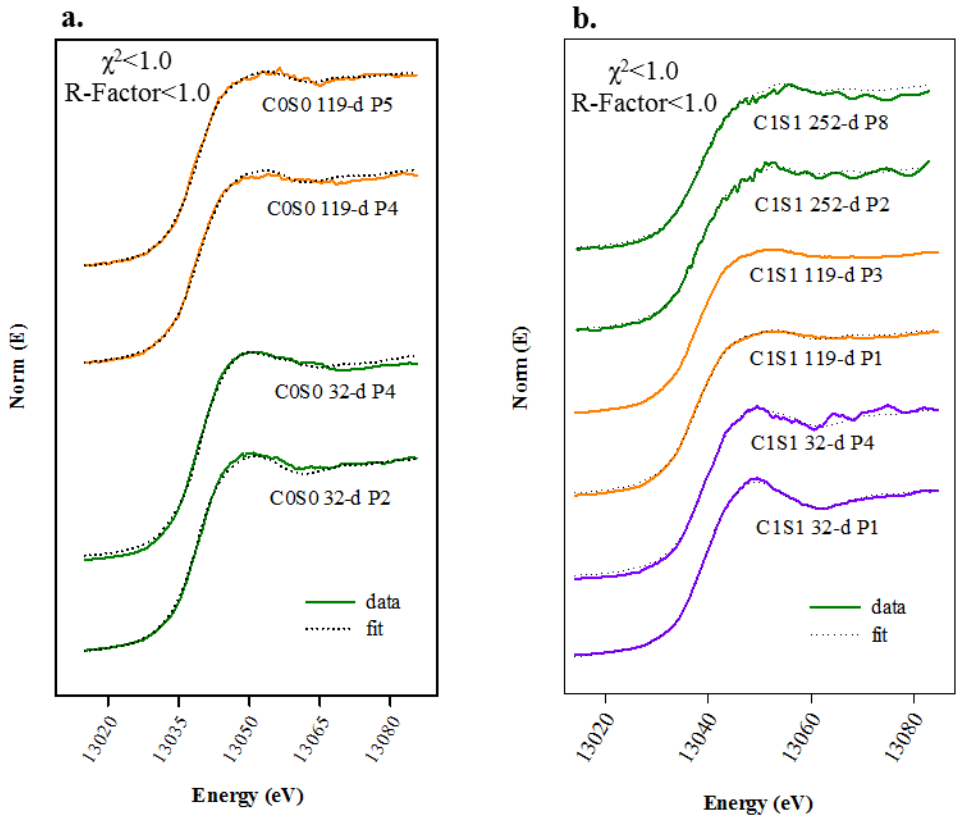

Figure 4-3: Micro Pb-XANES spectra a) for control (C0S0), b) OC plus S treated (C1S1) samples under short (32-day), medium-term (119-day), and long-term (252-day) submergence. In each spectrum, 'd' represents days of submergence, and P1-P5 represents the points selected on micro-XRF maps for XANES data collection. Solid lines represent the normalized spectra and the dotted lines represent the best fits obtained using statistical analyses; principal component analysis (PCA), and linear combination fitting (LCF).

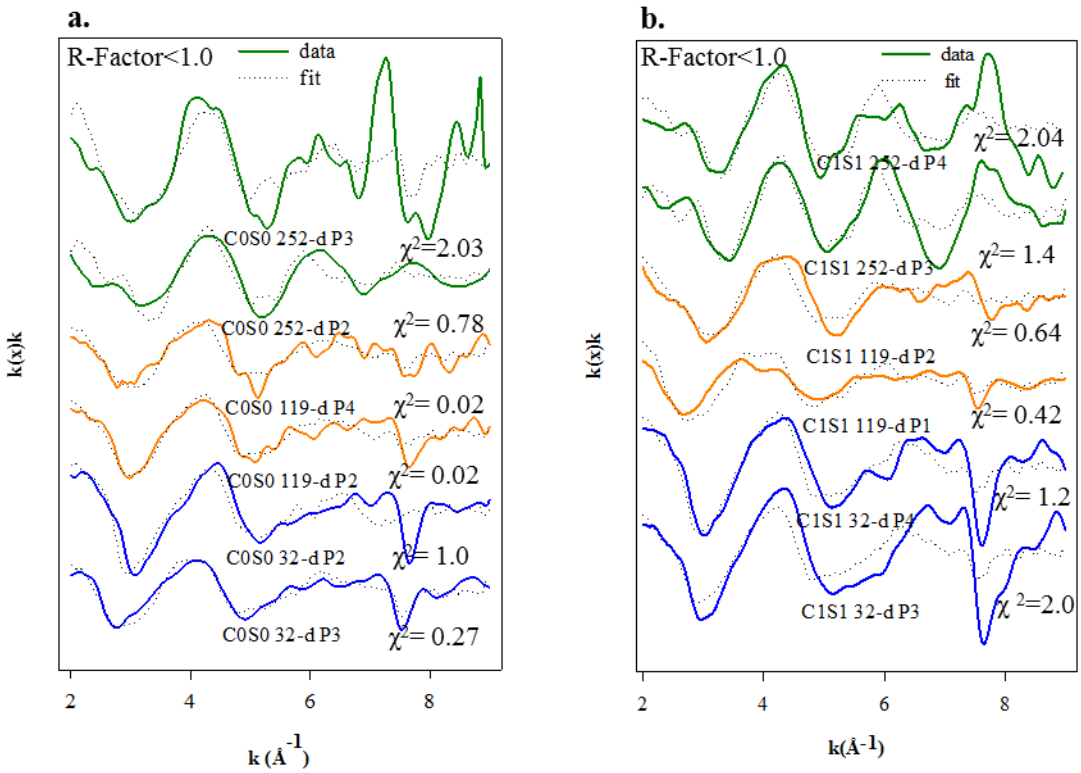

Figure 4-4: Micro Zn-XAFS spectra a) for control (C0S0), b) OC plus S treated (C1S1) samples under short (32-day), medium (119-day), and long-term (252-day) submergence. In each spectrum d represents days of submergence, and P1-P5 represents the points selected on micro-XRF maps for XAFS data collection. Solid lines represent the k^1-weighted χ-spectra, and the dotted lines represent the best fits obtained using statistical analyses; principal component analysis (PCA), and linear combination fitting (LCF).

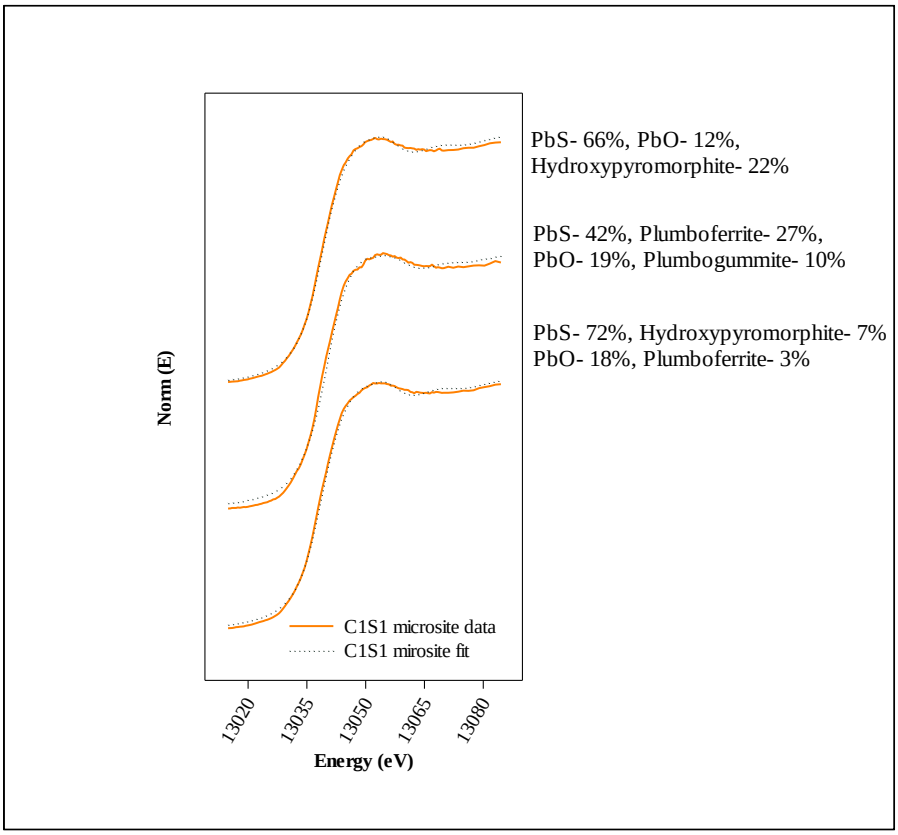

Figure 4-5: Micro Pb-XANES spectra collected from microsite formed in OC plus S treated (C1S1) submerged for 119-day. Solid lines represent the normalized spectra and the dotted lines represent the best fits obtained using statistical analyses; principal component analysis (PCA), and linear combination fitting (LCF).

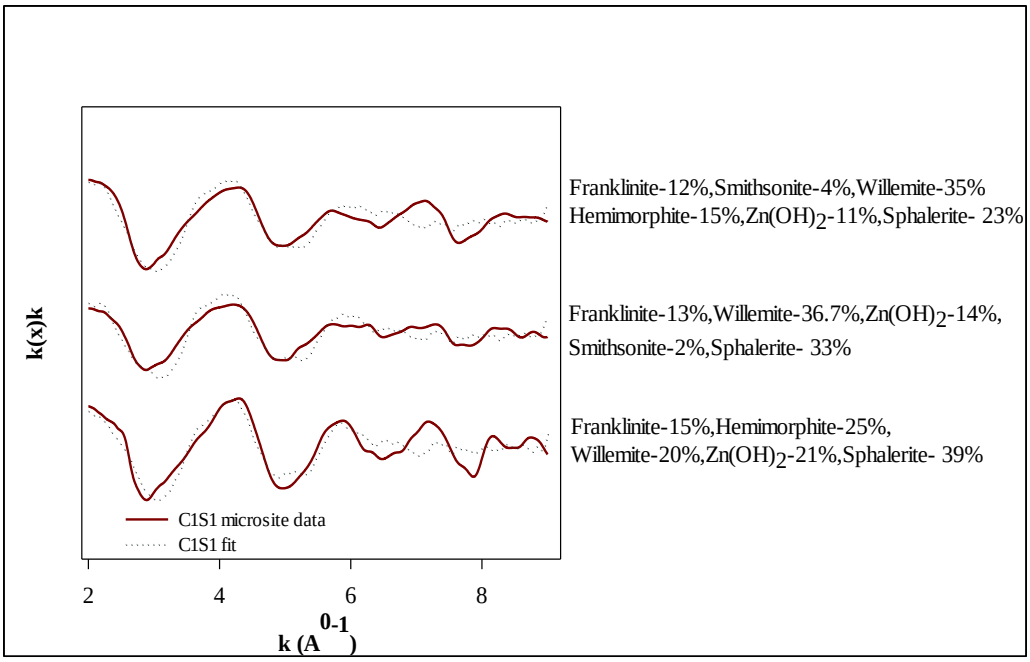

Figure 4-6: Micro Zn-XAFS spectra collected from microsite formed in OC plus S treated (C1S1) submerged for 119-day. Solid lines represent the k^1-weighted χ-spectra, and the dotted lines represent the best fits obtained using statistical analyses; principal component analysis (PCA), and linear combination fitting (LCF).

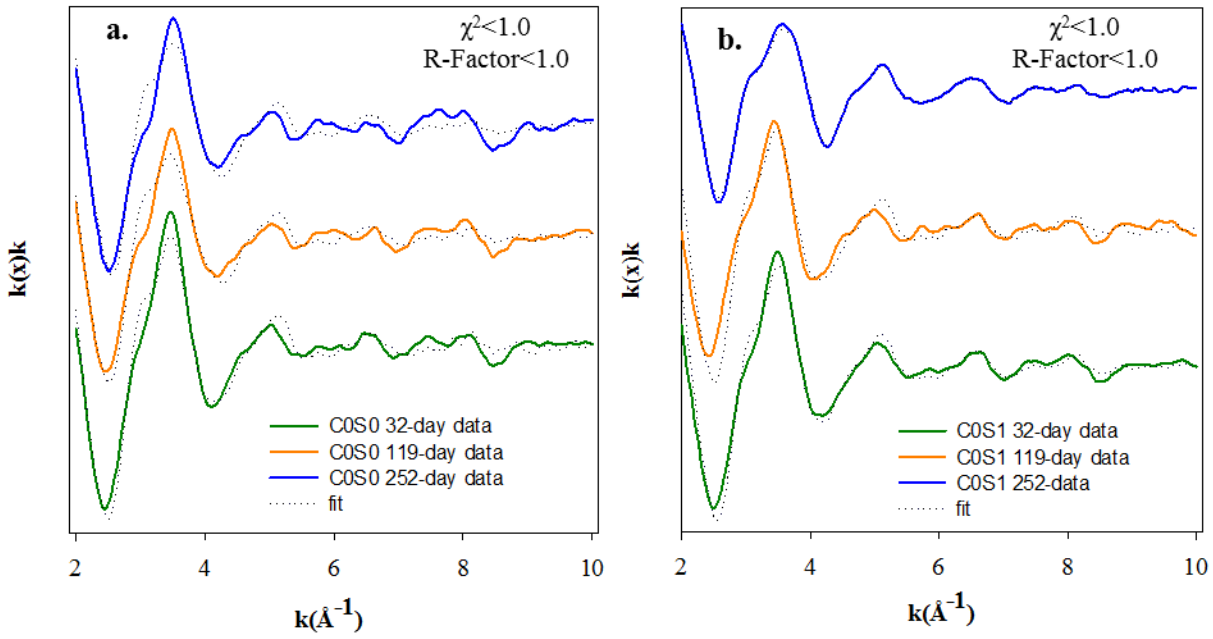

Figure 4-7: Bulk Pb-XAFS spectra collected for a) control (C0S0), and only S treated (C0S1) samples submerged for short (32-day), medium (119-day) and long-term (252-day) submergence. Solid lines represent the k^1-weighted χ-spectra, and the dotted lines represent the best fits obtained using statistical analyses; principal component analysis (PCA), and linear combination fitting (LCF).

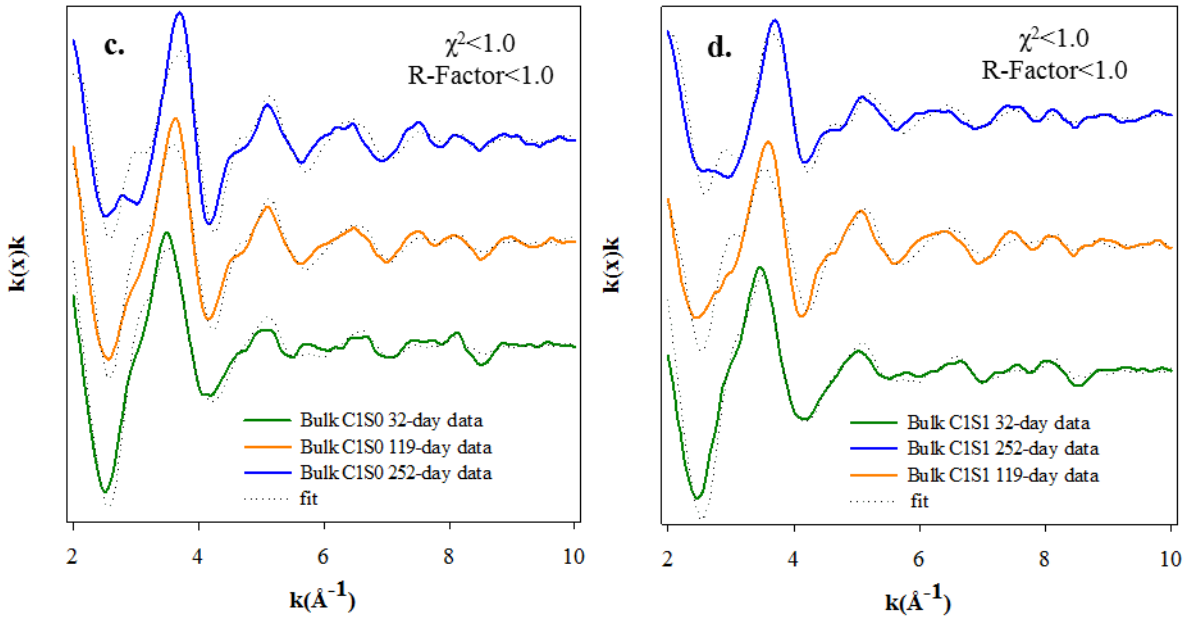

Figure 4-8: Bulk Pb-XAFS spectra collected for a) only OC treated (C1S0), and OC plus S treated (C1S1) samples submerged for short (32-day), medium (119-day) and long-term (252-day) submergence. Solid lines represent the k^1-weighted χ-spectra, and the dotted lines represent the best fits obtained using statistical analyses; principal component analysis (PCA), and linear combination fitting (LCF).

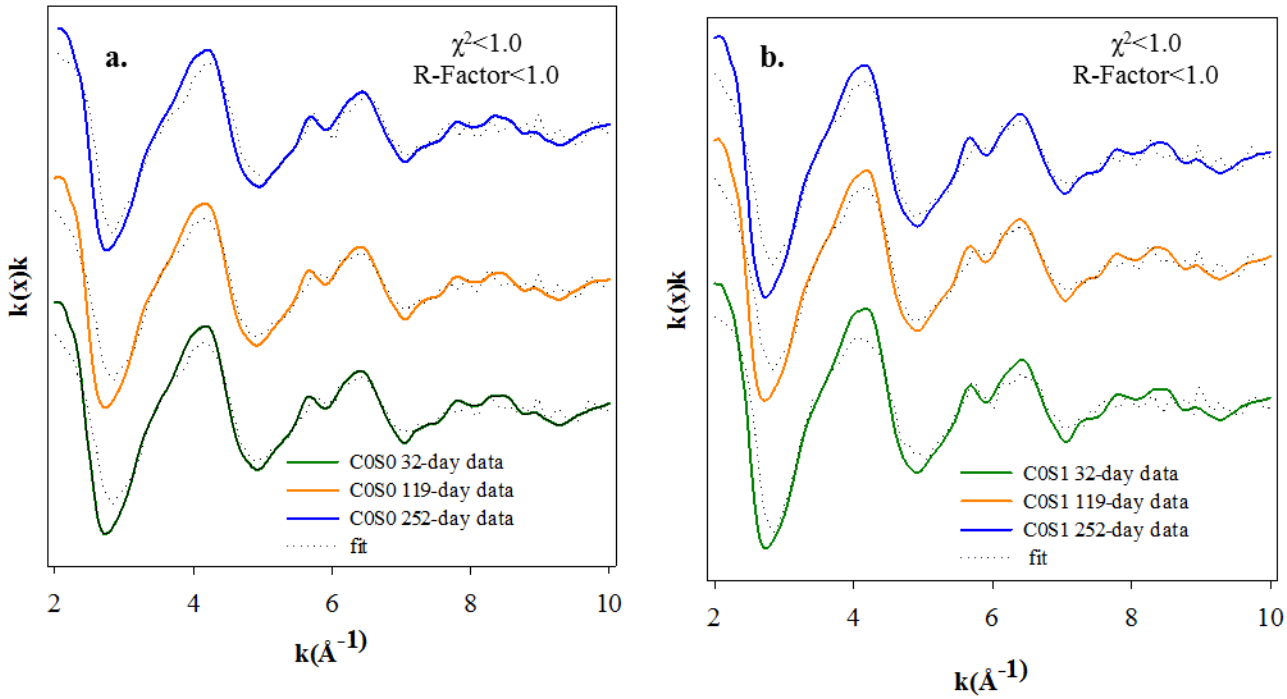

Figure 4-9: Bulk Zn-XAFS spectra collected for a) control (C0S0), and only S treated (C0S1) samples submerged for short (32-day), medium (119-day) and long-term (252-day) submergence. Solid lines represent the k^1-weighted χ-spectra, and the dotted lines represent the best fits obtained using statistical analyses; principal component analysis (PCA), and linear combination fitting (LCF).

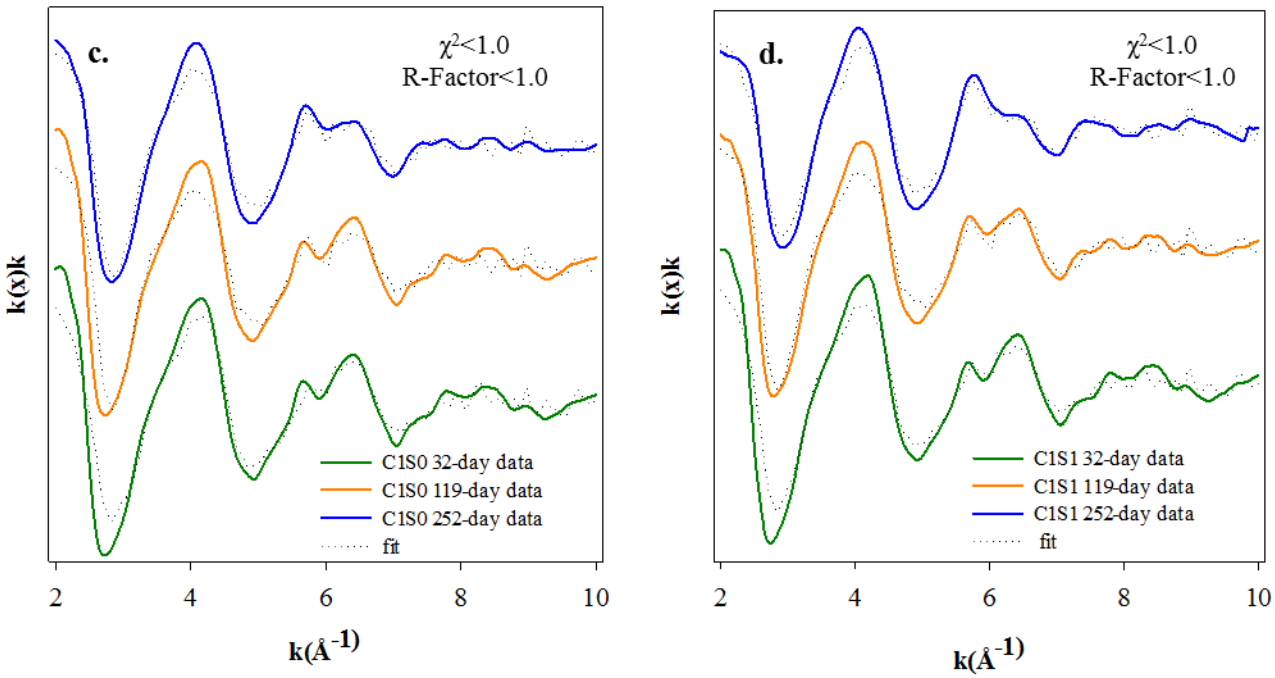

Figure 4-10: Bulk Zn-XAFS spectra collected for a) only OC treated (C1S0), and OC plus S treated (C1S1) samples submerged for short (32-day), medium (119-day) and long-term (252-day) submergence. Solid lines represent the k^1-weighted χ-spectra, and the dotted lines represent the best fits obtained using statistical analyses; principal component analysis (PCA), and linear combination fitting (LCF).

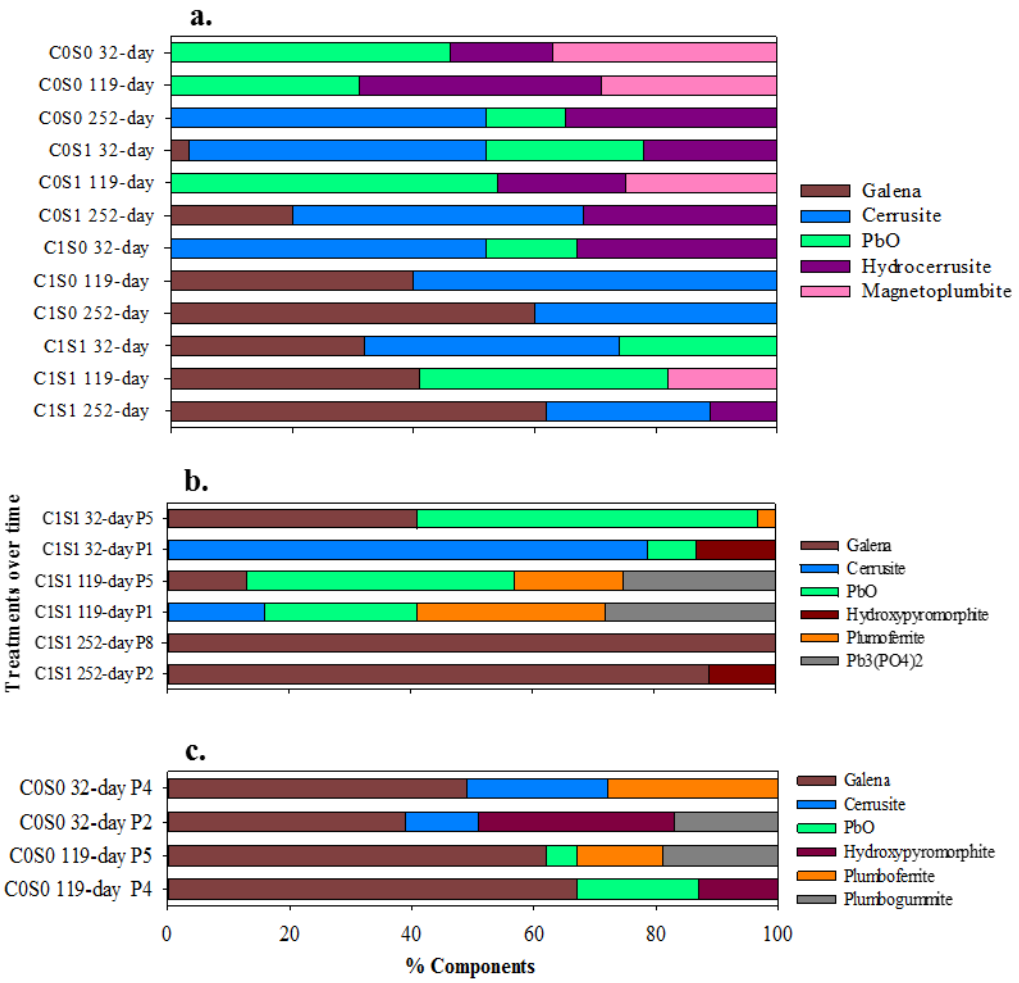

Figure 4-11: a) Bulk Pb-XAFS linear combination fitting (LCF) results for control (C0S0), only S treated (C0S1), only OC treated (C1S0), and OC plus S treated (C1S1), b) micro Pb-XANES LCF results for OC plus S treated (C1S1), c) micro Pb-XANES LCF results for control (C0S0) showing % components of Pb minerals formed under short (32-day), medium (119-day), and long-term (252-day) submergence.

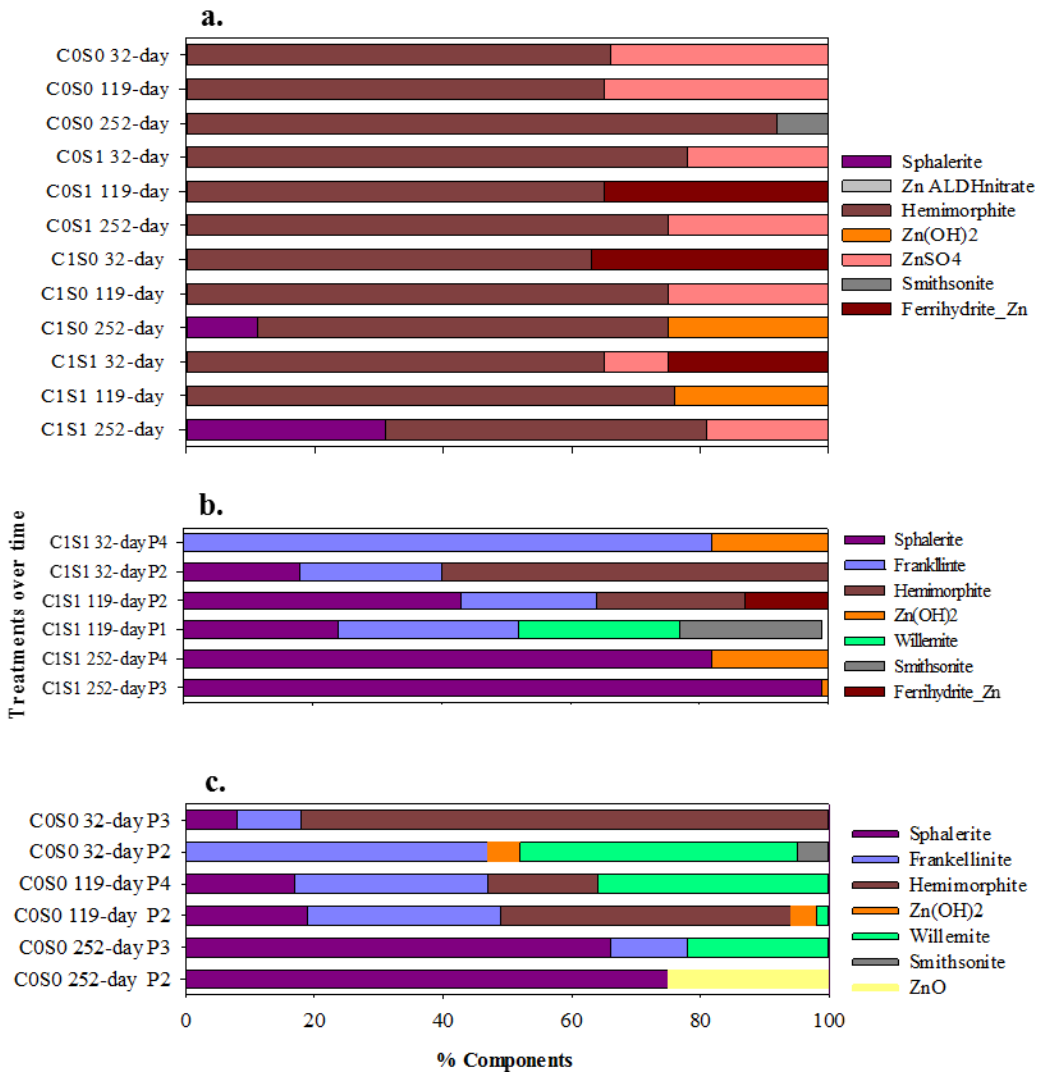

Figure 4-12: Bulk Zn-XAFS linear combination fitting (LCF) results for control (C0S0), only S treated (C0S1), only OC treated (C1S0), and OC plus S treated (C1S1), b) micro Zn-XANES LCF results for OC plus S treated (C1S1), c) micro Zn-XANES LCF results for control (C0S0) showing % components of Pb minerals formed under short (32-day), medium (119-day), and long-term (252-day) submergence.

Table 4-1: Total element concentration in minewaste collected from the Tri-State mining district.

Element	Cd	Pb	Zn	Fe	Mn	S
mg kg^{-1}	67	5048	23468	6834	97	9458

Chapter 5 - Microbial Population Dynamics, and Role of SRB Genes in Stabilizing Lead and Zinc under Subsurface Environment

Abstract

Milling and mining metal ores are some of the major sources of heavy metal contamination. The spring river, and its tributaries in southeast Kansas are contaminated with Pb, Zn and Cd, due to 120 years of historic mining activities conducted in the Tri-State mining district. Trace metal transformations and cycling in minewaste materials could greatly influence their mobility and toxicity and therefore affecting plant productivity ecosystem and human health. It has been hypothesized that under reduced conditions in sulfate rich environments, these metals can be transformed back into their sulfide forms limiting their mobility and toxicity. We have attempted to study biogeochemical transformation of Pb and Zn in flooded subsurface minewaste materials, natural or treated with organic carbon (OC), and sulfur (S), by combining advanced microbiological and X-ray microspectroscopic techniques. The specific objectives of the current study were to measure the effect of OC and S on the microbial community structure, and identify the dominant functional genes directly involved in the biogeochemical transformations, especially metal sulfide formation over time. Short-, medium- and long-term saturated column experiments were conducted. The samples collected from the medium- and long-term submerged columns were used to investigate the change in microbial community structure, their functional roles, and the key genes involved in biogeochemical transformations of Pb and Zn via functional gene array (FGA 4.2) that targets 740 functional genes, and 95847 probes. The total number of detected genes decreased under long-term submergence; however, major functional genes were much enhanced with the OC plus S treatment. The microbial

community was extremely responsive to OC and S addition, exhibiting a substantial change in structure. Sulfur reducing bacteria genes; dsrA/ B were identified as key players in metal sulfide formation via dissimilatory sulfate reduction. Integrating the microarray results with synchrotron X-ray based spectromicroscopic and solution chemistry analyses, it is suggested that OC plus S treatment would be a promising strategy for minewaste materials in the Tri-State mining district under similar conditions.

Introduction

The main environmental concern associated with milling and mining activities are related to the generation of huge amounts of wastes loaded with several heavy metal contaminants (Edwards et al., 2000; Baker et al., 2003; Bhattacharya et al., 2006). Heavy metals are dispersed via different pathways such as wind erosion, surface water runoff, and transport of metal laden sediments to neighboring water bodies (Johnson et al., 2005; Vega et al., 2006; Almendras et al., 2009). The Tri-State mining district in parts of southeast Kansas, southwest Missouri and northeast Oklahoma was one of the largest Pb and Zn ore mining districts in the world for 120 years until 1970. The movement of soluble metals and metal-laden sediments from the landscape into surface waters via surface runoff are the primary ecological concerns for both aquatic and terrestrial organisms (Pierzynski and Vaillant, 2006). The USEPA has suggested wetland construction as a remediation strategy for the highly contaminated abandoned minewaste materials with the hypothesis that under reduced conditions in sulfate-rich environments, these metals can be transformed back into their sulfide forms, limiting their mobility, and toxicity.

However, there are several challenges associated with this strategy. Minewaste material with low dissolved OC content could have significant impacts on redox processes (Zhang et al.,

2005; Hayes et al., 2006; Stein et al., 2007) as OC is the main driver of biogeochemical cycling of major and trace elements (Evans et al., 2006; Borch et al., 2009). Limited S in minewaste could limit sulfide formation, and promote carbonate precipitation, depending on pH and carbonate concentration (Toevs et al., 2006). Therefore, the addition of OC and S could allow these metals to be transformed back into their sulfide forms under reduced conditions thereby limiting their mobility and toxicity. A sulfate reduction reaction using organic matter (OM) as an electron donor is:

SO_4^{2-}+ OM (2C) +$2H_2O$→ H_2S+ $2HCO_3^-$ (pH<7.0) (Stein et al., 2007)

At high metal concentrations, metals tend to precipitate as metal sulfides at pH<7.0, as the rate of H_2S formation increases at pH of 7.0 to a maximum of 8.0 (Morris et al., 1972, Nielsen et al., 1988; Burton et al., 2008).

$H_2S+M^{2+}\rightarrow MS+2H^+$

The above mentioned reaction is the result of dissimilatory sulfate metabolism that has been successfully tested in removing contaminants via biostimulation. Of all the metal sulfide minerals, iron sulfide mineralization is most often attributed to microbial activity (McLean and Southam, 2007), especially to the activity of dissimilatory SRBs. Environmentally important activities displayed by SRBs are the result of metabolic production of high levels of sulfides that are reactive and participate in subsequent mineral formation (Lovely et al., 1995; Bazylinski and Frankel, 2003). Sulfate-reducing bacteria encompass 60 genera and 220 species (Barton et al., 2009) and are ubiquitous as they can tolerate a wide range of environmental conditions including temperatures below 5 °C and above 50 °C and pH values as low as 2.6 and as high as 9.5 (Lee et al., 1995; Stein et al., 2007). Sulfate-reducing bacteria can use a large variety of compounds as electron donors, and have been proven to perform dissimilatory reduction of U(VI) (Lovely,

1995), Cr(VI), Pd(II) as well as some organic compounds (Barton et al., 2009). In addition, SRBs biofilm reactors are reported to entrap or precipitate metals such as Cd, Cu and Zn reported possible stability of Zn, Cu, and Pb (Zn<Cu<Pb) using SRBs (White and Gadd, 2000; Labrenz, 2000; Almendras et al., 2009).

The ability of microbes to affect and/or mediate metal mobilization or immobilization processes depends upon its ability to influence metal distribution among soluble and insoluble phases (McLean et al., 2002; Gadd 2010). Most metal-microbes interactions have been studied as a means of removal, immobilization, and detoxification of metal or radionuclide pollutants (Eccles, 1999; Ramasamy et al., 2007). These previous studies have revealed that microbially mediated metals immobilization involves transformation of metals into insoluble and chemically stable forms. The mechanisms through which metal immobilizations occur are: biosorption, metal precipitation by sulfate reduction, redox transformation, methylation, and plant-microbe interactions (Gadd, 2002, 2010; Kosolapov et al., 2004).

Using a culture-dependent technique would not be feasible to study the complex microbial community as 99% of microorganisms have not been cultured yet (Whitman, 1998). Therefore culture independent techniques like functional gene arrays (FGA) are required (Van Nostrand et al., 2011; Tu et al., 2014). GeoChip 4.2 is a functional gene array targeting 740 functional genes, and 95847 probes involved in the biogeochemical processes and functional activities of microbial communities important to human health, ecosystem management, agriculture, energy, global climate change, and environmental cleanup and restoration including N, C, S and P cycling, metal reduction and resistance, and organic contaminant degradation (Tu et al., 2014). This technique allows detection, characterization and quantification of microorganisms in minewaste and to link microbial diversity to ecosystem processes and

functions (He et al., 2007; Loick et al., 2014). This technique has been successfully used for tracking the dynamics of metal-reducing bacteria and associated communities for an in situ bioremediation study (Wu et al., 2007; He et al., 2007; Zhou et al., 2008, Van Nostrand et al., 2009, 2011; Lu et al., 2012).

There are not many studies combining microbial analysis with solution chemistry, microscopic, and X-ray spectroscopic techniques to develop a molecular-scale understanding of complex biogeochemical processes affecting soil and water quality (Brown et al., 1999; Brantley et al., 2007). An attempt was made to explore an interplay between geochemical and biological processes in the transformation of Pb and Zn in natural subsurface environments biostimulated by the addition of OC and S. Stimulating the systems with OC and S would favor SRBs growth and activities. We expect that OC plus S treatment would result in a higher abundance of SRB genes compared to natural, OC alone, or S alone treatments. The study objectives were: a) to characterize the microbial community playing a role in the biogeochemical transformation of Pb and Zn under reduced conditions; b) to measure the change in microbial community structure with OC and/or S treatment over medium- and long-term submergence; and c) to identify the most dominant genes and the associated mechanisms involved in effective immobilization of Pb and Zn.

Materials and Methods

Sample collection, and experimental setup

The highly contaminated mine tailing materials were collected from a secured repository area in Baxter Springs, KS; a part of the Tri-State mining district that has a history of 120 years of Pb- and Zn-ore mining related activities. The minewaste was sieved to a 2 mm size and was digested following the aqua-regia reflux tube soil digestion method in order to determine the

background concentrations of selected elements (Zarcinas et al., 1996). Based on the sum of background elemental concentration of Pb, Zn, Cd, Fe, Mn, Na_2SO_4 solution was added to a portion of minewaste materials. The required amount of a Na_2SO_4 was calculated based on the 1: 2 mM ratio of Σ metals: S. The S treated minewaste material was equilibrated for 10 days at room temperature on a reciprocating shaker (6010, Eberbach Corporation, Ann Arbor, MI) at 192 reciprocates/min for 3 days, and at 98 reciprocates/min afterwards. The treated and equilibrated minewaste was further leached with deionized (DI) water until a target <2 mS cm^{-1} electric conductivity was achieved, and then air dried. The S retention after leaching with DI water was about 50% of total added S. Both S treated and untreated minewaste materials were inoculated with 0.5 g $100g^{-1}$ of soil slurry (Ivan, Kennebec, and Kahola silt loams) collected from the North Agronomy farm closer to the creek at Kansas State University, Manhattan, KS. Prior to its addition to the minewaste, a serial dilution (10^{-1} to 10^{-5}) of soil slurry was cultured on a petri dish using Postgate's medium (BP1420500) and incubated overnight at 34 ºC in an anaerobic jar (AG0025A used with the oxygen absorber; OXAN0025A, Fisher Scientific, USA). The black patches observed on the petridish indirectly confirmed the presence of SRBs in the soil slurry. The method used for SRB culturing was adapted from Luptakova et al. (2005). The minewaste materials (non-treated or treated with S) were well-mixed with soil slurry, and used to pack Plexiglas columns (20 cm length, 3.2 cm ID with 3 windows milled to achieve a bulk density of about 1.7 g cm^{-3}. The packed columns were saturated slowly with DI water using a Mariotte's bottle that delivers a constant rate of flow before eluent solution was supplied. The eluent consisted of a base of simulated groundwater (1 mM NaCl, 1mM $MgCl_2$, 1 mM KCl, 1 mM $CaCl_2$ adjusted to pH 7.2) with or without 10.7 mM Na-lactate (32 mM OC). This provided four treatments for the columns designated C0S0, C1S0, C0S1, and C1S1 where C0 designates

simulated groundwater without OC, C1 with OC, S0 designates simulated groundwater applied to columns without added S, and S1 designates simulated groundwater applied to columns with added S. The eluent solution was supplied using a syringe pump (KD scientific Inc., Holliston, MA) at the rate of 13 mm day^{-1} simulating slow groundwater discharge rate (Wan et al., 2005). Three series of column experiments, short-, medium- and long-term, were conducted based on a completely randomized design with a two-way factorial experiment (factor 1: OC with two levels, 0 and 10.7 mM L^{-1}; factor 2: S with two levels; 0 and 252.7 mg Kg^{-1}). Effluent samples were collected every week for medium-term and every two weeks for long-term submergence. At the end of each column experiments, about 20 g samples were collected from three windows located on the columns and frozen at -80 °C until DNA was extracted. All treatments from medium-term including C1S0, C0S1, C1S1 and C0S0 were used for microbial analysis.

It should be noted that we performed the microarray analysis only on C0S0 and C1S1 treatments from long-term submergence. The samples were selected based on the geochemical and spectroscopic results.

DNA extraction, labeling, hybridization, scanning, and data processing

About 5 g of soil was used for genomic DNA extraction using the PowerMAx® soil DNA isolation kit (Mo Bio, Carlsbad, CA, USA). Raw DNA extracts were purified using Wizard® Plus *SV* Minipreps purification system (Promega, USA). Purified DNA was quantified using the Quant-iT™ PicoGreen® dsDNA assay kit. DNA was labeled and then hybridized at 42 °C on the array as described in Lu et al. (2012). The hybridized arrays were scanned with a NimbleGen MS 200 Microarray Scanner and scanned images were extracted and quantified using Nimble Scan software (Roche NimbleGen, Madison, WI, USA), followed by data preprocessing (Lu et al., 2012). Positive and negative controls, including (i) 8 degenerate probes targeting 16S rRNA

sequences for positive controls, (ii) 563 strain-specific probes targeting 7 hyper thermophile genomes for negative controls, and (iii) common oligonucleotide reference standard for data normalization and comparison were included for grid alignment and data normalization and comparison (Liang et al., 2010). All hybridization data are available at the Institute for Environmental Genomics, University of Oklahoma, OK, USA.

Results and Discussions

Geochemical dynamics after organic carbon (OC), and sulfur (S) additions

The minewaste material consisted of 85% sand (2000 to 50 µm), 11.3% silt (50 to 2 µm), and 3.4% clay (<2 µm). The total N and C were 0.03 g kg^{-1} and 1.56 g kg^{-1}, respectively. The pH of the water extract (DI water: geomaterial mass ratio, 2:1) was 7.2 and the electrical conductivity was 2.31 mS cm^{-1}. The major element composition of fine geomaterial obtained through aqua-regia digestion is listed in Table 5-1. The standard reference material 2711a (National Institute of Standards and Technology, Gaithersburg, MD) was digested along with the geomaterial in order to assure the recovery percentage of each element that ranged from 79-109%.

In the current study, solution chemistry data from medium- and long-term submergence indicated that both C1S0 and C1S1 treatments showed rapid immobilization of Pb, Zn and Cd. The observed SO_4^{-2} reduction in relation to the decreasing OC concentration indicated dissimilatory sulfate reduction was playing a role in metal' immobilization. Similar results were observed during a study focused on uranium (U) reduction in a contaminated aquifer by Van Nostrand et al. (2011), where dissimilatory sulfate reduction was revealed to play a role in U reduction. Scanning electron microscopy- energy dispersive X-ray provided indirect evidence of sulfide formation via enhanced colocalization of Pb, Zn and Fe with S (Karna et al., 2014a

(Chapter 3)). This indirect evidence of metal sulfide formation was further supported with both bulk- and micro-scale XAS directly (Karna et al., 2014b (Chapter 4)). Bulk XAS data indicated about 62% galena (PbS) formation with C1S0 and C1S1 (Figure 5-1) compared to C0S1 and C0S0 under long-term submergence. In addition to this, cerrusite ($PbCO_3$) was another dominant Pb mineral formed when only OC was added. Zinc was mostly transformed as silicate minerals such as hemimorphite in C1S0 and C0S1 treatments, whereas 31% sphalerite (ZnS) formation was observed in C1S1 (Figure 5-2). Metal sulfides are more stable than carbonates over a wide range of pH, and are highly resistant to the desorption effects of chlorides of Zn, Cu, Cd, Pb, hydroxides and bicarbonates of Zn under anoxic conditions (Moraes et al., 2005; Du Liang et al., 2009). Precipitation of metal sulfides can act as a sink for trace metal contaminants (Nordstrom, 1999). The literature suggest that metal carbonate formation may potentially become the dominant process controlling metal solubility due to alkaline pH under reduced conditions (Chen et al., 1997; Komárek, 2004; Boynton et al., 2009), and insufficient S may limit sulfide formation in the long-term (Toevs et al., 2006). Based on our bulk XAS results it appears that the OC plus S treatment would be a better strategy over the OC only treatment for facilitating metal sulfide formation. More details on solution chemistry, and synchrotron based X-ray analysis can be found in Karna et al. (2014a, b) (Chapter 3 and 4).

Functional gene diversity

The p-value from Bray-Curtis dissimilarity test was <0.05 indicating significant dissimilarity between the treatments (Table 5-3) over medium- and long-term submergence. The p-values provided in the table are based on the total number of detected genes. Functional gene richness, indicated by the total number of genes detected, was enhanced in C1S1 under medium-

term submergence compared to the other treatments; C0S0, C0S1, C1S0 (Figure 5-3). However, under long-term submergence, the total number of detected genes were much lower in C1S1 treatment (Figure 5-3). The significant increase in microbial community in C1S1 followed by a significant decline may indicate a rapid oxidation of added OC coupled with reduction of available terminal electron acceptors (TEAs) and a subsequent decline as suitable TEAs are exhausted. This could be explained by the trend that was observed with DOC concentration in the current study. Initial concentration of DOC in the eluent was 32 Mm that was reduced to 30 mM in effluent at 7-day submergence, and further decreased to <detection limit (DL) under long-term submergence in OC added treatments. On the other hand, non OC treated columns showed about <3 mM DOC with no significant change over long-term submergence (Table 5-2). Similar result was reported by Brodie et al. (2006), where initial enrichment in total functional genes was observed that was subsequently declined with OC addition. On the other hand, no such enhancement in functional gene richness was observed without OC addition. This could be due to decreased availability of OC (<3 mM) (Table 5-2). Previous literatures revealed that addition of OC stimulates biomass and microbial activity in these typically nutrient-poor environments and has a significant impact on the microbial biomass, microbial community structure and functional genes (Homles et al., 2002; Martin et al., 2002; Nevin et al., 2003; Brodie et al., 2006; Yergeau et al., 2007). Sufficient labile OC must be available for sulfate reduction and is a key rate limiting factor of metal sulfide formation (Morse et al., 2002; Ku et al., 2008). This process can be accelerated by the action of indigenous microorganisms fueled through the addition of exogenous carbon (Khan et al., 2010).

Relationships among the microbial communities

Detrended correspondence analysis (DCA) was used to examine the overall functional structure changes in the microbial communities with the OC plus S treatment under medium- and long-term submergence. In the DCA ordination plot, more similar samples will cluster more closely (Ramette et al., 2007). The overall DCA ordination plot obtained from all detected genes resulted in clear clustering of samples from medium- and long-term submergence (Figure 5-4). When samples from medium- and long-term submergence were plotted individually, separate clusters for each treatment were formed, thus indicating an overall effect of OC and/ or S treatments and time on the community structure in relation to dynamics of geochemistry and enhanced reduction (Figure 5-4). The positive effect of OC, S and N via enhancement of corresponding functional genes, and impact on change in microbial community structure has been observed by several studies (Kleikemper et al., 2002; Tokunaga et al., 2003; Furham et al., 2009). The DCA was also performed for metal resistance (Figure 5-5), C-cycling (Figure 5-6) and S-cycling (Figure 5-7) categories separately. The DCA results for metal resistance and S-cycling genes showed clear clusters (Figure 5-5, 5-7), however DCA ordination plot for C-cycling genes showed slight overlapping.

The DCA was also conducted with individual S- cycling genes; dsrA/ B (Figure 5-8, 5-9) that revealed more clear clusters with dsrB compared to dsrA genes. Overall DCA results indicated that decrease in metal resistance and organic remediation functional genes, and enrichment in S- and C-cycling functional genes were mainly involved in the observed community shift. The change in microbial community structure was observed due to direct and indirect involvement of certain functional genes in bioremediation of U study using microarray (Van Nostrand et al., 2011). There are several other studies conducted by using other DNA

fingerprinting techniques such as phospholipid fatty acid analysis (PLFA), and polymerase chain reactions- denaturing gradient gel electrophoresis (PCR-DGGE) that reported changes in microbial community structure with addition of OC as substrate (Griffiths et al., 1998; Ellier et al., 2003; Calbrix et al., 2009).

Total abundance of functional genes categories

The shifts that were observed in the DCA ordination plots were likely the results of changes in total abundance of functional genes. The results from individual gene categories revealed that S- and C-cycling functional genes abundance was enhanced by 35%, and 27%, respectively with compared to C0S0 over time. On the other hand, metal resistance and organic remediation functional genes were decreased by 26% (Figure 5-10) and 21% (Figure 5-11) in C1S1, respectively with compared to C0S0. Thus significant enrichment of S- and C-cycling genes, and a large decrease in metal resistance and organic remediation genes by 50-60% within both treated and untreated samples over time could have resulted in community structure changes. As previously mentioned, this could be due to either their direct involvement or absence of involvement in bio-reduction (Van Nostrand et al., 2011). For example, if organic remediation genes are considered to represent background functional genes, these were greatly decreased (Figure 5-11) probably due to lack of involvement in bio-reduction and the corresponding genes directly involved in bio-reduction (i.e., dsrA/B) which was also reported by Van Nostrand et al. (2011).

The abundance of stress related functional genes (Figure 5-11), and metal resistance genes decreased over long-term submergence with both C1S1 and C0S0 indicated that in addition to OC and S, submergence time is also an evident factor playing role in decreasing toxicity in these systems. Heavy metals are predicted to represent a major stress on the microbial

community, and adaptation to metal stress may be of particular importance that has been playing a major role in shaping microbial community structure (Hemme et al., 2010). There are several studies that indicated impact of heavy metals on microbial activities, and their community structure (Gao et al., 2010; Hemme et al., 2010; Khan et al., 2010). A study conducted on the effect of Pb and Cd on soil microbial activities and their community structure via denaturing gradient gel electrophoresis (DGGE) indicated that Pb and Cd together has highly decreased the number of bacteria when no nutrients were supplied, and also revealed significant impact on community structure dynamics particularly at high Pb and Cd concentrations (Khan et al., 2010).

On the other hand functional genes involved in S- and C-cycling were significantly enhanced in C1S1 despite the total number of detected genes was decreased under long-term submergence indicating direct involvement of S- and C-cycling genes in biogeochemical transformations processes. Increased activities of S-cycling functional genes could be due to readily available sulfate as TEA under more reduced condition thereby favoring dissimilatory sulfate reduction (Brodie et al., 2003; Muyzer et al., 2008). Relationship observed between enhanced dissimilatory sulfate reduction and increased S-cycling functional genes can be further supported by the decrease of sulfate-S concentration in effluent sample (table 5-2) and increase in metal sulfide formation (Figure 5-1, 5-2) observed in the current study. Similar results were reported by Huerta-Diaz et al. (1998) indicating direct involvement of C-cycling and S-cycling genes in dissimilatory S reduction via rapid consumption of OC followed by sulfate reduction.

Changes in S-, C-cycling, and metal resistance genes

To better understand the differences observed in the categories above, changes in individual genes were examined. Sulfate-reducing bacteria (SRB) mediate the direct

and indirect reduction of heavy metals and metalloids (White et al., 1997; Hao, 2000), and have been considered as a key player in anaerobic bioremediation for contaminated soils, waters, and subsurfaces (Franzmann et al., 2002; Kirk et al., 2002; Janssen and Temminghoff, 2004). For SRB community, dsr gene encodes the dissimilatory sulfite reductase enzyme with subunits; A/B that is a key enzyme in reducing sulfite to sulfide and is required by all sulfate reducers (Klein et al., 2001). Thus, dsr genes provide the insight into SRB activities and their functional role in sulfate reduction. Under S- cycling, dsrA, dsrB, and csyJ were more abundant by 31%, 35%, and 40%, respectively, in C1S1 compared to C0S0 under long-term submergence (Figure 5-12) indicating their major role in dissimilatory sulfate reduction. Similarly among C-cycling functional genes; phenol_oxidase, and endochitinase were the most dominant genes and they were 35%, and 30% more abundant in C1S1 compared to the C0S0 (Figure 5-12). Metal resistance genes for Cd, Zn and Pb were examined and cadA (Cd resistance gene), czcA (Zn resistance gene) and pbrA (Pb resistant gene) decreased by 29%, 24% and 15%, respectively, in C1S1 compared to C0S0 over time (Figure 5-14). Decrease in some functional genes with subsequent increase in some other types of functional genes could be explained as some microbial species can be diminished, while tolerant species survive and gets more abundant that results due to physiological adaptation and genetic modifications in tolerant species, which may lead to replacement of more sensitive species (Briuns et al. 2000). In addition, available favorable electron acceptors and sufficient OC availability are other major reasons as previously discussed.

Relationships of microbial community with environmental factors

Canonical correspondence analysis (CCA) was performed to examine the relationship between microbial community structure and geochemistry (Figure 5-14) to correlate the

environmental variables with the functional community structure and determine the most significant variable causing the change in community structure. Environmental variables such as dissolved organic carbon (DOC), SO_4^{2-}, total S, and NO_3^- were used to perform CCA. In CCA, the environmental variables are represented as arrows starting at the origin and going out. The longer the arrow the more important that variable is in controlling or influencing the community. The closer a sample to an arrow, the more that variable influences the sample or important to that sample. Arrows going in opposite directions indicates a negative correlation between those variables. The smaller the angle between arrows, the more related they are, and have similar influence on the community (Wilson et al., 1983; Austin et al., 1987, Witten et al., 2009). Our CCA results shows that DOC and S are closer with a small angle indicating these variables have a stronger correlation and have similar influence on the microbial communities. Dissolved organic carbon and NO_3^- had a larger angle, indicating these variables have a stronger correlation, and have a similar influence on the microbial communities. Dissolved OC and NO_3^- had a larger angle, indicating a weaker correlation and are influencing the microbial communities in different manners. The SO_4^{2-} and total S vectors are in opposite directions indicating that these factors are negatively correlated.

Metal precipitation is one of the most significant processes involved in the long-term retention of metals in artificial and natural wetlands. Such processes may be accompanied by other indirect reductive metal precipitation (such as redox transformation) including dissimilatory sulfate reduction and the subsequent precipitation of metal sulfides (Finneran et al., 2002). Dissimilatory sulfate reduction helps formation of FeS, and FeS_2; the systems with pyrite (FeS_2) formation are more resistant to solubilization of metals (Huerta-Diaz et al., 1998). There are several studies reporting dissimilatory sulfate reduction as a major mechanism in

immobilizing metals. Our results suggest that appropriate microbial communities were stimulated by OC plus S treatments resulting in biogeochemical transformations of Pb and Zn under reduced conditions. The total gene abundance in C1S0 was similar to C1S1 under medium-term submergence, which was also supported by bulk XAS indicating similar amount of galena formations over time. However, limited S concentration and enhanced pH in C1S0 treatment, metal carbonates could potentially dominate controlling metal solubility and carbonates are not as stable as sulfide minerals. Similar results were observed by Falkowski et al. (2000); Toevs et al. (2007) that reported more carbonate formations under alkaline pH under anaerobic condition. Metal sulfides are more resistant to oxidation, therefore even less sulfide formation would help to maintain low metal concentrations in water, down to permissible levels, for long time. There are a handful of studies that looked at non redox sensitive element removal via constructed wetland treatment systems (White and Gadd, 2000; Almendras et al., 2009). Earlier studies done by Almendras et al. (2009) testing Pb, Cu and Zn stability via sulfide formations showed that biostimulation plays a vital role in stabilizing Pb and Zn in the subsurface environment. The results from our study also suggest that wetland construction can be a better alternative for stabilizing non redox sensitive elements such as Pb and Zn present in minewaste materials, or similar geomaterial.

Conclusions

The results obtained from the current study indicated that OC and S addition stimulated the microbial growth and activities causing change in functional microbial community structure via enhancement or reduction of functional genes in saturated minewaste materials enriched with Pb and Zn. The decrease in metal resistance genes with reduced toxicity over time, and enrichment of S- and C-cycling genes in OC plus S treated samples (C1S1) indicated that these

members played significant roles in maintaining the microbial communities in the subsurface environment. Sulfur reducing bacteria gene; dsrA/ B appeared to be a key player in forming metal sulfides, which was significantly enhanced in C1S1 over the long-term submergence. On the other hand, there was no significant difference in the functional gene richness under any categories in C0S0 treatment over time. The information obtained from this study help concluding that biostimulation would be helpful for inducing metal sulfide formations in minewaste materials and SRBs can be used as key players for *in situ* bioremediation of Pb and Zn in subsurface treatment wetlands. The results are in agreement with solution chemistry and molecular scale synchrotron based X-ray data and help understanding of the biogeochemical processes involved in Pb and Zn removal via dissimilatory sulfate reductions under reduced conditions.

Acknowledgements

We acknowledge Kansas State University Research and Extension, Kansas State University, Manhattan, KS for conducting this experiment. We highly acknowledge committee members: Drs. Charles W. Rice, Gary M. Pierzynski, Gerard Kluitenberg and Saugata Datta, for their helpful suggestions and insightful discussions. We also acknowledge Jizhong Zhou, Tong Yuan, Joy Van Nodstrand, and Ye Deng for their help with microarray data collection and inputs for analysis, and Yared Assefa Mulisa for helping with statistics. We also thank Dr. Ari Jumponnen and his students for providing lab space to conduct initial procedure in DNA extraction and purification procedures.

References

Almendras, M., Wiertz, J., and Chamy, R. 2009. Heavy metals immobilization in contaminated smelter soils using microbial sulfate reduction. Advanced Materials Research. 71:577-580.

Austin, M. P. 1987. Models for the analysis of species' response to environmental gradients. Vegetation. 69:35-45.

Baker, B. J., and Banfield, J. F. 2003. Microbial communities in acid mine drainage. FEMS Microbiology Ecology. 44:139-152.

Barton, L. L., and Fauque, G. D. 2009. Biochemistry, physiology and biotechnology of Sulfate-Reducing bacteria. Advances in Applied Microbiology. 68:41-98.

Bazylinski, D. A., and Frankel, R. B. 2003. Biologically controlled mineralization in prokaryotes. Reviews in Mineralogy and Geochemistry. 54:217-247.

Bhattacharya, J., Ji, S. W., Lee, H. S., Cheong, Y. W., Yim, G. J., and Min, J. S. 2008. Treatment of acidic coal mine drainage: Design and operational challenges of successive alkalinity producing systems. Mine Water and the Environment. 27:12-19.

Borch, T., Kretzschmar, R., Kappler, A., Cappellen, P. V., Ginder-Vogel, M., and Voegelin, A. 2009. Biogeochemical redox processes and their impact on contaminant dynamics. Environmental Science and Technology. 44:15-23.

Boynton, W. V., Ming, D. W., Kounaves, S. P., Young, S. M., Arvidson, R. E., and Hecht, M. H. 2009. Evidence for calcium carbonate at the mars phoenix landing site. Science (New York, N.Y.). 325:61-64.

Brantley, S. L., Goldhaber, M. B., and Ragnarsdottir, K. V. 2007. Crossing disciplines and scales to understand the critical zone. Elements. 3:307-314.

Briuns, M. R., Kapil, S., and Oehme, F. W. 2000. Microbial resistance to metals in the environment. Ecotoxicol Environ Safety. 45:198–207.

Brookes, P. C. (1995). The use of microbial parameters in monitoring soil pollution. Biol Fertil Soils. 19:269–279.

Brodie, E. L., Desantis, T. Z., Joyner, D. C., Baek, S. M., Larsen, J. T., Andersen, G. L. 2006. Application of a high-density oligonucleotide microarray approach to study bacterial population dynamics during uranium reduction and reoxidation. Applied and Environmental Microbiology. 72:6288-6298.

Burton, E. D., Bush, R. T., Sullivan, L. A., and Mitchell, D. R. 2008. Schwertmannite transformation to goethite via the Fe (II) pathway: Reaction rates and implications for iron–sulfide formation. Geochimica Et Cosmochimica Acta. 72:4551-4564.

Calbrix, R., Barray, S., Chabrerie, O., Fourrie, L., and Laval, K. 2007. Impact of organic amendments on the dynamics of soil microbial biomass and bacterial communities in cultivated land. Applied Soil Ecology. 35:511-522.

Chen, K. Y., and Morris, J. C. 1972. Kinetics of oxidation of aqueous sulfide by oxygen. Environmental Science and Technology. 6:529-537.

Chen, X., Wright, J. V., Conca, J. L., and Peurrung, L. M. 1997. Effects of pH on heavy metal sorption on mineral apatite. Environmental Science and Technology. 31:624-631.

Edwards, K. J., Bond, P. L., Druschel, G. K., McGuire, M. M., Hamers, R. J., and Banfield, J. F. 2000. Geochemical and biological aspects of sulfide mineral dissolution: Lessons from iron mountain, California. Chemical Geology. 169:383-397.

Eiler, A., Langenheder, S., Bertilsson, S., and Tranvik, L. J. 2003. Heterotrophic bacterial growth efficiency and community structure at different natural organic carbon concentrations. Applied and Environmental Microbiology. 69:3701-3709.

Evans, M., Warburton, J., and Yang, J. 2006. Eroding blanket peat catchments: Global and local implications of upland organic sediment budgets. Geomorphology. 79:45-57.

Fontaine, S., Mariotti, A., and Abbadie, L. 2003. The priming effect of organic matter: A question of microbial competition? Soil Biology and Biochemistry. 35:837-843.

Fuhrman, J. A. 2009. Microbial community structure and its functional implications. Nature. 459:193-199.

Gadd, G. M. 2010. Metals, minerals and microbes: Geomicrobiology and bioremediation. Microbiology (Reading, England). 156:609-643.

Griffiths, B., Ritz, K., Ebblewhite, N., and Dobson, G. 1998. Soil microbial community structure: Effects of substrate loading rates. Soil Biology and Biochemistry. 31:145-153.

He, Z., Gentry, T. J., Schadt, C. W., Wu, L., Liebich, J., Chong, S. C. 2007. GeoChip: A comprehensive microarray for investigating biogeochemical, ecological and environmental processes. The ISME Journal. 1:67-77.

Hemme, C. L., Deng, Y., Gentry, T. J., Fields, M. W., Wu, L., Barua, S. 2010. Metagenomic insights into evolution of a heavy metal-contaminated groundwater microbial community. The ISME Journal. 4:660-672.

Holmes, D. E., Finneran, K. T., O'Neil, R. A., and Lovley, D. R. 2002. Enrichment of members of the family *Geobacteraceae* associated with stimulation of dissimilatory metal reduction in uranium-contaminated aquifer sediments. Applied Environmental Microbiology. 68:2300-2306.

Johnson, D. B., and Hallberg, K. B. 2005. Acid mine drainage remediation options: A review. Science of the Total Environment. 338:3-14.

Khan, S., Hesham, A. E., Qiao, M., Rehman, S., and He, J. 2010. Effects of Cd and Pb on soil microbial community structure and activities. Environmental Science and Pollution Research. 17:288-296.

Kleikemper, J., Schroth, M. H., Sigler, W. V., Schmucki, M., Bernasconi, S. M., and Zeyer, J. 2002. Activity and diversity of sulfate-reducing bacteria in a petroleum hydrocarbon-contaminated aquifer. Applied and Environmental Microbiology. 68:1516-1523.

Kosolapov, D., Kuschk, P., Vainshtein, M., Vatsourina, A., Wiessner, A., and Kästner, M. 2004. Microbial processes of heavy metal removal from Carbon-Deficient effluents in constructed wetlands. Engineering in Life Sciences. 4:403-411.

Loick, N., and Weisener, C. 2014. Novel molecular tools to assess microbial activity in contaminated environments. Geomicrobiology and biogeochemistry. p. 17-35.

Lovley, D. R. 1995. Bioremediation of organic and metal contaminants with dissimilatory metal reduction. Journal of Industrial Microbiology. 14:85-93.

Lu, Z., Deng, Y., Van Nostrand, J. D., He, Z., Voordeckers, J., and Zhou, A. 2012. Microbial gene functions enriched in the deepwater horizon deep-sea oil plume. The ISME Journal. 6:451-460.

Luptakova, A., and Kusnierova, M. 2005. Bioremediation of acid mine drainage contaminated by SRB. Hydrometallurgy. 77:97-102.

Martin, T., Oswald, O., and Graham, I. A. 2002. Arabidopsis seedling growth, storage lipid mobilization, and photosynthetic gene expression are regulated by carbon: Nitrogen availability. Plant Physiology. 128:472-481.

McLean, E. J., Robinson, R. I., Teat, S. J., Wilson, C., and Woodward, S. 2002. Transformation of sulfur dioxide to sulfate at a palladium centre. Journal of the Chemical Society, Dalton Transactions. 18:3518-3524.

McLean, L., Pray, T., Onstott, T., Brodie, E., Hazen, T., and Southam, G. 2007. Mineralogical, chemical and biological characterization of an anaerobic biofilm collected from a borehole in a deep gold mine in South Africa. Geomicrobiology Journal. 24:491-504.

Moraes, P. B., and Bertazzoli, R. 2005. Electrodegradation of landfill leachate in a flow electrochemical reactor. Chemosphere. 58:41-46.

Moreau, J. W., Webb, R. I., and Banfield, J. F. 2004. Ultrastructure, aggregation-state, and crystal growth of biogenic nanocrystalline sphalerite and wurtzite. American Mineralogist. 89:950-960.

Muyzer, G., and Stams, A. J. 2008. The ecology and biotechnology of sulfate-reducing bacteria. Nature Reviews Microbiology. 6:441-454.

Nevin, K. P., Finneran, K. T., and Lovley, D. R. 2003. Microorganisms associated with uranium bioremediation in a high-salinity subsurface sediment. Appl. Environ. Microbiol. 69:3672-3675.

Pierzynski, G. M., and Vaillant, G. C. 2006. Remediation to reduce ecological risk from trace element contamination: A decision case study. Journal of Natural Resources and Life Sciences Education. 35:85-94.

Ramasamy, K., and Banu, S. P. 2007. Bioremediation of metals: Microbial processes and techniques. Environmental bioremediation technologies, Springer- Verlag, New York. p. 173-187.

Ramette, A. 2007, Multivariate analyses in microbial ecology. FEMS Microbiology Ecology. 62:142–160.

Schwab, A., and Lindsay, W. 1983. Effect of redox on the solubility and availability of iron. Soil Science Society of America Journal. 47:201-205.

Smith, W. L., and Gadd, G. M. 2000. Reduction and precipitation of chromate by mixed culture sulfate-reducing bacterial biofilms. J. Appl. Microbiol. 88:983-991.

Stein, O. R., Borden-Stewart, D. J., Hook, P. B., and Jones, W. L. 2007. Seasonal influence on sulfate reduction and zinc sequestration in subsurface treatment wetlands. Water Research. 41:3440-3448.

Toevs, G. R., Morra, M. J., Polizzotto, M. L., Strawn, D. G., Bostick, B. C., and Fendorf, S. 2006. Metal (loid) diagenesis in mine-impacted sediments of Lake Coeur d'Alene, Idaho. Environmental Science and Technology. 40:2537-2543.

Tokunaga, T. K., Wan, J., Firestone, M. K., Hazen, T. C., Olson, K. R., and Herman, D. J. 2003. In situ reduction of chromium (VI) in heavily contaminated soils through organic carbon amendment. Journal of Environmental Quality. 32:1641-1649.

Tu, Q., Yu, H., He, Z., Deng, Y., Wu, L., and Nostrand, J. D. 2014. GeoChip 4: A functional gene-array-based high-throughput environmental technology for microbial community analysis. Molecular Ecology Resources. 14:914-928.

Van Nostrand, J. D., Wu, W., Wu, L., Deng, Y., Carley, J., and Carroll, S. 2009. GeoChip-based analysis of functional microbial communities during the reoxidation of a bioreduced uranium-contaminated aquifer. Environmental Microbiology. 11:2611-2626.

Van Nostrand, J. D., Wu, L., Wu, W. M., Huang, Z., Gentry, T. J., and Deng, Y. 2011. Dynamics of microbial community composition and function during in situ bioremediation of a uranium-contaminated aquifer. Applied and Environmental Microbiology. 77:3860-3869.

Vega, F. A., Covelo, E. F., and Andrade, M. 2006. Competitive sorption and desorption of heavy metals in mine soils: Influence of mine soil characteristics. Journal of Colloid and Interface Science. 298:582-592.

Wan, J., Tokunaga, T. K., Brodie, E., Wang, Z., Zheng, Z., Herman, D. 2005. Reoxidation of bioreduced uranium under reducing conditions. Environmental Science and Technology. 39:6162-6169.

White, C., and Gadd, G. 2000. Copper accumulation by sulfate-reducing bacterial biofilms. FEMS Microbiology Letters. 183:313-318.

Whiteman, M., Armstrong, J. S., Chu, S. H., Jia-Ling, S., Wong, B., and Cheung, N. S. 2004. The novel neuromodulator hydrogen sulfide: An endogenous peroxynitrite 'scavenger'? Journal of Neurochemistry. 90:765-768.

Wilson, M. V., and Mohler, C. L. 1983. Measuring compositional change along gradients. Vegetation. 54:129-41.

Wu, L. 2001. Development and evaluation of functional gene arrays for detection of selected genes in the environment. Applied Environmental. Microbiology. 67:5780–5790.

Yergeau, E., Kang, S., He, Z., Zhou, J., and Kowalchuk, G. A. 2007. Functional microarray analysis of nitrogen and carbon cycling genes across an Antarctic latitudinal transect. The ISME Journal. 1:163-179.

Zarcinas, B. A., McLaughlin, M. J., and Smart, M. K. 1996. The effect of acid digestion technique on the performance of nebulization systems used in inductively coupled plasma spectrometry. Communications in Soil Science and Plant Analysis. 27:1331-1354.

Zhang, S., Xue, X., Liu, R., and Jin, Z. 2005. Current situation and prospect of the comprehensive utilization of mining tailings [J]. Mining and Metallurgical Engineering. 3: 44-48.

Zhou, J., Kang, S., Schadt, C., and Garten Jr, C. 2008. Spatial scaling of functional Gene diversity across various microbial taxa. Procedures of National Academy of Sciences, USA. 105:7768-7773.

Table 5-1: Total element concentration in minewaste materials collected from the Tri-State mining district.

Element	Cd	Pb	Zn	Fe	Mn	S
mg kg^{-1}	67	5048	23468	6834	97	9458

Table 5-2: Chemical data for the effluent samples that were collected at 119-day and 252-day. The soil samples collected at these time points were used for microarray analysis.

	µg/L			mg/L			
Sample	**Zn**	**Cd**	**Pb**	**pH**	**DOC**	**sulfate-S**	**Nitrate-N**
C0S0 119-day	723	432	<DL	7.57	5	474	2.0
C0S0 252-day	517	28	<DL	8.41	62	571	2.0
C0S1 119-day	30	2	<DL	8.00	4	468	1.8
C0S1 252-day	<DL	1	36	6.39	65	¶	2.2
C1S0 119-day	<DL	1	<DL	8.18	5	503	1.9
C1S0 252-day	<DL	<DL	<DL	7.58	<DL	474	2.0
C1S1 119-day	<DL	1	<DL	7.40	4	437	1.8
C1S1 252-day	<DL	<DL	<DL	7.02	<DL	288	1.9

*DL corresponds to detection limit. Detection limit of 0.6 for Cd, and 0.7 μgL^{-1} for Pb was determined.

¶ indicates data not collected

Table 5-3: Bray Curtis dissimilarity test giving p-value for each treatments submerged for short (119-day) and long-term (252-day). The p-values were calculated based on total number of detected genes.

Group	Adonis Bray
Whole	0.001
C0S0 119-day vs C0S0 252-day	0.001
C0S0 119-day vs C1S1 119-day	0.001
C0S0 119-day vs C1S1 252-day	0.001
C0S0 119-day vs C0S1 119-day	0.001
C0S0 119-day vs C1S0 119-day	0.132
C0S0 252-day vs C1S1 119-day	0.11
C0S0 252-day vs C1S1 252-day	0.039
C0S0 252-day vs C0S1 119-day	0.09
C0S0 252-day vs C1S0 119-day	0.013
C1S1 119-day vs C1S1 252-day	0.068
C1S1 119day vs C0S1 119-day	0.001
C1S1 119-day vs C1S0 119-day	0.001
C1S1 252-day vs C0S1 119-day	0.497
C1S1 252-day vs C1S0 119-day	0.001
C0S1 119-day vs C1S0 119-day	0.305

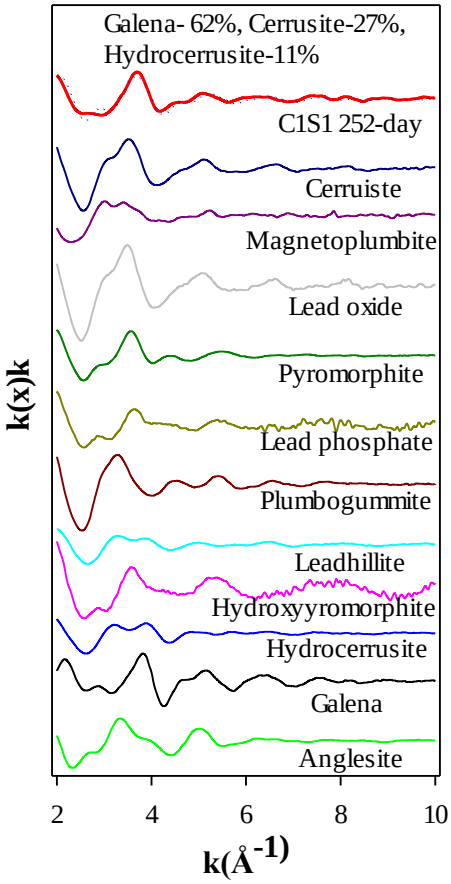

Figure 5-1: Pb-XAFS of selected Pb standards and bulk XAFS spectra for OC plus S treated sample (C1S1) showing Galena (PbS) formation under long-term (252-day) submergence. Solid lines represent the k^1-weighted *x*-spectra and the dotted lines represent the best fits obtained using statistical analyses; principal component analysis (PCA), and linear combination fitting (LCF).

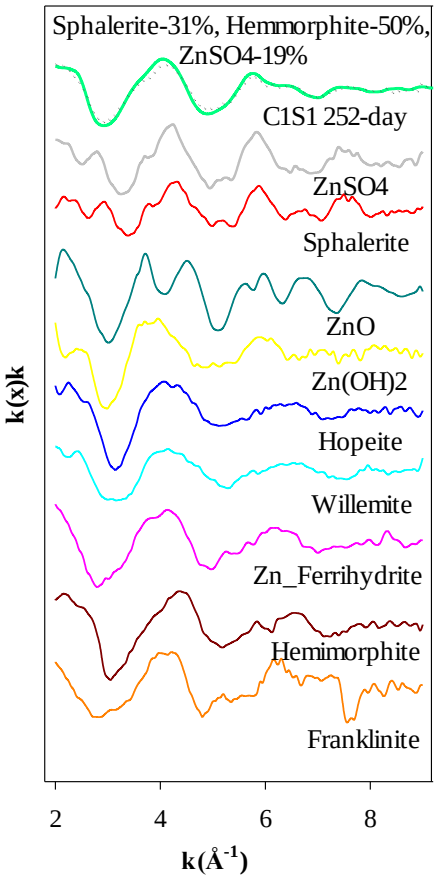

Figure 5-2: Zn-XAFS of selected Zn standards and bulk Zn XAFS spectra for OC plus S treated sample (C1S1) showing Sphalerite (ZnS) formation under long-term (252-day) submergence. Solid lines represent the k^1-weighted *x*-spectra and the dotted lines represent the best fits obtained using statistical analyses; principal component analysis (PCA), and linear combination fitting (LCF).

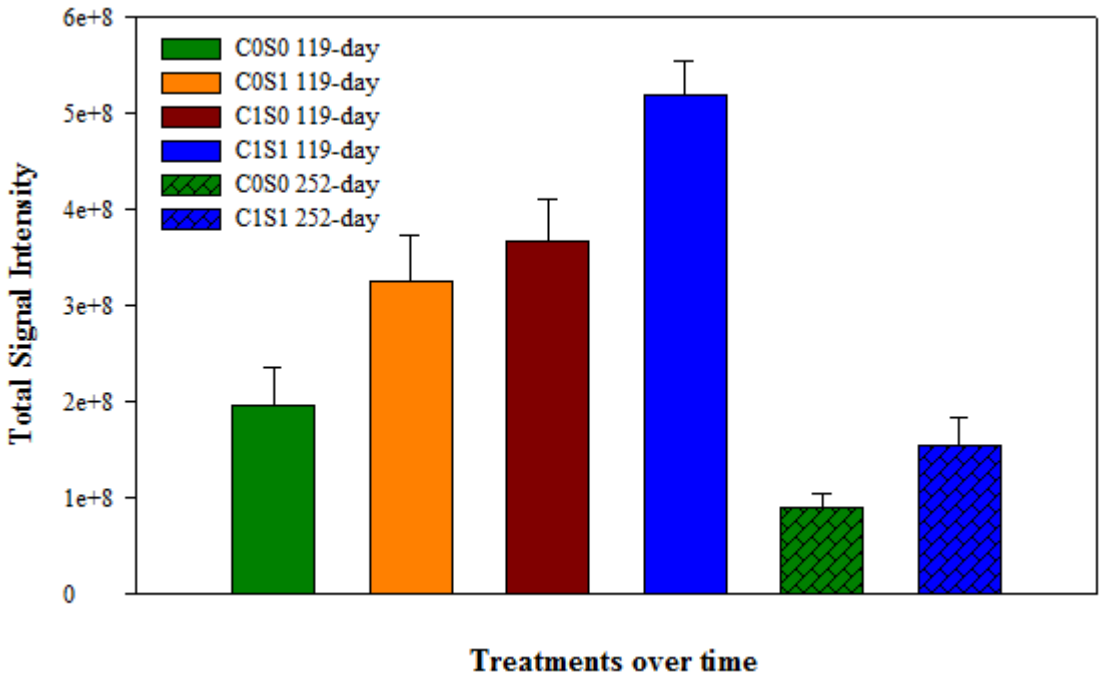

Figure 5-3: Functional Gene richness under medium (119-day), and long-term (252-day) submergence.

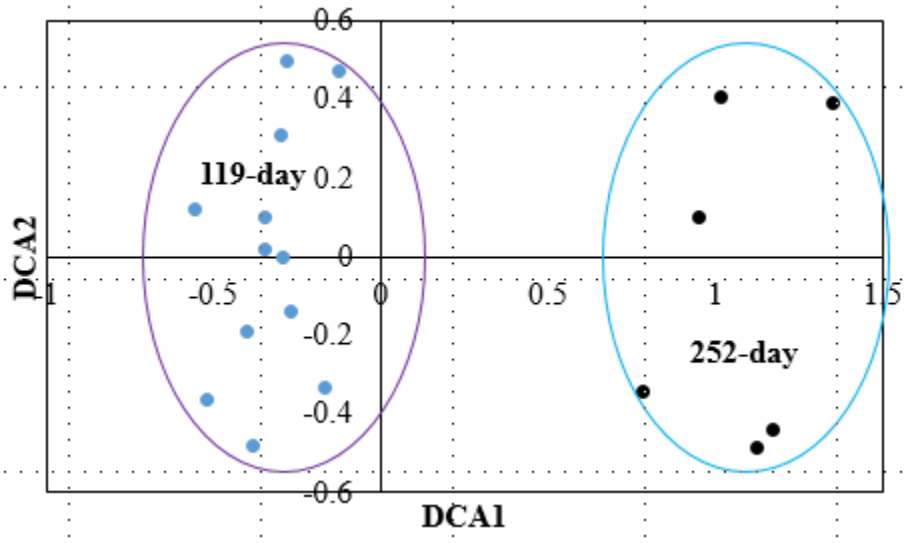

Figure 5-4: Detrended correspondence analysis (DCA) for total number of detected genes under medium (119-day), and long (252-day) submergence indicating community structure changes.

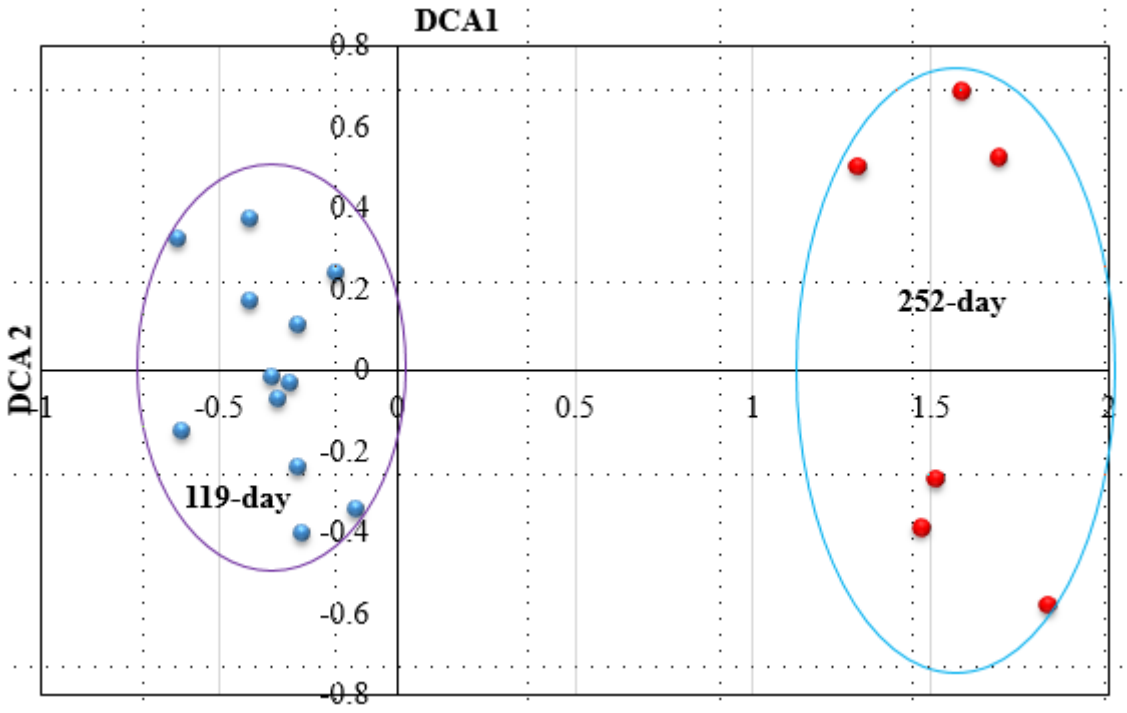

Figure 5-5: Detrended correspondence analysis (DCA) of functional genes under metal resistance category showing change in community structure under medium (119-day), and long (252-day) submergence.

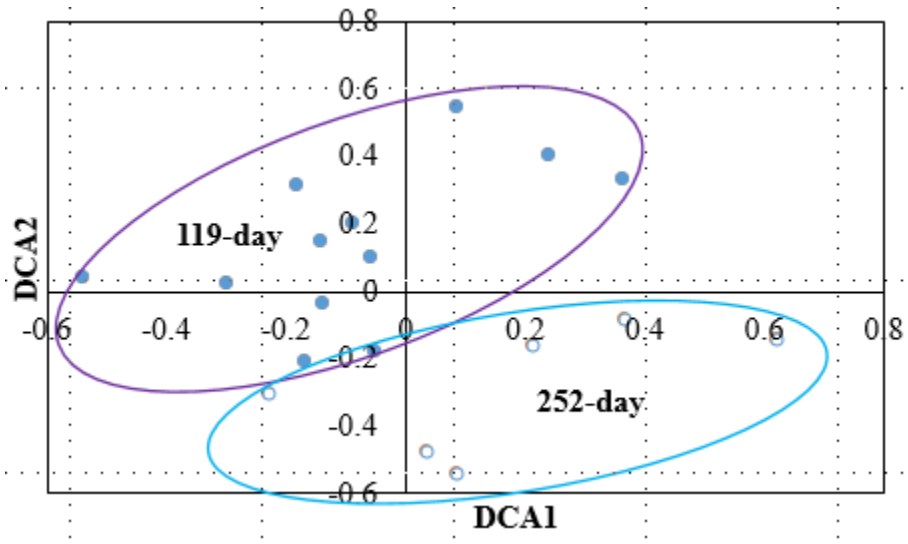

Figure 5-6: Detrended correspondence analysis (DCA) of functional genes under C-cycling category showing change in community structure under medium (119-day), and long (252-day) submergence.

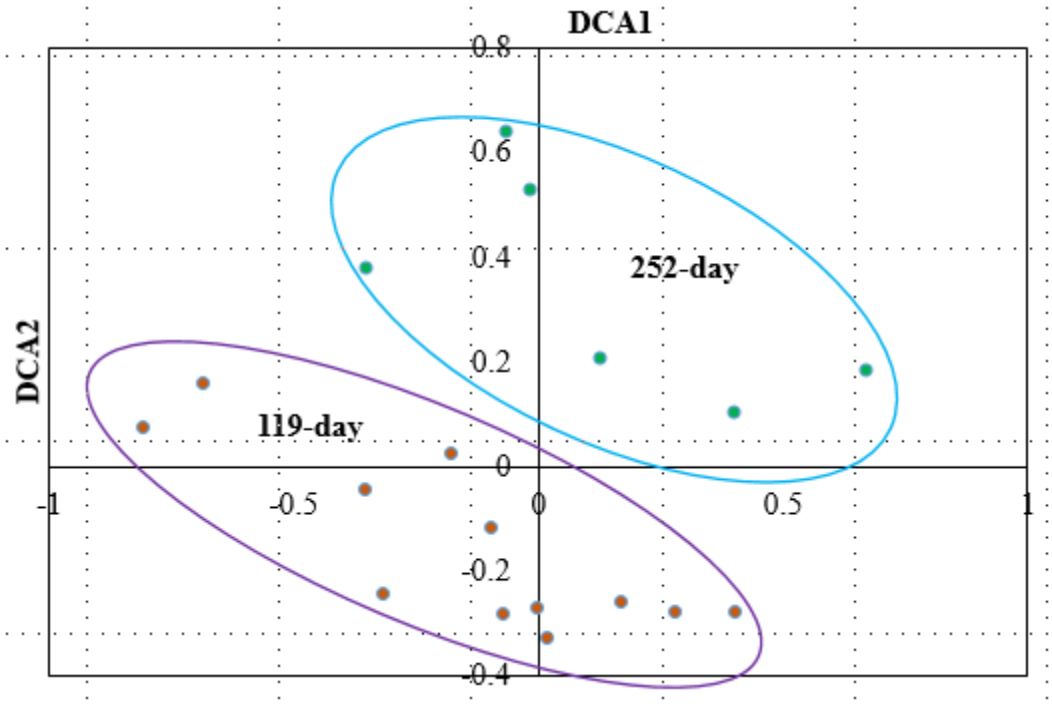

Figure 5-7: Detrended correspondence analysis (DCA) of functional genes under sulfur category showing change in community structure under medium (119-day), and long (252-day) submergence.

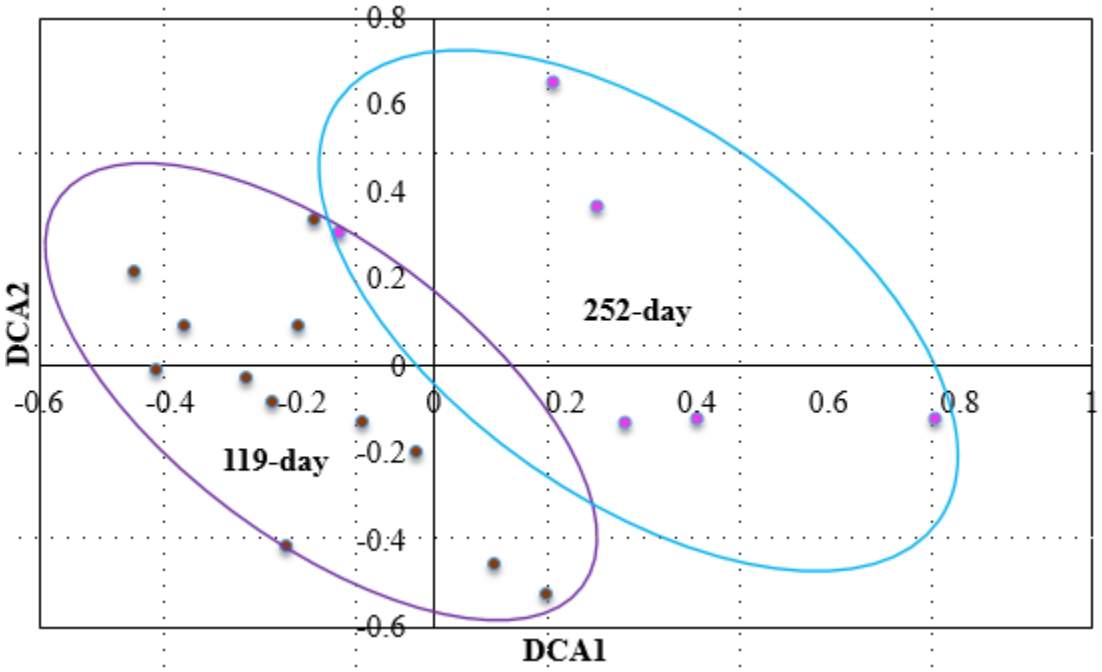

Figure 5-8: Detrended correspondence analysis (DCA) of dsrA showing change in community structure under medium (119-day), and long (252-day) submergence.

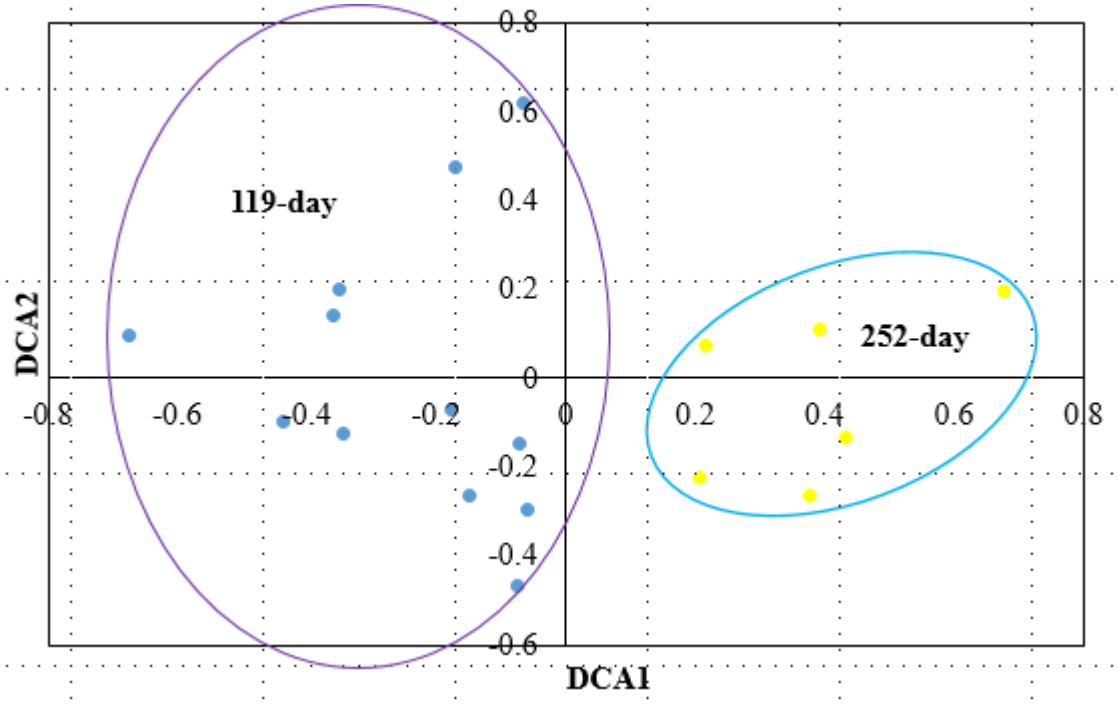

Figure 5-9: Detrended correspondence analysis (statistics) of dsrB showing change in community structure under medium (119-day), and long (252-day) submergence.

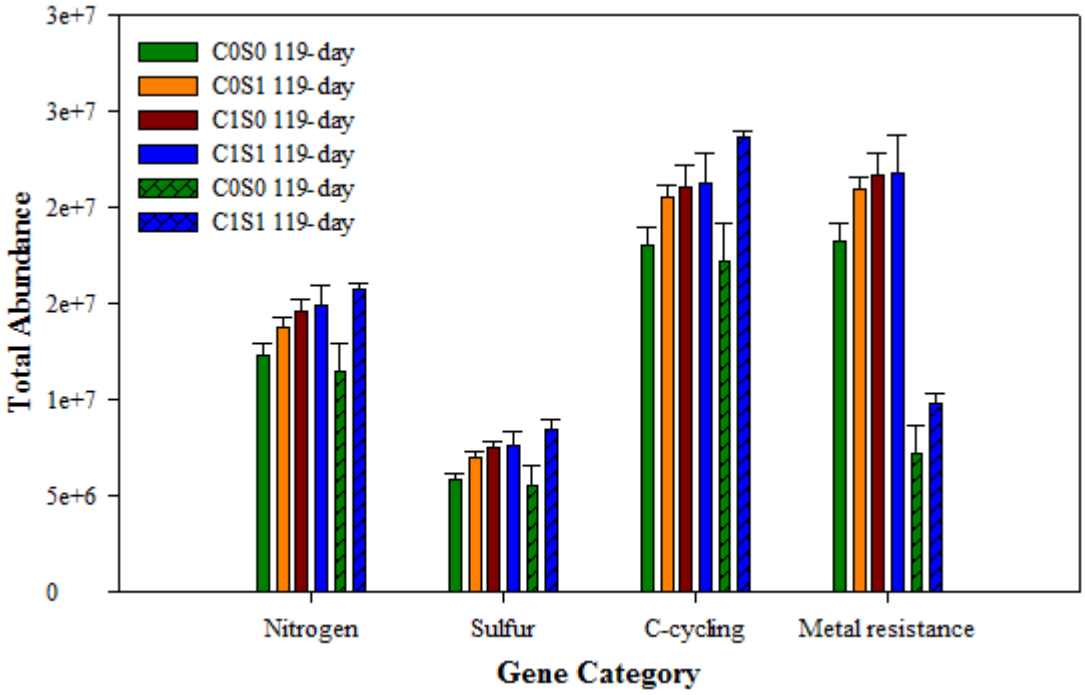

Figure 5-10: Total abundance of function genes under selected categories for the samples submerged for both medium (119-day) and long term (252-day) submergence.

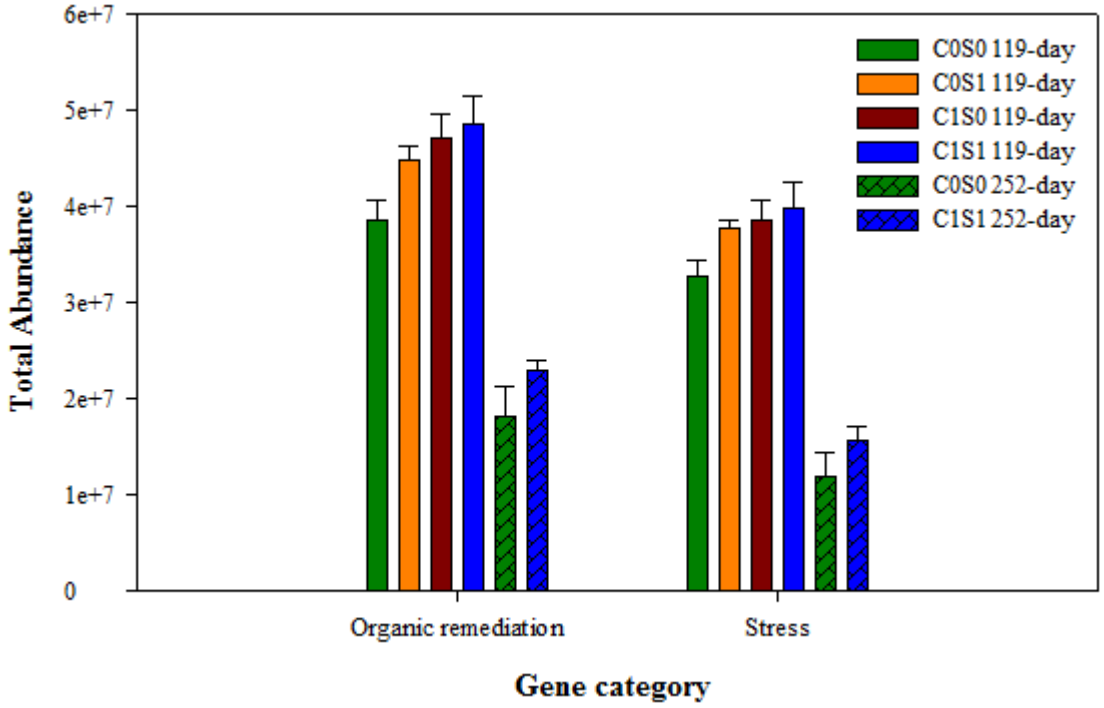

Figure 5-11: Total abundance of functional genes under organic remediation, and stress category under medium (119-day) and long (252-day) submergence.

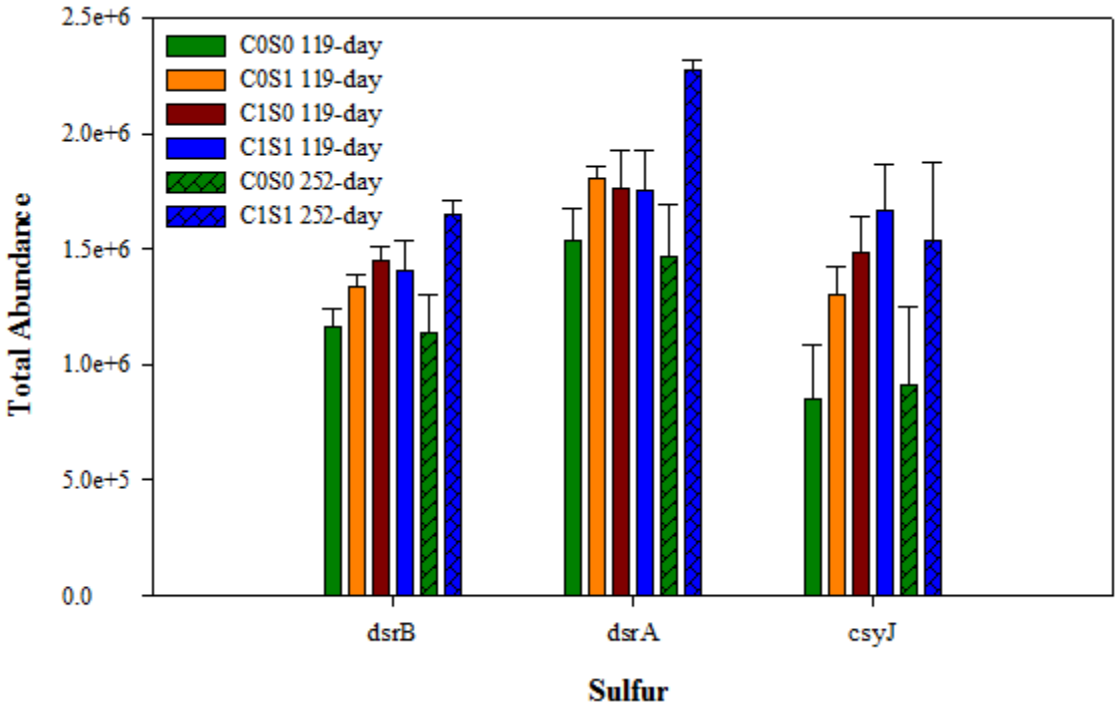

Figure 5-12: Total abundance of dsrA/dsrB, and csyJ under sulfur category under medium (119-day) and long (252-day) submergence.

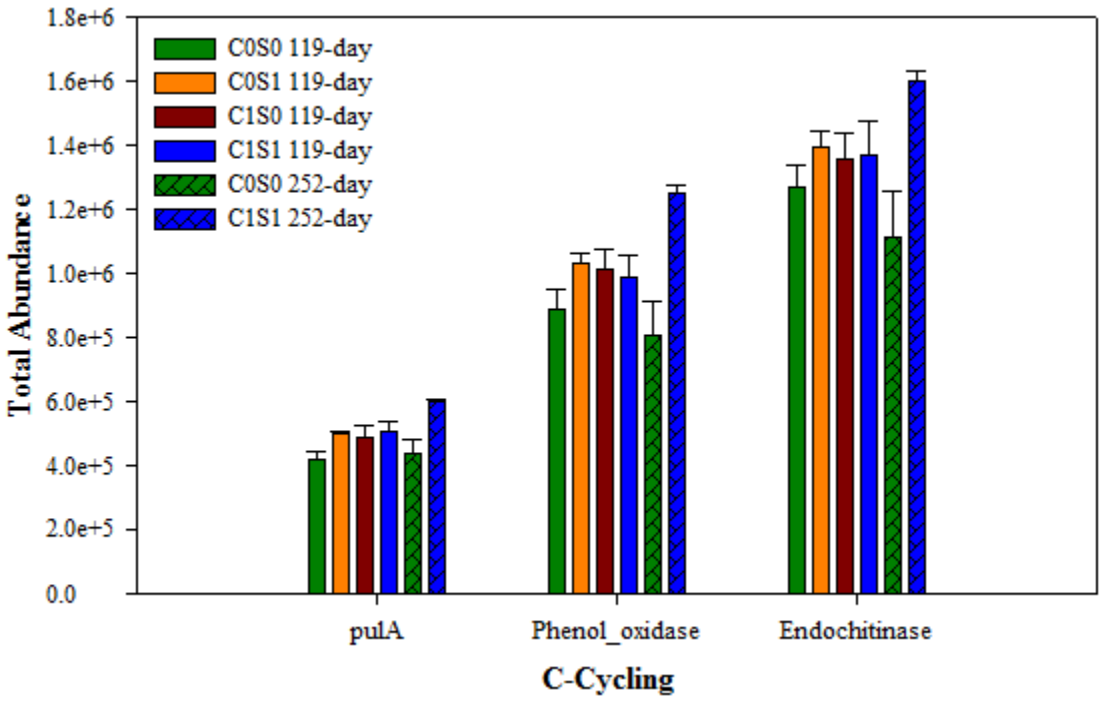

Figure 5-13: Total abundance of selected functional genes under C-cycling category under medium (119-day) and long (252-day) submergence.

.

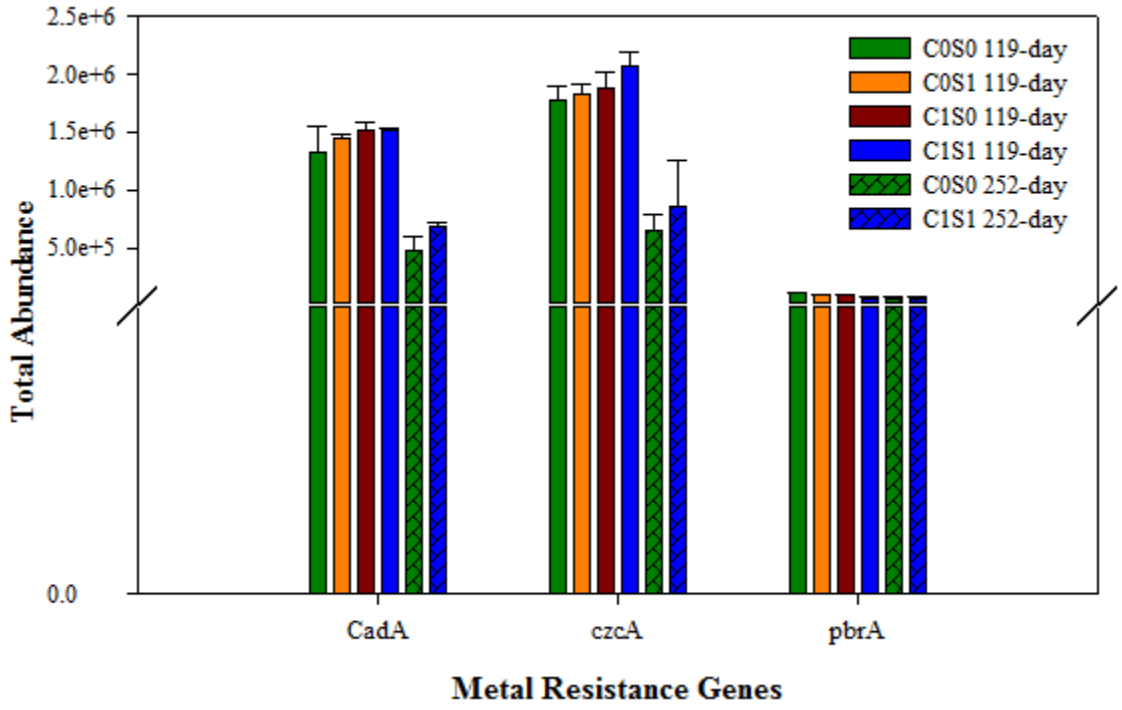

Figure 5-14: Total abundance of functional genes under metal resistance category indicating reduction of Cd resistance gene (CadA), Zn resistance gene (czcA), and negligible change in Pb resistance gene.

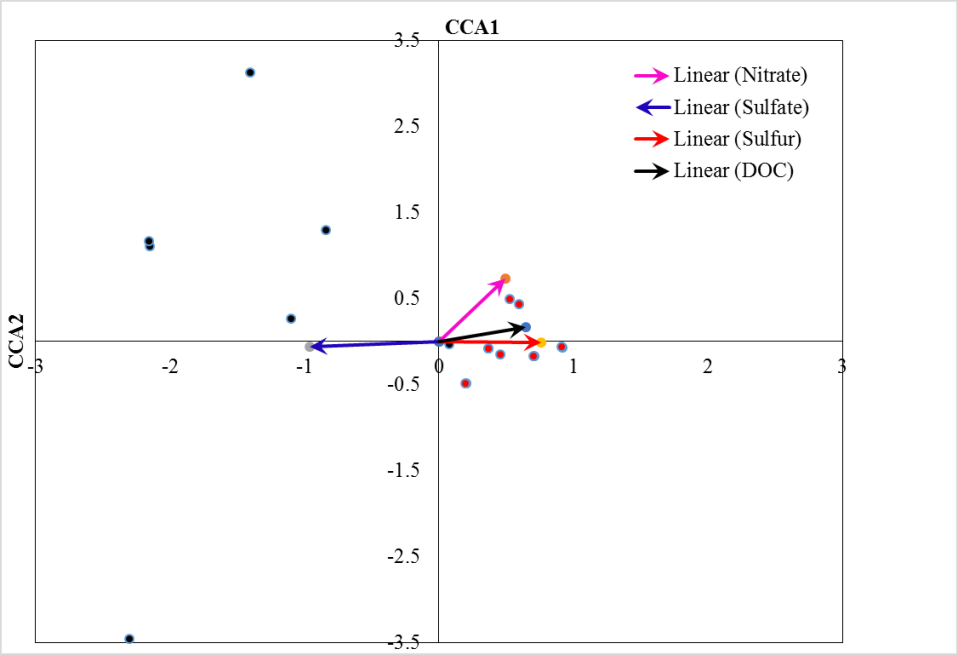

Figure 5-15: Canonical correspondence analysis (CCA) indicating relationship between microbial communities with environmental factors.

Chapter 6 - Overall Conclusion

The solution chemistry data from our current study indicated that metals were effectively immobilized under both medium- and long-term submergence in all the treatments, however C1S1 showed an enhanced effect. Metal immobilization effects observed in this study was supported by SEM-EDXA that indicated colocalization of metals with S in the black patches observed over medium-term submergence indicating indirect evidence of metal sulfide formation. This was further confirmed via synchrotron based fluorescence and absorption X-ray analyses. Bulk XAS provided overall speciation indicating enhanced sulfide formation with C1S0, and C1S1 treatments. The results obtained from the current study indicated that OC and S addition stimulated the microbial growth and activities causing change in functional microbial community structure via enhancement or reduction of functional genes in saturated minewaste materials enriched with Pb and Zn. Sulfur reducing bacteria gene; dsrA/ B appeared to be the key player in forming metal sulfides, which was significantly enhanced in C1S1 over long term submergence. Colloidal assisted metal transportation (<1% of both Pb and Cd) occurred during initial submergence. Retention filters are suggested to avoid colloidal metal transport in order to meet the maximum concentration limit for Pb and Cd in groundwater.

Based on the overall results, it seemed that C1S0 treatment revealed similar results, however considering long term stability of metals, insufficient S could promote carbonate formation at alkaline pH under reduced conditions. Considering the fact that sulfides are more stable than carbonates addition of OC and S would be the best strategy for stabilizing metals in the minewaste materials in the Tri-State mining district and any other similar geomaterials.

This research enhances our understanding of the redox processes associated with the sequestration of non-redox sensitive metals through dissimilatory reduction of sulfates in mine waste materials and/ or waste water and provides regulators with useful scientific evidence for optimizing remediation goals.

The results are in agreement with solution chemistry and molecular scale synchrotron based X-ray data and help understanding of the biogeochemical processes involved in Pb and Zn removal via dissimilatory sulfate reductions under reduced conditions.

Appendix A

Figures and tables relevant to Chapter 4

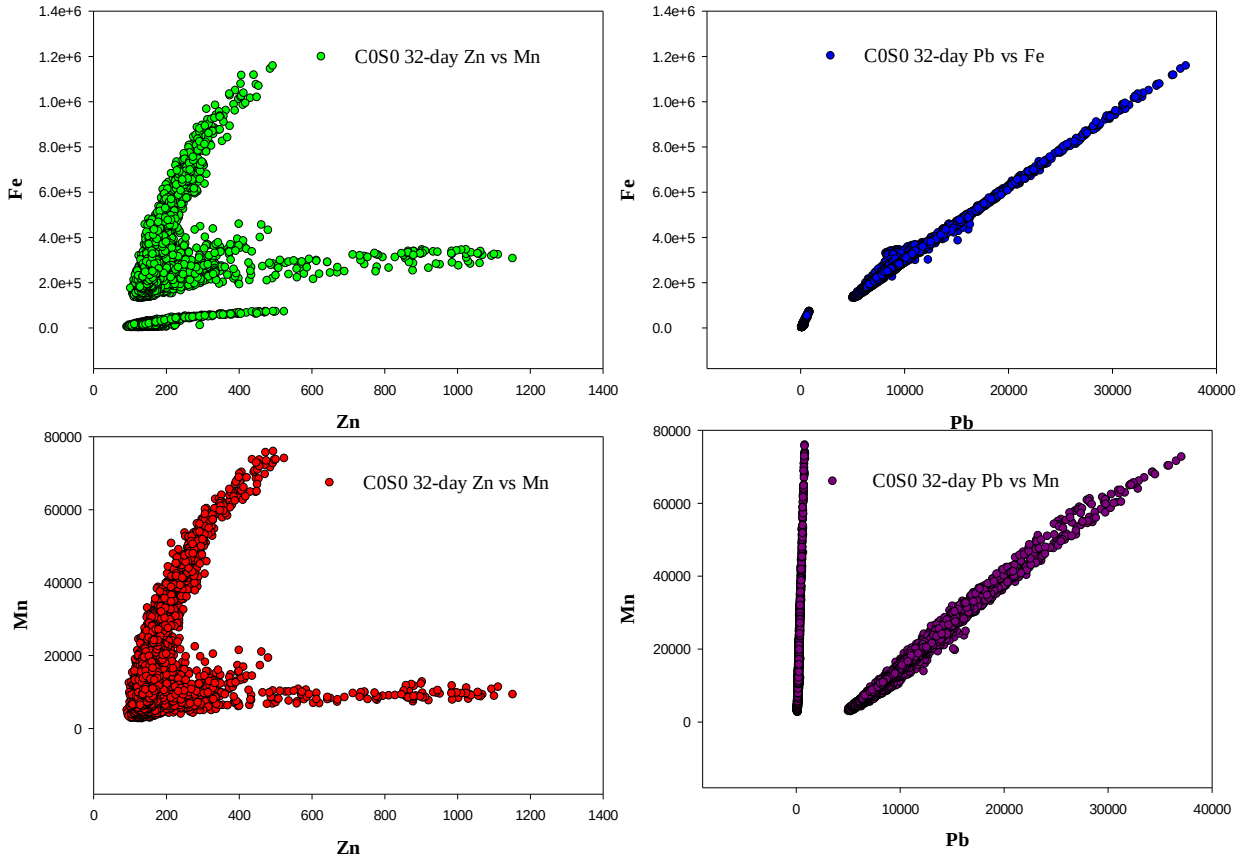

Figure A-1 Correlations between the fluorescence signals of Pb, Zn with Fe and Mn in control (C0S0) samples submerged for short term (32-day) The fluorescence signals of Pb, Zn, Fe, and Mn were collected at 14 000 eV. Each point on the graph represents a pixel in Figure 1.

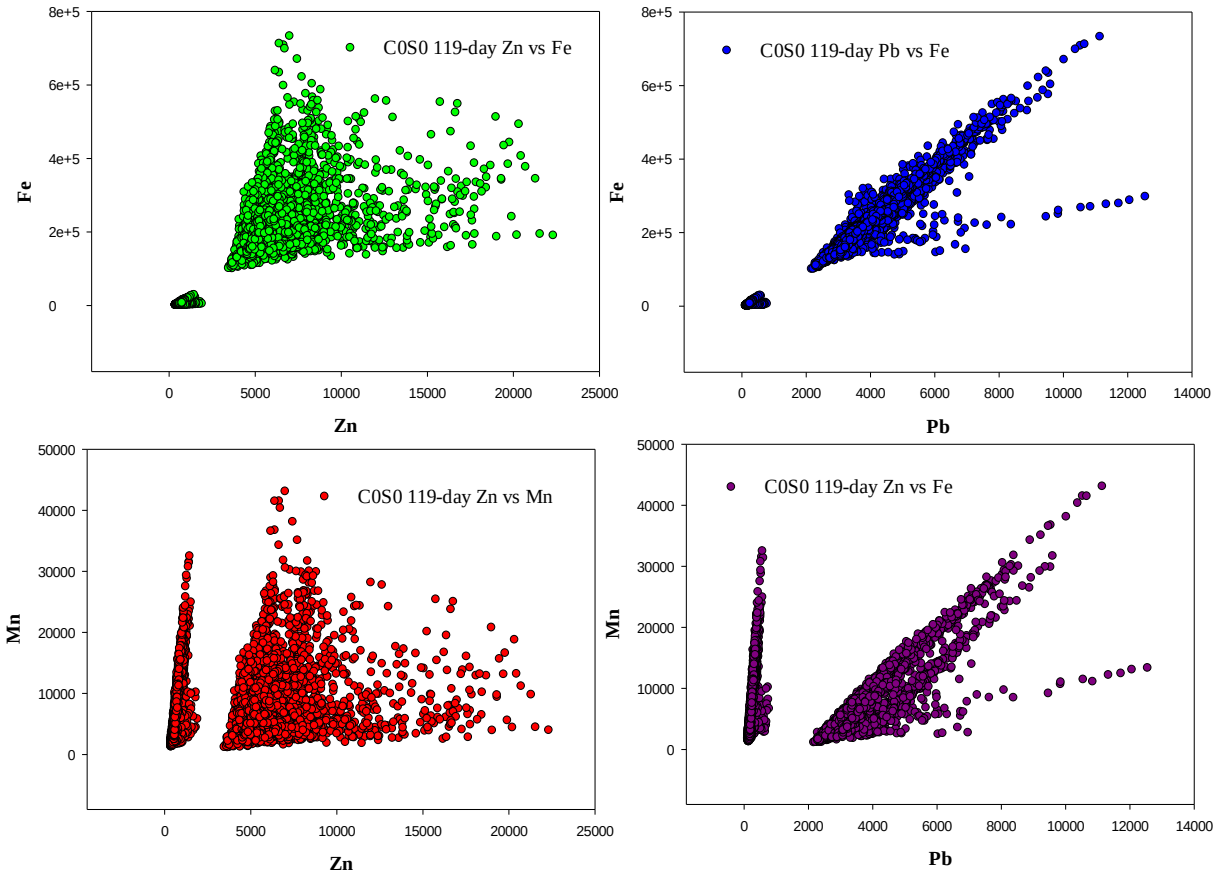

Figure A-2: Correlations between the fluorescence signals of Pb, Zn with Fe and Mn in control (C0S0) samples submerged for medium term (119-day) The fluorescence signals of Pb, Zn, Fe, and Mn were collected at 14 000 eV. Each point on the graph represents a pixel in Figure 1.

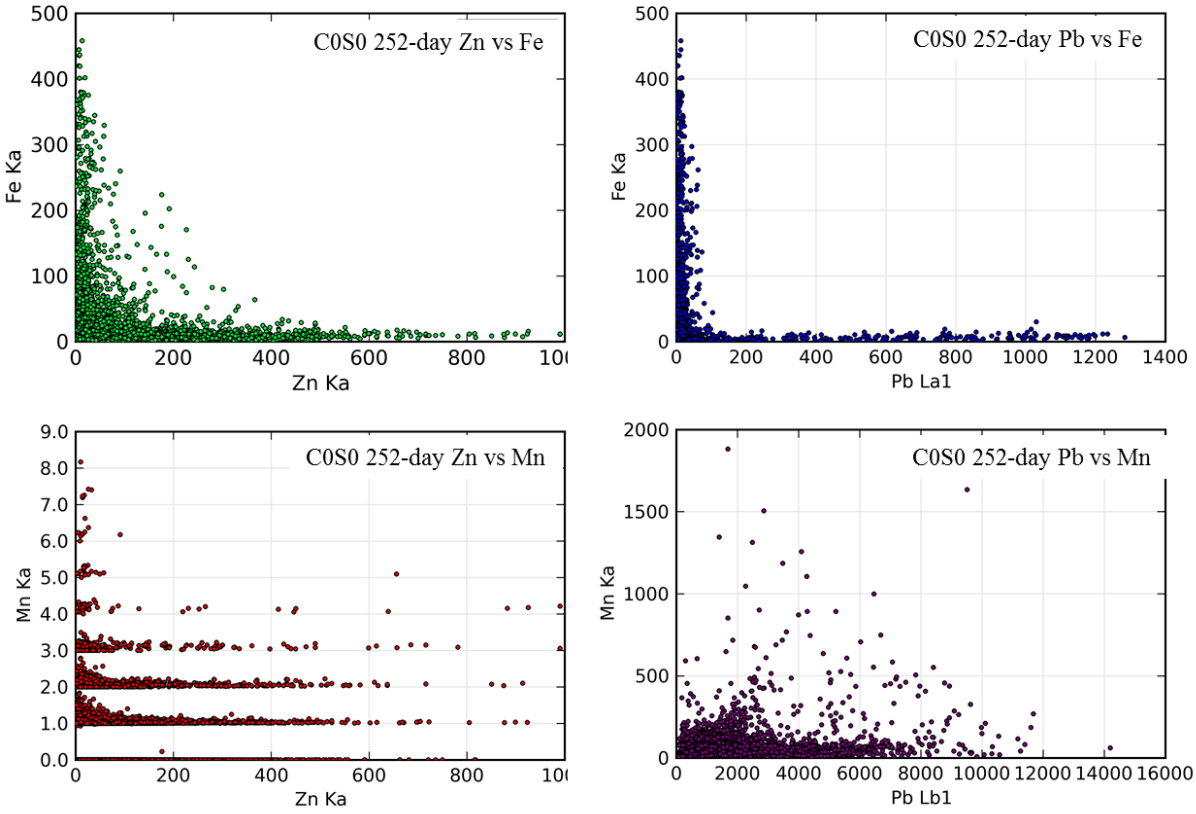

Figure A-3: Correlations between the fluorescence signals of Pb, Zn with Fe and Mn in control (C0S0) samples submerged for long term (252-day).The fluorescence signals of Pb, Zn, Fe, and Mn were collected at 14000 eV. Each point on the graph represents a pixel in Figure 1.

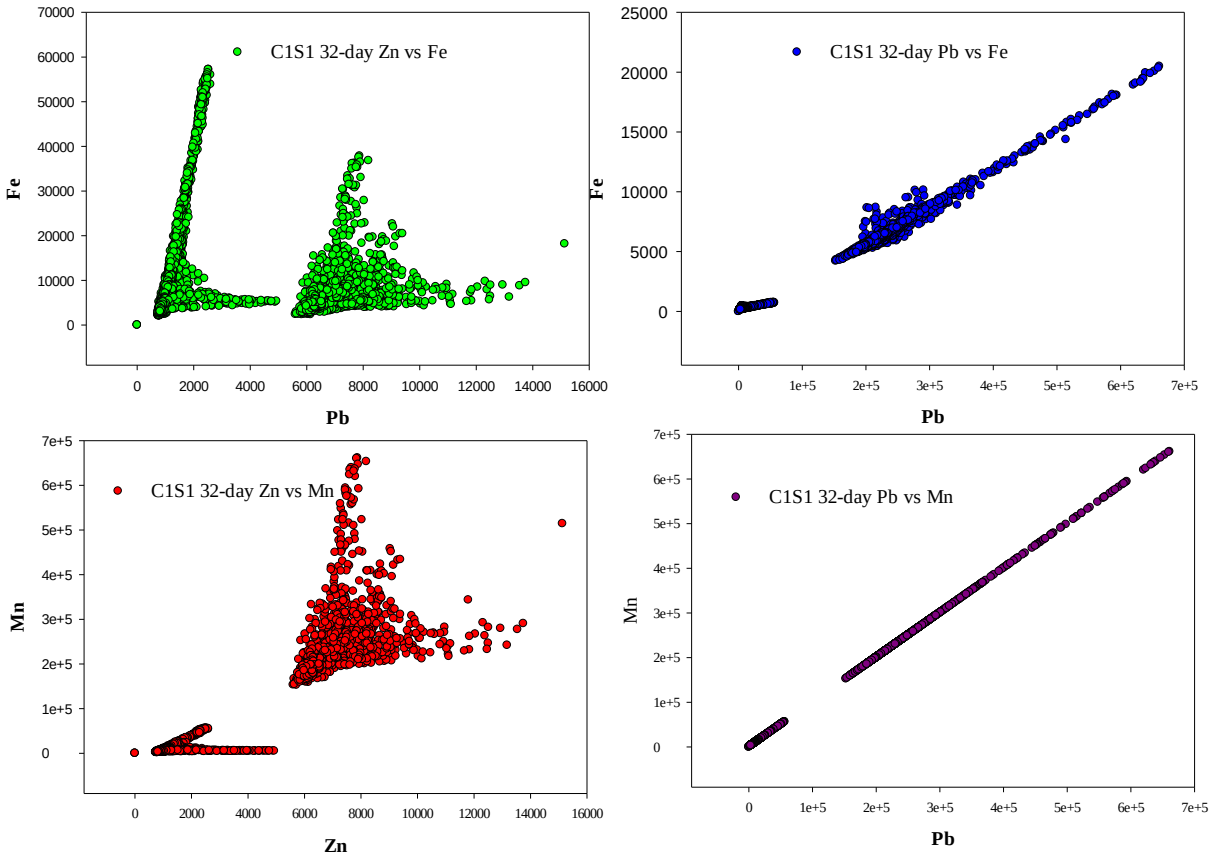

Figure A-4: Correlations between the fluorescence signals of Pb, Zn with Fe and Mn in OC plus S treated (C0S0) samples submerged for short term (32-day). The fluorescence signals of Pb, Zn, Fe, and Mn were collected at 14 000 eV. Each point on the graph represents a pixel in Figure 2.

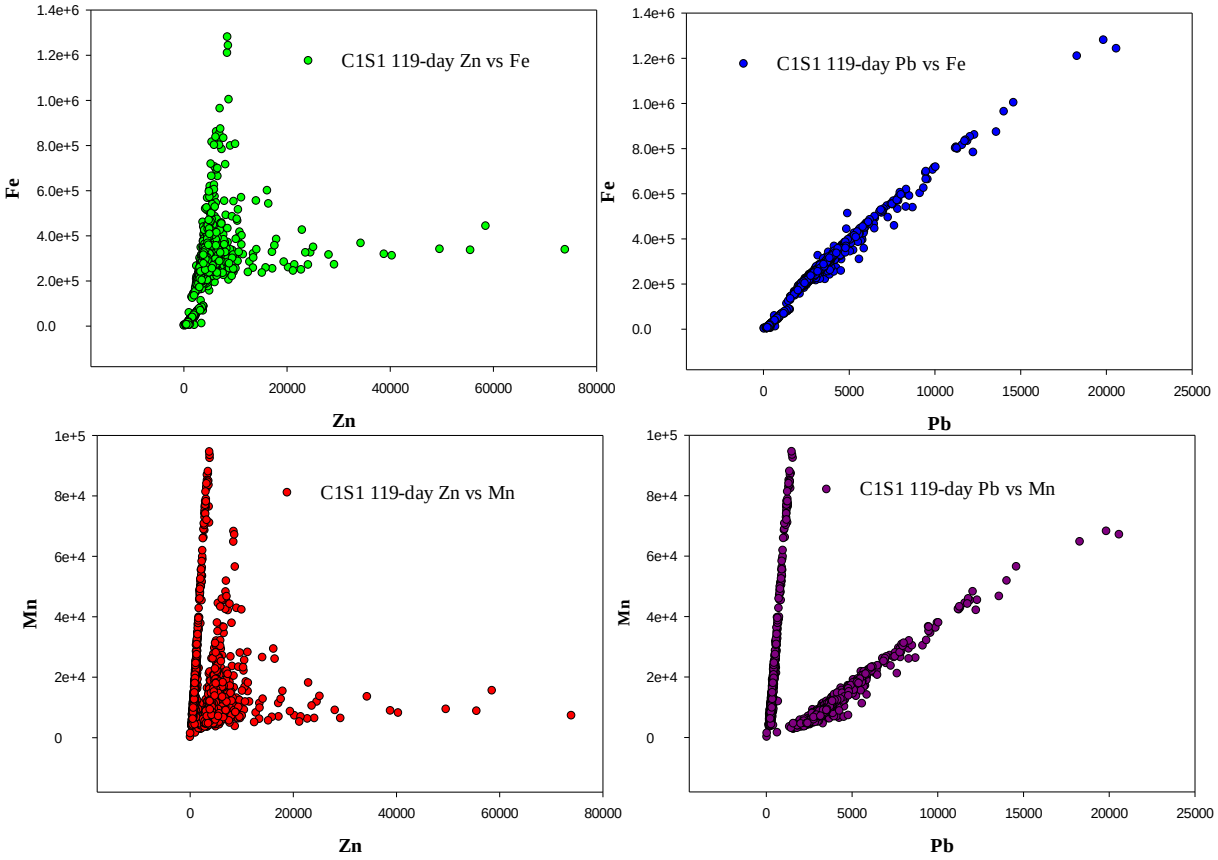

Figure A-5: Correlations between the fluorescence signals of Pb, Zn with Fe and Mn in control (C0S0) samples submerged for medium term (119-day). The fluorescence signals of Pb, Zn, Fe, and Mn were collected at 14000 eV. Each point on the graph represents a pixel in Figure 2.

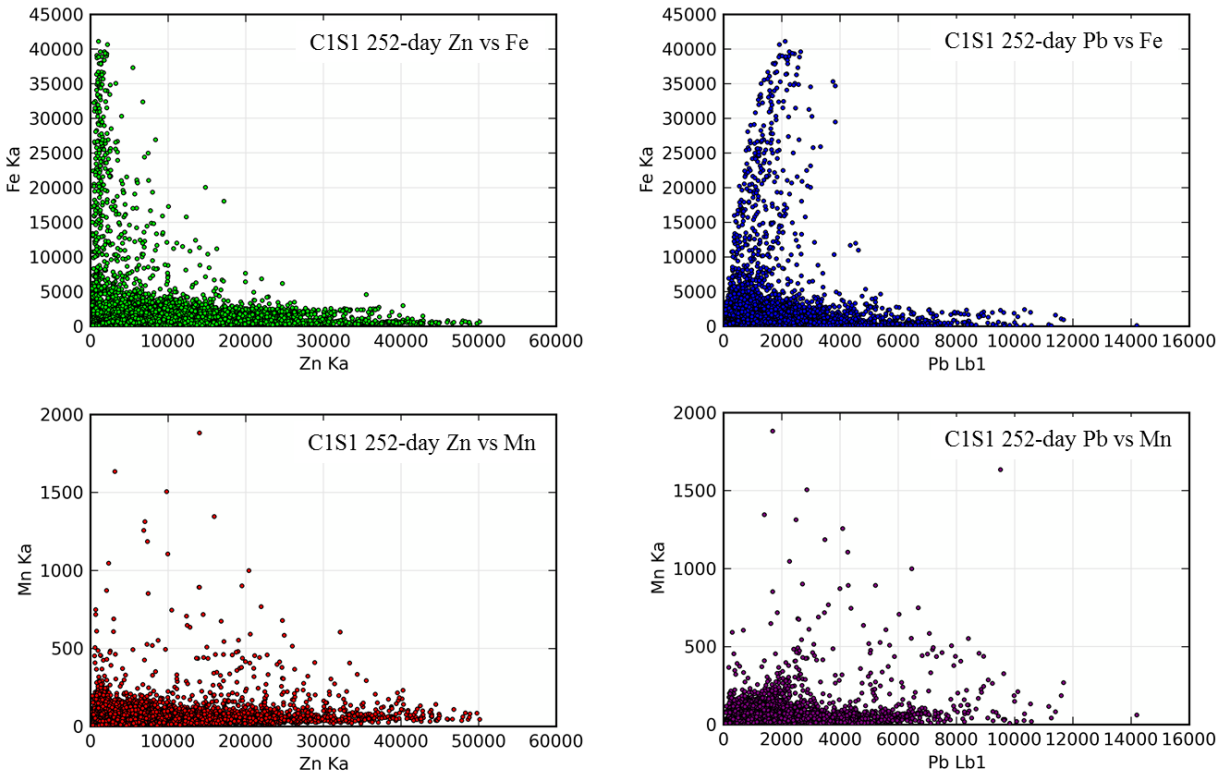

Figure A-6: Correlations between the fluorescence signals of Pb, Zn with Fe and Mn in control (C0S0) samples submerged for long term (252-day). The fluorescence signals of Pb, Zn, Fe, and Mn were collected at 14000 eV. Each point on the graph represents a pixel in Figure 1.

Table A-1: Principle component analysis (PCA) results showing spoil values for Pb and Zn mineral standards.

Zinc minerals	Spoil value	Lead minerals	Spoil value
Ferrihydrite	3.71*	Anglesite	7.19
Frnklinte	9.87	Cerrusite	0.97*
Ganhnite	9.49	Galena	2.54*
Hemimorphite	1.57*	Hydrocerrusite	3.53*
Hopeite	6.38	Hydroxypyromorphite	7.29
Hydrozincite	2.74*	Leadhillite	3.75*
Scholzite	5.23	Magnetoplumbite	2.51*
Smithsonite	2.62*	Lead oxide	1.63*
Willemite	9.92	Lead phosphate	4.7*
Zincite	15.4	Plumboferrite	9.63
ZnAl_LDH	2.65*	Plumbogummite	4.21
Zinc hydroxide	3.2*	Plumboyrosite	7.68
Sphalerite	2.31*	Pyromorphite	6.15
Zinc sulfate	1.97*	Lead hindsalite	8.01
Zinc oxide	20.5	Plumbonacrite	5.45

The mineral standards <4 were selected. *on the value indicates the standards that were used to run linear combination fittings for bulk Zn-XAFS, and Pb-XAFS.

Table A-2: Principle component analysis (PCA) results showing spoil values for Pb and Zn mineral standards

Zinc minerals	Spoil value	Lead minerals	Spoil value
Ferrihydrite	2.63*	Anglesite	3.71
Frnklinte	2.66*	Cerrusite	3.83*
Ganhnite	5.64	Galena	1.89*
Hemimorphite	2.23*	Hydrocerrusite	1.96*
Hopeite	2.19*	Hydroxypyromorphite	2.76*
Hydrozincite	5.63	Leadhillite	1.98*
Scholzite	3.11*	Magnetoplumbite	3.45
Smithsonite	2.73	Lead oxide	4.4
Willemite	2.03*	Lead phosphate	2.29*
Zincite	3.0*	Plumboferrite	2.31*
ZnAl_LDH	3.56*	Plumbogummite	3.85*
Zinc hydroxide	3.68*	Plumboyrosite	4.76
Sphalerite	2.73*	Plumbonacrite	2.46*
Zinc sulfate	4.34	Lead phosphate	2.29*
Zinc oxide	2.07*	Pyromorphite	5.81

The mineral standards <4 were selected. *on the value indicates the standards that were used to run linear combination fittings for bulk Zn-XAFS, and Pb-XAFS.

Table A-3: Micro Pb-XAS linear combination fitting results showing % components of different Pb-minerals formed with OC plus S treated (C1S1) samples under short term (32-day), medium term (119-day), and long term (252-day) submergence.

Treatments over time	Galena	Cerrusite	PbO	Hydroxypyromorphite	Plumboferrite	Plumbogummite	Pb3(PO4)2	$\chi 2$	R-factor
C1S1 252-day P1*	–	–	–	–	–	–	–	–	–
C1S1 252-day P2	89	–	–	11	–	–	–	0.02	0.0006
C1S1 252-day P8	100	–	–	–	–	–	–	0.05	0.001
C1S1 252-day P6*	–	–	–	–	–	–	–	–	–
C1S1 252-day P7*	–	–	–	–	–	–	–	–	–
C1S1 119-day P1	–	16	25	–	31	–	28	0.005	0.000065
C1S1 119-day P2	–	–	66	–	34	–	–	0.02	0.000308
C1S1 119-day P3	6	59		26	9	–	2	0.0188	0.000268
C1S1 119-day P4	29	–	51	–	–	20	–	0.01265	0.000166
C1S1 119-day P5	13	–	44	–	18	–	25	0.0162	0.000234
C1S1 32-day P1	–	79	8	13	–	–	–	0.018	0.00026
C1S1 32-day P3	71	–	–	–	8	21	–	0.0189	0.00013
C1S1 32-day P4	20	–	69	11	–	–	–	0.0084	0.00012
C1S1 32-day P5	41	–	56	–	3	–	–	0.055	0.000804
C1S1 32-day P6	–	67	21	5	7	7	–	0.02212	0.000322

P1-Pn represents the point of interest (POI) on the µ-XRF maps (Figure 1). *indicates the POIs where XAS data collected were not useable.

Table A-4: Micro Zn-XAS linear combination fitting results showing % components of different Zn-minerals formed with control (C0S0) samples under short term (32 and 119-day), and long term (252-day) submergence.

Treatments over time	Sphalerite	Frankellinite	Hemimorphite	Zn(OH)2	Willemite	Smithsonite	Ferrihydrite_Zn	ZnAl-LDH	ZnSO4	$\chi 2$	R-factor
C1S1 252-day P2	–	64	–	–	–	–	–	–	36	3.4	0.49
C1S1 252-day P3	99	–	–	1	–	–	–	–	–	1.4	0.33
C1S1 252-day P4	82	–	–	18	–	–	–	–	–	2.04	0.51
C1S1 252-day P6	44	–	–	–	56	–	–	–	–	0.94	0.67
C1S1 252-day P7	72	–	–	28	–	–	–	–	–	1.23	0.99
C1S1 119-day P1	24	28	–	–	25	22	–	–	–	0.42	0.53
C1S1 119-day P2	43	21	23	–		–	13	–	–	0.64	0.29
C1S1 119-day P3*	–	–	–	–		–	–	–	–	–	–
C1S1 119-day P4	24	17	–	5	48	2	–	4	–	0.02	0.49
C1S1 119-day P5	16	21	–	2	44	17	–	–	–	0.28	0.32
C1S1 32-day P1*	–	–	–	–	–	–	–	–	–	–	–
C1S1 32-day P2	18	22	67	–	–	–	–	–	–	5.86	0.7
C1S1 32-day P3	–	5	5	–	–	–	–	–	–	2.84	0.42
C1S1 32-day P4	–	82	–	18	–	–	–	–	–	1.23	0.26
C1S1 32-day P5*	–	–	–	–	–	–	–	–	–	–	–

P1-Pn represents the point of interest (POI) on the µ-XRF maps (Figure 3). *indicates the POI where XAS data collected were not useable.

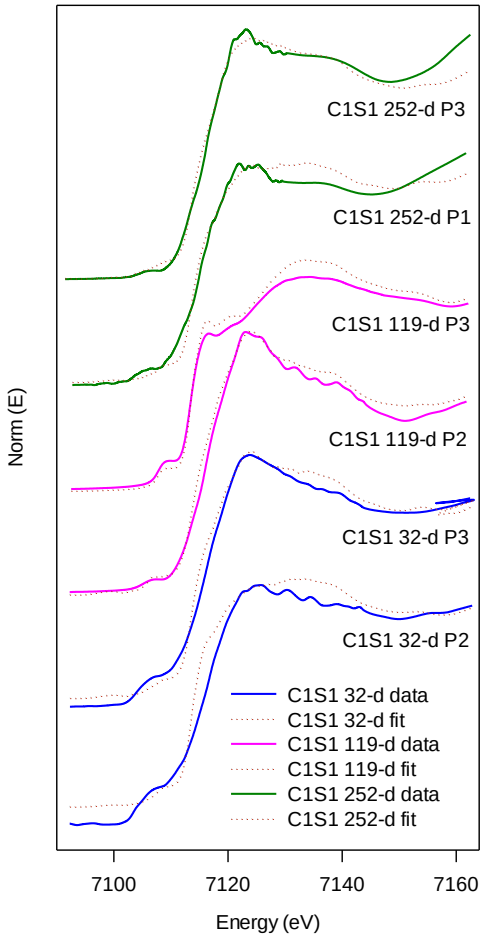

Figure A-7: Micro Fe-XANES spectra OC plus S treated (C1S1) samples under short (32-day), medium term (119-day), and long term (252-day) submergence. In each spectrum d represents days of submergence, and P1-P5 represents the points selected on micro-XRF maps for Fe-XANES data collection. Solid lines represent the normalized spectra and the dotted lines represent the best fits obtained using statistical analyses; principal component analysis (PCA), and linear combination fitting (LCF).

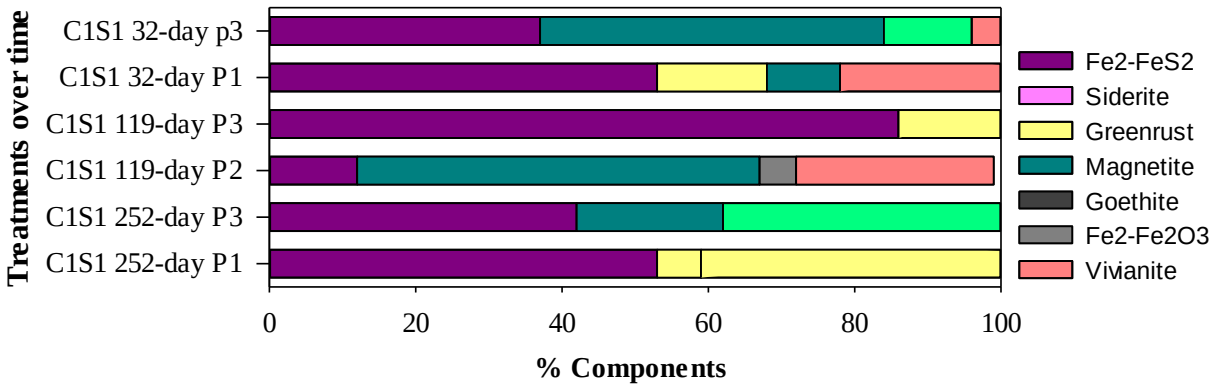

Figure A-8: Micro Fe-XANES linear combination fitting (LCF) results for control OC plus S treated (C1S1) showing % components of Fe^{2+}, and Fe^{3+} minerals formed representing redox status of system under short (32-day), medium term (119-day), and long term (252-day) submergence.

Appendix B

Material summary

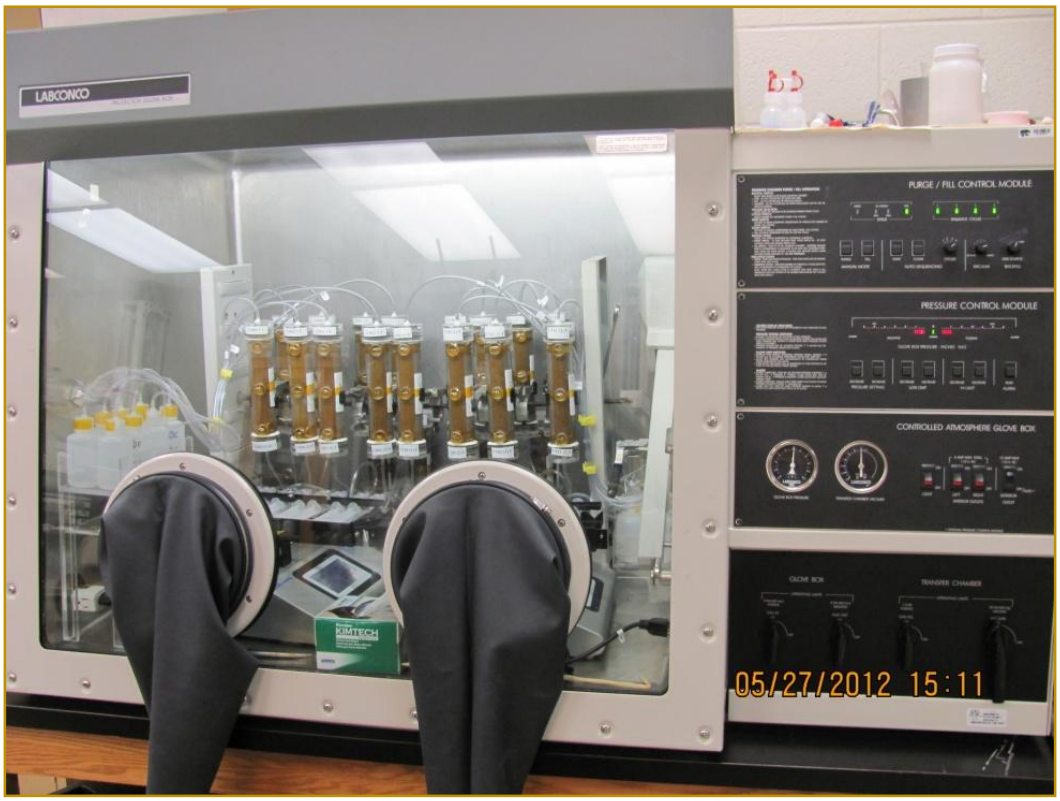

Figure B-1: Column experiment setup inside an anaerobic chamber.

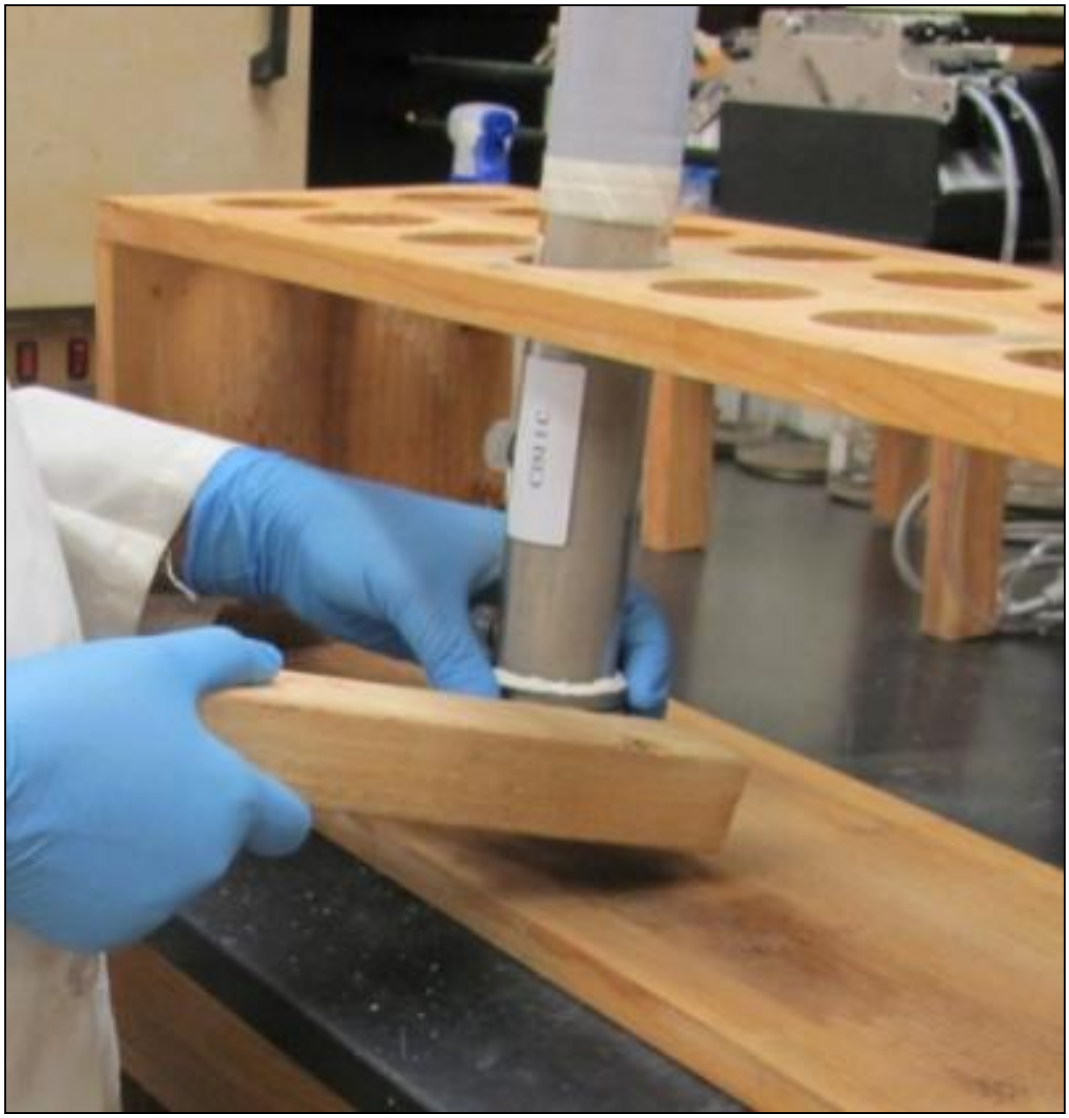

Figure B-2: Column packing.

Figure B-3: Eluent solution supply using syringe pump.

Figure B-4: Effluent sample collection.

Figure B-5: Soil sample collection at the end of experiment.

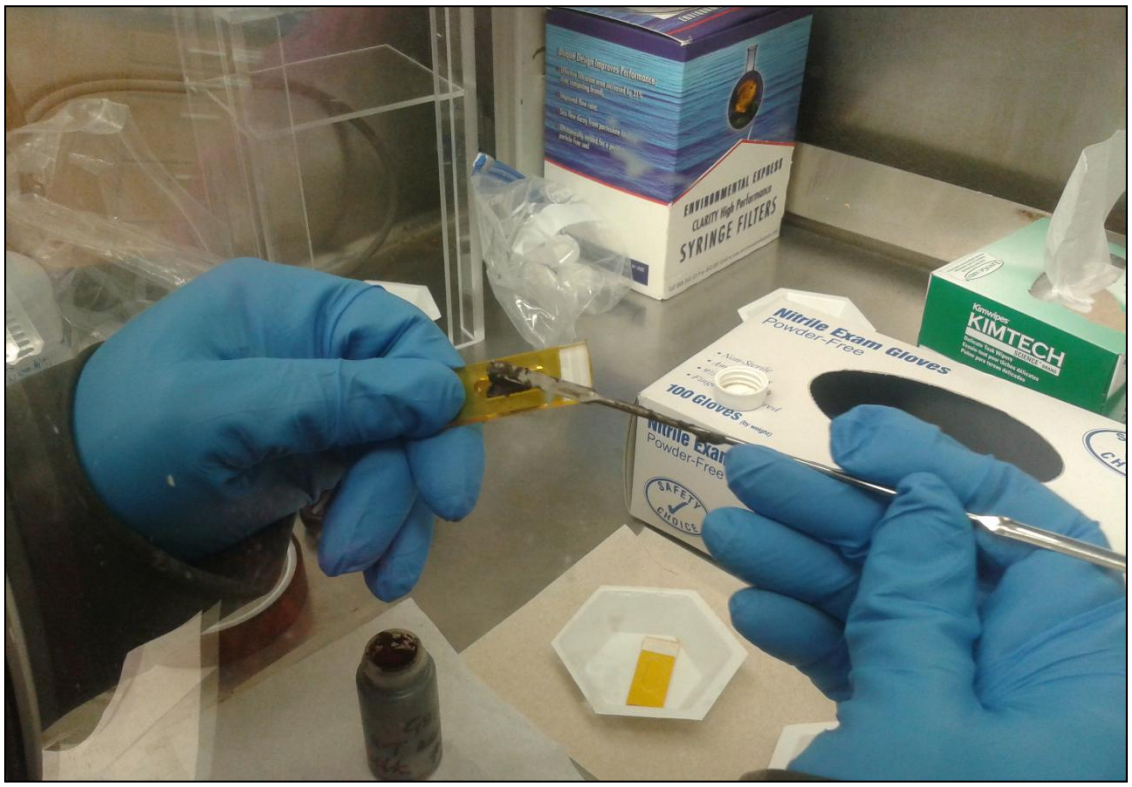

Figure B-6: Sample preparation for bulk X-ray analysis.

Figure B-7: Soil smear mounted on epoxy for micro-X-ray analysis.